Human Brain Project
Education Programme

Co-funded by
the European Union

3RD HBP STUDENT CONFERENCE

On Interdisciplinary Brain Research

Ghent University, Belgium - February 6–7, 2019

BOOK OF ABSTRACTS

frontiers Event Abstracts

3RD HBP STUDENT CONFERENCE ON INTERDISCIPLINARY BRAIN RESEARCH

ISBN: 978-2-88963-596-2
DOI: 10.3389/978-2-88963-596-2
Citation: Gabriel Urbain, Sandra Diaz-Pier, Marcelo Armendariz, Guillaume Bellec, Petrut Bogdan, Andrea Santuy, Alexander van Meegen, Stefan Mittermayr, Theresa Rass. (2019). 3rd HBP Student Conference on Interdisciplinary Brain Research.

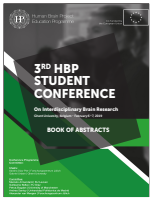

February 6–7, 2019, Ghent University, Belgium

Table of Contents

Welcome to the 3rd HBP Student Conference on Interdisciplinary Brain Research

The human brain is such a complex system that it can only be understood by combining knowledge and practices from multiple scientific fields. The 3rd HBP Student Conference provided an open forum for the exchange of new ideas among young researchers working across various aspects of science relevant to the Human Brain Project (HBP). The conference offered a space for extensive scientific dialogue, both intra- and interdisciplinary, among peers and faculty through a variety of discussion sessions, lectures and social events.

LIST OF ORGANIZERS

Chairs
Gabriel Urbain, Ghent University, Belgium
Sandra Diaz-Pier, Forschungszentrum Jülich, Germany

Committee
Marcelo Armendariz, KU Leuven, Belgium
Guillaume Bellec, TU Graz, Austria
Petrut Bogdan, University of Manchester, UK
Andrea Santuy, Universidad Politécnica de Madrid, Spain
Alexander van Meegen, Forschungszentrum Jülich, Germany

HBP Education Programme Office
Stefan Mittermayr, Medical University Innsbruck
Theresa Rass, Medical University Innsbruck

Transmittance and diattenuation of brain tissue explained by *finite-difference time-domain* simulations

Miriam Menzel[1,2]*, Markus Axer[1], Katrin Amunts[1,3], Hans De Raedt[4], Kristel Michielsen[5,2]

AQ1

[1]Institute of Neuroscience and Medicine (INM-1), Forschungszentrum Jülich GmbH, Germany
[2]Department of Physics, RWTH Aachen University, Germany
[3]Cécile and Oscar Vogt Institute for Brain Research, University of Düsseldorf, Germany
[4]Zernike Institute for Advanced Materials, University of Groningen, the Netherlands
[5]Jülich Supercomputing Centre (JSC), Forschungszentrum Jülich GmbH, Germany
**m.menzel@fz-juelich.de*

INTRODUCTION/MOTIVATION

The neuroimaging technique *3D-Polarized Light Imaging (3D-PLI)* reconstructs the microscopic nerve fiber architecture of the brain by measuring the birefringence (anisotropic refraction) of unstained histological brain sections [1]. The anisotropic structure of the nerve fibers leads to diattenuation (anisotropic attenuation), which can be measured by means of *Diattenuation Imaging (DI)* [2]. Here, we study the polarization-independent attenuation (*transmittance*) and the polarization-dependent attenuation (*diattenuation*) both with experimental studies and with *finite-difference time-domain (FDTD)* simulations and show that they contain valuable information about the brain tissue structure.

METHODS

The experimental studies were performed on 60 µm thick sections of a vervet monkey brain embedded in 20% glycerin solution. The transmittance images (Fig. 1a) were obtained from 3D-PLI measurements with a resolution of 1.33 µm/px as described by Axer et al. [1]. The diattenuation images (Fig. 1d) were obtained from combined 3D-PLI and DI measurements with a resolution of 43 µm/px as described by Menzel et al. [2]. The propagation of the polarized light wave through the brain tissue was simulated by means of a massively parallel 3D Maxwell Solver based on an FDTD algorithm as described by Menzel et al. [3].

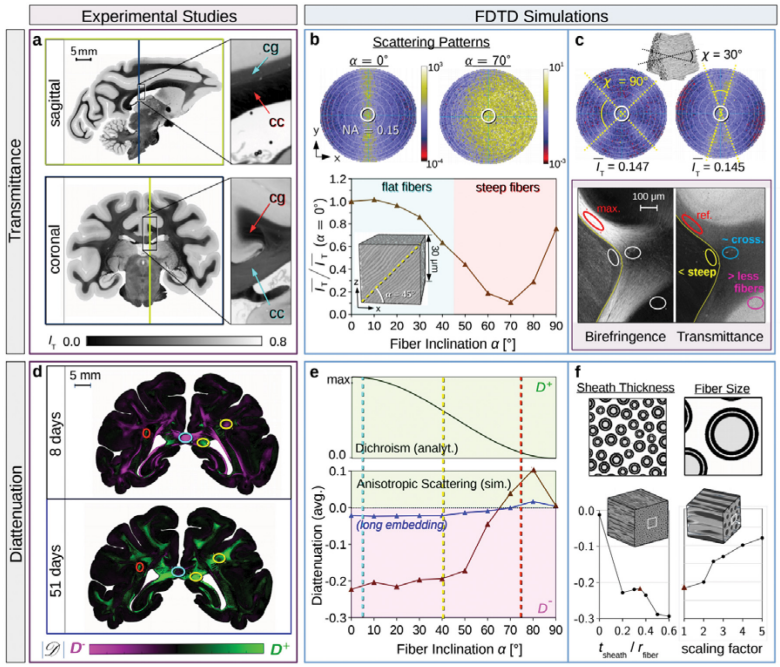

FIGURE 1: (**a**) Transmittance images of a sagittal and coronal vervet brain section (the enlarged regions show the cingulum (cg) and corpus callosum (cc)). (**b**) Scattering patterns and normalized average transmittance values obtained from FDTD simulations of an artificial nerve fiber bundle (inset) with different inclination angles (α = {0,10,...90}°). (**c**) Scattering patterns of two crossing fiber bundles with crossing angle χ. The images below show a region in the occipital lobe, demonstrating how the transmittance (right) can be used to distinguish regions with small birefringence signal (white circles, left): the transmittance in the region with maximum birefringence signal (red) is used as reference value; regions with similar (lower/larger) transmittance values are expected to contain in-plane crossing (steep/less) fibers. (**d**) Diattenuation images of a coronal vervet brain section measured 8 and 51 days after tissue embedding. Diattenuation values belonging to D^+ (D^-) regions are marked in green (magenta). The colored circles highlight regions with flat, intermediate, and steep fiber inclinations: α = 5° (cyan), α = 40° (yellow), α = 75° (red). (**e**) Diattenuation curves (average diattenuation plotted against the fiber inclination) caused by dichroism (analytical model [5]) and by anisotropic scattering (simulated for the artificial fiber bundle shown in (b)). (**f**) Average diattenuation of the horizontal fiber bundle simulated for different myelin sheath thicknesses (relative to the fiber radius) and for different fiber sizes. Parts of this figure have been published in [4,5].

RESULTS AND DISCUSSION

Our experimental studies reveal that the transmittance decreases with increasing out-of-plane inclination angle of the nerve fibers (see Fig. 1a): flat fibers with small inclinations (cyan arrows) show larger transmittance values than steep fibers (red arrows). With FDTD simulations, we could demonstrate that this effect is caused by isotropic light scattering in combination with the small numerical aperture (NA = 0.15) of the imaging system (see Fig. 1b). Furthermore, we found that the transmittance of in-plane crossing fibers does not depend on the crossing angle and can therefore be used to distinguish in-plane crossing from steep fibers (see Fig. 1c), which both yield small birefringence signals and cannot be distinguished with 3D-PLI [4].

Combined 3D-PLI and DI measurements have shown that brain tissue exhibits two different types of diattenuation: for some brain regions, the transmitted light intensity becomes maximal (minimal) when the polarization of light is oriented parallel to the nerve fibers, referred to as D^+ (D^-) effect [2]. With increasing time after embedding the brain sections, the D^- effect decreases (see Fig. 1d). With FDTD simulations, we could show that anisotropic light scattering leads to an inclination-dependent diattenuation (D^- for flat, D^+ for steep fibers), which decreases with increasing embedding time (see Fig. 1e). Finally, we could demonstrate that the diattenuation also depends on other brain tissue properties like myelin sheath thickness and nerve fiber size [5] (see Fig. 1f). This allows, for example, to distinguish brain regions with many small nerve fibers from regions with few large fibers, which makes DI a promising imaging technique revealing unknown brain tissue properties.

AQ2

REFERENCES

[1] M. Axer et al. A novel approach to the human connectome: Ultra-high resolution mapping of fiber tracts in the brain. *NeuroImage*, 54(2):1091-1101, 2011.

[2] M. Menzel et al. Diattenuation of brain tissue and its impact on 3D polarized light imaging. *Biomedical Optics Express*, 8(7):3163-3197, 2017.

[3] M. Menzel et al. Finite-Difference Time-Domain Simulations for Three-dimensional Polarized Light Imaging. In BrainComp 2015, *Lecture Notes in Computer Sciences*, Vol. 10087, Chp. 6. Springer International Publishing, Cham., 2016.

[4] M. Menzel et al. Transmittance assisted interpretation of 3D nerve fibre architectures. *arXiv:1806.07157,* 2018.

[5] M. Menzel et al. Diattenuation Imaging reveals different brain tissue properties. *arXiv:1806.07712*, 2018.

Spike latency reduction generates efficient predictive coding

AQ1

Pau Vilimelis Aceituno*, Masud Ehsani*, Jürgen Jost*

Max Planck Institute for Mathematics in the Sciences, Germany
**aceituno@mis.mpg.de; *ehsani@mis.mpg.de; *jjost@mis.mpg.de*

INTRODUCTION

Electrophysiology experiments have consistently reported recurrent spike trains with regular inter-spike times that have milisecond-level precision and can last up to a few seconds [1]. As the brain has evolved under heavy constraints on energy consumption and performance. Therefore, if some patterns are repeated very often, the neurons that receive and process them should transmit that information fast – to reduce the time spent on processing that specific spike train – and with fewer spikes – to reduce the metabolic costs of the most common stimuli –. In this work we argue that the core mechanism behind this process is the latency reduction due to synaptic plasticity. Furthermore, we show that the same mechanism explains how predictive coding can emerge.

METHODS

We study leaky-integrate and fire neurons with a refractory period (LIF), each one getting an input spike train that is repeated many times. The weights of the synapses change following the Synaptic Time-Dependent Plasticity (STDP) with soft bounds [5]. We to go from STDP dynamics on a single neuron to coding in 3 steps:

- Short Temporal Effects: STDP and LIF neurons have time constants on the order of 10 ms, and thus we analyze how do postsynaptic spikes evolve. We start with a simple toy model (Fig. 1) and we show that a single postsynaptic spike reduces its latency, meaning that it happens earlier. We also prove that, within normal parameter ranges [3,4] if two postsynaptic spikes are close in time, the latter disappears.

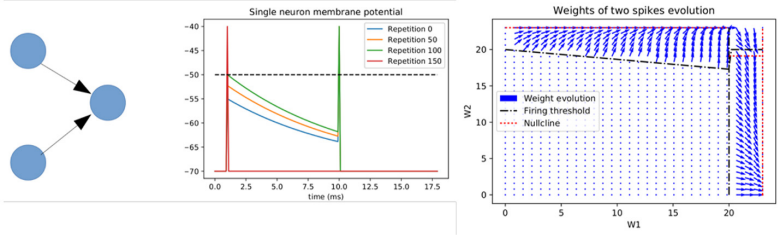

FIGURE 1: Simple explanation of local latency reduction through STDP. Two presynaptic neurons send their spikes to a postsynaptic one (left). Originally, the membrane potential of the postsynaptic one reaches the threshold at only after receiving the two presynaptic spikes, but after many repetitions, the first presynaptic synapse is strong enough to trigger a postsynaptic spike uppon receiving the first spike (center). The weights of the two presynaptic spikes evolve following STDP rules, which define a dynamical system in which the with four regions (separated by the black dotted lines), each one with its own nullclines (red dorred lines) in which the weight evolves (following the blue arrows) to a final attractor where the weight associated to the first spike at its maximum and the second weight at zero (right plot).

- Long Temporal Effects: Knowing how postsynaptic times evolve locally, we derive their behaviour in longer timescales. We prove that the post-synaptic spike train becomes very dense at input onset and that the number of postsynaptic spikes reduces exponentially with the number of repetitions (Fig. 2 A).

- Coding Consequences: Since STDP makes postsynaptic neurons fire at the onset of the input, the delay between the postsynaptic spike and the stimulus is reduced. If the presynaptic spike train includes a pre-stimulus clue, the postsynaptic neuron does not differentiate between clue and stimulus – neurons do not have direct stimulus information – and will fire before the stimulus arrives (Fig. 2 B). Note that we could interpret this as having neurons that change what they encode, but this is a common feature of all prediction schemes: a neuron that "predicts" a stimulus simply encodes a preceding stimulus.

Our results are analytical, using a combination of combinatorial and probability methods as well as told from dynamical systems theory and differential equations with delays. All our results are supported by simulations.

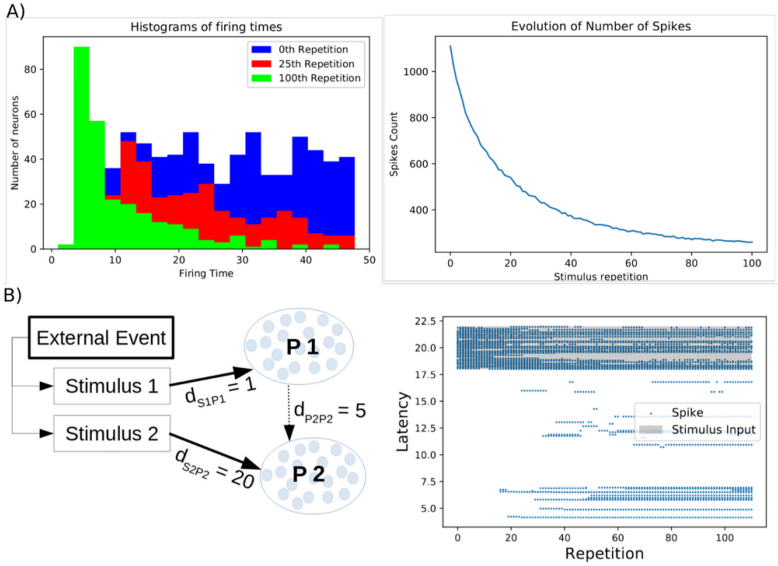

FIGURE 2: (**A**) Evolution of long postsynaptic spike trains: We simulated a population of 200 postsynaptic neurons, each one receiving 100 presynaptic spikes with random but fixed arrival times during a time interval of 200 ms. The distribution of postsynaptic spikes (left plot) changed from a constant firing rate (blue), to concentrate the spikes at the onset of the spike train (green) as the same input spikes are repeated. As STDP weakens spikes arriving after a postsynaptic one, two postsynaptic arriving very close in time cannot coexist, and thus the number of postsynaptic spikes decreases (right plot) as the input is repeated. (**B**) Predictive Coding through Latency Reduction: We show that STDP can lead to predictive coding through a simple schema where a single event generates two stimulus S1, S2 which trigger spikes on two neural populations P1 P2 at different times so that P1 always precedes P2. If we add a few connections from P1 to P2, the neurons in P2 receive a few spikes that systematically precede the spikes associate to S2. As they do not differentiate between the two spike trains, they treat both as equal. Since each neuron tends to fire at the onset of the presynaptic spike train (see Fig. 2 A), some neurons in P2 will fire upon receiving spike trains from P1, even earlier than the presynaptic spikes from S2. Thus, they fire earlier than the stimulus. The left plot shows the schema, while the right plot shows the firing times of neurons in P2.

RESULTS AND DISCUSSION

We showed that STDP in combination with regularly timed presynaptic spikes generates postsynaptic codes that are efficient and explain how forecasting are phenomena that emerge in an unsupervised way with a simple

mechanistic interpretation. We believe that this idea offers an interesting complement to classical supervised predictive coding schemes in which prediction errors are feed back into the coding neurons. Furthermore, the concentration of postsynaptic spikes at stimulus onset can be interpreted in information theoretical terms as a way to improve the code in terms of error-resilience (not shown). Finally, we speculate that the fact that the same mechanism can be used to generate predictions as well as improve the effectiveness and metabolic efficiency of the neural code might give insights into how the ability of the nervous system to forecast might have evolved.

AQ2

REFERENCES

[1] Fellous, J. M., Tiesinga, P. H., Thomas, P. J., & Sejnowski, T. J. Discovering spike patterns in neuronal responses. Journal of Neuroscience, 24(12), 2989-3001. 2004.

[2] Dayan, P., Abbott, L. F., & Abbott, L.. Theoretical neuroscience MIT Press 2001.

AQ3

[3] Song, S., Miller, K. D., & Abbott, L. F. Competitive Hebbian learning through STDP. Nature neuroscience, 3, 919. 2000.

[4] Guyonneau, R., VanRullen, R., & Thorpe, S. J. Neurons tune to the earliest spikes through STDP. Neural Computation, 17(4), 859-879. 2005.

[5] Sjöström, J., & Gerstner, W. Spike-timing dependent plasticity. Spike-timing dependent plasticity, 35. 2010.

Ligand tethered dendrimers for brain delivery of Anti-AD agents: Better pharmacokinetics and behavioral responses

AQ1

Avinash Gothwal[1]*, Kartik T. Nakhate[2], Umesh Gupta[1]*

[1]Department of Pharmacy, School of Chemical Sciences and Pharmacy, Central University of Rajasthan, Bandarsindri, Ajmer

[2]Rungta College of Pharmaceutical Sciences and Research, Kohka Road, Kurud, Bhilai, Chhattisgarh

**umeshgupta175@gmail.com; *avgothwal20@gmail.com*

INTRODUCTION

To bypass the BBB and to deliver the therapeutic agent into the brain several approaches such as pharmacological, physiological, invasive and non-invasive have been used so far and each has some merits and demerits [1]. As the BBB is the biggest challenge in drug delivery to the brain in all the brain ailments including Alzheimer's Disease (AD), Parkinson and brain tumor etc [2] . For the instance, there is no disease-modifying cure or prevention for the AD [3], one of the effective approaches for the AD is an anti-AChE (i.e. rivastigmine, donepezil) treatment strategy [4] and NMDA (N-methyl D-aspartate) antagonists [5] (memantine) which only gives a symptomatic relief. The BBB controlled uptake limits bioavailability of the bio-actives into the brain. Therefore, we are proposing a new approach, dendrimer-ligand mediated targeted delivery of the bio-actives to the brain for the effective delivery to the brain. Dendrimers are the hyper-branched, unimiceller, monodispersed, globular, versatile and synthetic macromolecules with higher molecular weight. We hypothesized that dendrimer-ligand conjugate would facilitate the process of BBB crossing which would lead to higher brain uptake.

METHODOLOGY

A ligand was chemically conjugated to PAMAMs (polyamidoamine) dendrimers of different generations. Conjugation was confirmed by FT-IR, 1H-NMR (proton-nuclear magnetic resonance), 2D-NMR spectroscopy and AFM (atomic force microscopy) techniques. Further, rivastigmine (RIV) and memantine (MEM) were physically encapsulated to PAMAM and conjugates, separately.

In-vitro and ex vivo studies such as release, hemotoxicity, encapsulation determination etc. were performed. HPLC was used to quantify the drug loading and also for the estimation of drug amount in pharmacokinetic and bio-distribution methods. Brain targeting potential of the conjugates and behavioral responses were investigated in Sprague– Dawley rat model in vivo.

RESULTS AND DISCUSSION

Spectroscopic analysis confirmed the conjugation, size of the conjugate was 100.03±3.1 nm after RIV (PAMAM-ligand-RIV) and MEM (PAMAM-ligand-MEM) loading the size was increased up to 336±8.3 and 131.72±4.73 nm, respectively. Ex-vivo hemotoxicity of PAMAM-ligand-RIV and PAMAM-ligand-MEM was less than the 10 percent. The bioavailability of the RIV and MEM was enhanced by almost 7 and 9 folds compared to pure drugs with other improved pharmacokinetic parameters. Brain uptake was significantly ($p<0.005$) higher than the pure drugs in vivo. No kind of neuronal death or necrosis was observed in the treated animals (Figure 1).

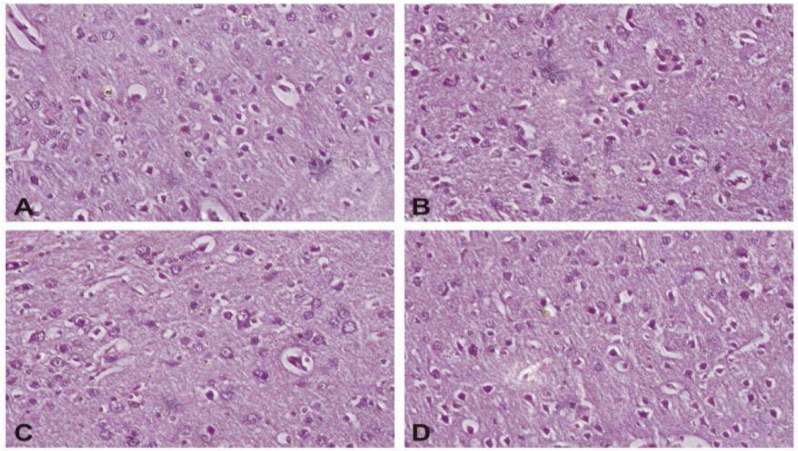

FIGURE 1: Hematoxylin and eosin-stained brain sections of rats treated with (**A**) control, (**B**) RIV, (**C**) PAMAM-RIV and (**D**) PAMAM-ligand-RIV. The neuronal degeneration was not observed following any of the treatment.

Additionally, the memory (long and short-term) and motor tasks were significantly improved when treated with RIV based formulations. while no significant improvement was observed in MEM based formulations.

CONCLUSION

PAMAM-ligand conjugates were synthesized, characterized to attain higher drug loading and effective delivery of RIV and MEM to the brain. The results revealed that the developed system could be promising in brain delivery and may have possible applications in Alzheimer's disease (AD).

AQ2

REFERENCES

[1] Upadhyay RK. BioMed Research International. http://dx.doi.org/10.1155/2014/869269.

[2] Jeffrey P, Summerfield SG. Xenobiotica. 2007 Oct-Nov;37(10-11):1135-51.

[3] Cummings J, Ritter A, Zhong K. J Alzheimers Dis. 2018;64(s1): S3-S22.

[4] Mathew M, Subramanian S. https://doi.org/10.1371/journal.pone.0086804.

[5] Marum RJV. Neuropsychiatr Dis Treat. 2009; 5: 237–247.

Temporal harmonics of brain activity reveal sleep stage transitions

Joan Rué-Queralt[1]*, Angus Stevner[2,3], Enzo Tagliazucci[4], Helmut Laufs[5], Morten Kringelbach[2,3], Gustavo Deco[1,6,7,8], Selen Atasoy[2,3]

AQ1

[1]Computational Neuroscience Group, Universitat Pompeu Fabra, Barcelona, Spain
[2]Department of Psychiatry, University of Oxford, UK
[3]Center for Music in the Brain, Aarhus University, Denmark
[4]Department of Neurology and Brain Imaging Center, Goethe University, Frankfurt, Germany
[5]Department of Neurology, Christian Albrechts University, Kiel, Germany
[6]Institució Catalana de la Recerca i Estudis Avançats (ICREA), Barcelona, Spain
[7]Department of Neuropsychology, Max Planck Institute for Human Cognitive and Brain Sciences, Leipzig, Germany
[8]School of Psychological Sciences, Monash University, Clayton, Melbourne, Australia
**joan.rue01@estudiant.upf.edu*

INTRODUCTION

The complex spatiotemporal patterns of brain activity have been the subject of intense study over the last two decades. Recent evidence has demonstrated that brain activity is constrained by the connectome and can usefully be described by a frequency-specific representation of brain activity – so-called 'connectome harmonics'. Here we describe a novel Temporal Manifold Harmonics method for recovering the low-dimensional manifold underlying the complexity of brain signals. As a proof of concept, we apply this method to fMRI data acquired over the human sleep cycle, and show how temporal manifold harmonics reveal how fMRI BOLD activity during the sleep cycle can be accurately mapped onto simple smooth manifolds.

METHODS

The fMRI BOLD signal from subjects sleeping in the scanner is used in this work to estimate the phase coupling between 90 brain regions defined

by automated anatomical labeling (AAL) template the at each time point. We then construct a sparse graph, in which the nodes are the defined as the time points, and the edges are defined as connections between only those time points that share similarities in their patterns of phase synchrony. A manifold learning technique is then applied, namely Laplacian eigenmaps, in order to map the high dimensional feature vector containing activity signal at each area to a lower dimensional manifold, which we termed 'Temporal Manifold Harmonics' (TMH) of brain activity. Linear classification of time points belonging to different sleep stages (which have been labeled by an expert, using the simultaneously recorded polysomnography) is performed in this low dimensional embedding through Support Vector Machines (SVM) to assess the capability of TMH to characterize different sleep stages. As Laplacian eigenmaps do not constrain this embedding to be linear, natural nonlinearities in the dynamics, if present, are captured in TMH. For this reason, we compare the accuracies of TMH with those obtained through a linear dimensionality reduction algorithm, the Principal Component Analysis (PCA). Sensitivity and specificity of these trained classifiers is assessed with a Receiver Operating Characteristic (ROC) analysis. An statistical analysis using Monte-carlo random reordering of the temporal signals is performed to discard any preprocessing artifact.

RESULTS

When the TMH are constructed for each individual subject, following a 6-fold cross-validation, the results indicate a high separability between sleep stages (the average accuracy being 91 ± 5 %, with all stage-to-stage comparisons being significant, p-value<.01, Monte-Carlo simulations, corrected for multiple comparisons via FDR, see Fig. 1). Great sensitivity and specificity scores in a binary classification even along a single dimension of the TMH (area under the ROC of 0.96). When TMH are constructed for al subjects, following a leave-one-subject-out cross-validation, the average accuracy for the group analysis is 83 ± 9 %, with all stage-to-stage comparisons being significant, p-value<.05, Monte-Carlo simulations, corrected for multiple comparisons via FDR, see Fig. 1).

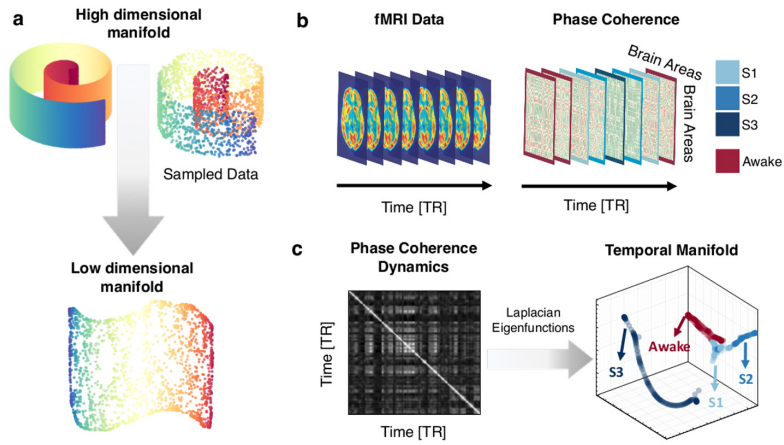

FIGURE 1: Pipeline to embed fMRI BOLD data onto their temporal harmonics. (**a**) Swiss Roll example to illustrate manifold learning: Three dimensional data points sampled from an intrinsically lower dimensional object are embedded on a two-dimensional manifold. (**b**) fMRI BOLD signal is transformed into instantaneous phase. The pairwise phase coherence provides a spatial pattern that characterizes the synchrony relations between the activity of all pairs of brain areas at each time point. (**c**) The Coherence Connectivity Dynamics (CCD) is derived as the similarity matrix between such the patterns of between-area synchronization for a time point in a pairwise manner. A sparse characterization of the CCD containing only local information is obtained through the Relaxed Minimum Spanning Tree (RMST) algorithm. The eigenfunctions of the Graph Laplacian applied to this sparse matrix define an embedding onto the Temporal Manifold Harmonics of the data.

DISCUSSION

Overall, this work demonstrates that TMH provide an accurate representation of the spatiotemporal dynamics of brain activity for characterizing the intrinsic nature of the different states in functional neuroimaging data. Furthermore, these results strongly evidence that all subjects share a common smooth manifold underlying the dynamics of their brain activity, given that the different sleeping stages can be accurately classified under the intrinsic structure found by their shared TMH.

AQ2

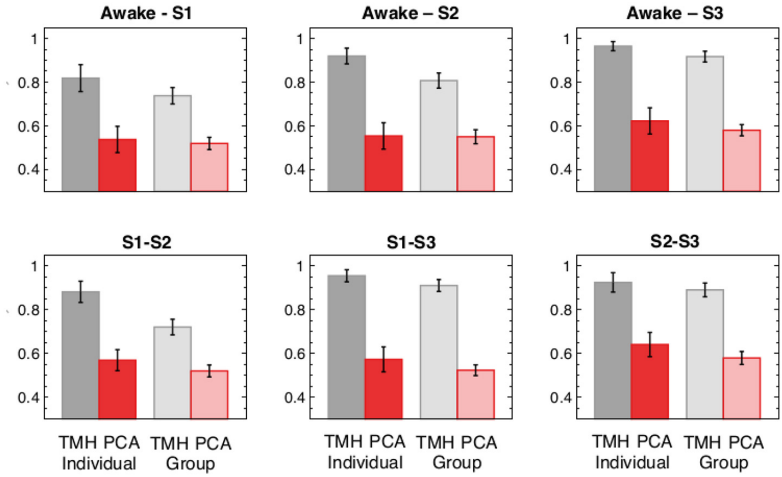

FIGURE 2: Accuracies of the support vector machines wakefulness-sleep stage-to-stage classification. For each stage pairwise comparison, there is an equal number of test elements for each class and the minimum accuracy is thus 0.5. Errorbars indicate the standard error of the mean. Legend: TMH, PCA individual, Temporal manifold harmonics or PCA embedding computed for each subject. TMH, PCA group: Temporal manifold harmonics or PCA embedding computed for the grouped data of all subjects. For all comparisons, temporal manifold harmonics yield much better classification accuracies, indicating that nonlinearities are crucial to characterize the differences amongst the different sleep stages.

AQ4

Brainnets: An open-source graph theoretical analysis library and application

AQ1

Avraam Marimpis[1,2]*, Rainer Goebel[1,2]*

[1]*Cognitive Neuroscience Department, Maastricht University, The Netherlands*
[2]*Brain Innovation B.V., Maastricht, The Netherlands*
**avraam.marimpis@maastrichtuniversity.nl; *r.goebel@maastrichtuniversity.nl*

Graph theoretical analysis attracts increasing attention in recent years, highlighting its importance and usefulness in neuroimaging, specifically, to brain connectivity [1, 2]. Through this new collection of tools, researchers drew astonishing conclusions about the underlying dynamics governing the brain [3] and even proposed network models that help understand the complex organization of the brain [4, 5].

In this work, we present, "brainnets" a new, opensource C++ library for graph analysis, specifically tailored for exploring functional brain connectivity. Functional connectivity refers to the statistical analysis of usually distinct brain regions [6]. Functional connectivity analysis based on graph analysis gains increasing popularity in the field of neuroimaging with applications in a wide variety of fMRI studies (see [7, 8] for a short survey); it can help unveil vulnerable brain networks' characteristics and possibly comprise important biomarkers. Neurodegenerative and neurodevelopmental disorders, such as Alzheimer's, Parkison's, Schizophrenia and ADHD are of special interest in utilizing graph theoretic approaches due to the disrupted connectivity patterns. Such cases, for example include, the loss of small-worldness has been observed in patients who have Alzheimer's [9, 10]. Moreover, in Schizophrenic patients, a significant reduction of betweenness centrality was observed, suppressing the centrality hubness of the studied regions [11]. Another complementary topic incorporates studies solely focused on the reliability of graph features between/within subjects [12] as well as their reproducibility [13].

The developed tool focuses on the analysis and visualization of graph features and graph distances. The usual method to compare connectivity matrices is based on statistical approaches, such as performing a t-test. In this toolbox, however, we employ well-established graph theoretical methods [14, 15, 16] that operate on the graphs' spectrum, thus retaining any topological and structural information. We plan to employ brainnets as a framework to

FIGURE 1: The connectivity between ROIs or voxels is visualized using a circular scatter plot. In our example, we demonstrate the functional connectivity between the Right and Left hemispheric V5 of one subject, as is estimated from their mean values.

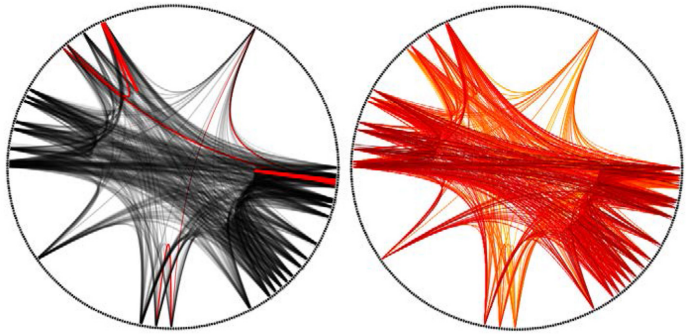

FIGURE 2: The estimated connectivity within the Left V5 (between voxels). The circular plot on the left the, the graph is passed through the Minimum Spanning Tree algorithm, and the resulting tree is highlighted in red lines. On the right plot, the connectivity matrix is plotted using the weights are colors.

further study and develop these methods. Considering the graph features, the toolbox contains all the necessary methods to explore the segregation, integration, and centrality from both global and nodal aspects of a network. A few selected graph featuers are demonstrated in Figures 3 and 4.

While the open source brainnets library can be used in combination with any neuroimaging software, we here demonstrate its usage and efficacy in combination with BrainVoyager (Brain Innovation, Maastricht) [17] by using it as a plugin with a developed graphical user interface (GUI). The plugin provides a graphical, intuitive way to load and plan a graph theoretical study on a subject. As already shortly discussed, graph features can unveil important information and insights about a brain organization. The planning of a study is as easy as loading the data and configuring the pipeline (i.e., choosing a connectivity estimator, graph thresholding, etc.). Subsequently, the options for interactive visualization (standard block matrix or circular plot) and graph analysis become available. The implemented graph features (both global and nodal) are accessible under their associated tab alongside with descriptions

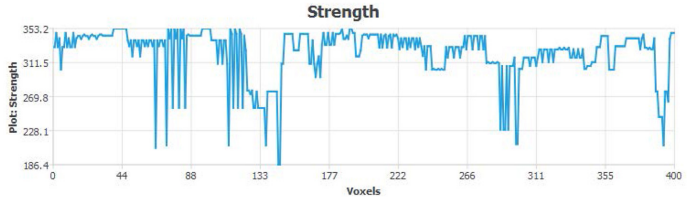

FIGURE 3: The strength of each node (voxel) of the left V5, on the full weighted matrix.

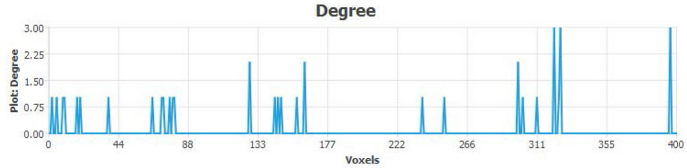

FIGURE 4: The degree of each node (voxel) of the left V5 connectivity matrix, filtered with the Minimum Spanning Tree.

and more visualization options (Figures 1 and 2). However, it is often required to draw comparisons between the connectivity profiles between subjects. Our proposed toolbox provides methods to perform a group analysis, using the corresponding options.

Brainnets is built on top of other well-established, mature, and community-driven scientific projects, namely Eigen C++ and Boost. The source code is available at https://github.com/makism/brainnets under the very liberal license MIT.

AQ2

REFERENCES

[1] M. Rubinov and O. Sporns. Complex network measures of brain connectivity: uses and interpretations. *Neuroimage*, 52(3), 1059-1069, 2010.

[2] F. D. V. Fallani, J. Richiardi, M. Chavez, and S. Achard. Graph analysis of functional brain networks: practical issues in translational neuroscience. *Phil. Trans. R. Soc. B,* 369(1653), 20130521, 2014.

[3] O. Sporns. The non-random brain: efficiency, economy, and complex dynamics. *Frontiers in computational neuroscience*, 5, 5, 2011.

[4] D. J. Watts and S. H. Strogatz. Collective dynamics of 'small-world'networks. nature, 393(6684), 440, 1998.

[5] D. S. Bassett and E. D. Bullmore. Small-world brain networks. *The neuroscientist*, 12(6), 512-523, 2006.

[6] B. Biswal, F. Zerrin Yetkin, V. M. Haughton and J. S. Hyde. Functional connectivity in the motor cortex of resting human brain using echo-planar MRI. *Magnetic resonance in medicine*, 34(4), 537-541, 1995.

[7] E. W. Lang, A. M. Tomé, I. R. Keck, J. M. Górriz-Sáez, and C. G. Puntonet. Brain connectivity analysis: a short survey. *Computational intelligence and neuroscience* 8, 2012.

[8] J. Wang, X. Zuo and Y. He. Graph-based network analysis of resting-state functional MRI. *Frontiers in systems neuroscience*, 4, 16, 2010.

[9] E. J. Sanz-Arigita, M. M. Schoonheim, J. S. Damoiseaux, S. A. Rombouts, E. Maris, F. Barkhof and C. J. Stam. Loss of 'small-world' networks in Alzheimer's disease: graph analysis of FMRI resting-state functional connectivity. *PloS one*, 5(11), e13788, 2010.

[10] M. John, T. Ikuta and J. Ferbinteanu. Graph analysis of structural brain networks in Alzheimer's disease: beyond small world properties. *Brain Structure and Function*, 222(2), 923-942, 2017.

[11] M. P. v.d. Heuvel, R. C. Mandl, C. J. Stam, R. S. Kahn and H. E. H. Pol. Aberrant frontal and temporal complex network structure in schizophrenia: a graph theoretical analysis. *Journal of Neuroscience*, 30(47), 15915-15926, 2010.

[12] U. Braun, M. M. Plichta, C. Esslinger, C. Sauer, L. Haddad, O. Grimm, H. Walter. Test–retest reliability of resting-state connectivity network characteristics using fMRI and graph theoretical measures. *Neuroimage*, 59(2), 1404-1412, 2012.

[13] T. Welton, D. A. Kent, D. P. Auer and R. A. Dineen. Reproducibility of graph-theoretic brain network metrics: a systematic review. *Brain connectivity*, 5(4), 193-202, 2015

[14] R. C. Wilson and P. Zhu. A study of graph spectra for comparing graphs and trees. *Pattern Recognition*, 41(9), 2833-2841, 2008.

[15] D. Jakobson and I. Rivin. Extremal metrics on graphs I. arXiv preprint math/0001169, 2000.

[16] B. Pincombe. Detecting changes in time series of network graphs using minimum mean squared error and cumulative summation. *ANZIAM Journal*, 48, 450-473, 2007.

[17] R. Goebel, F. Esposito and E. Formisano. Analysis of functional image analysis contest (FIAC) data with BrainVoyager QX: From single-subject to cortically aligned group general linear model analysis and self-organizing group independent component analysis. *Human brain mapping*, 27(5), 392-401, 2006.

Postdictive properties of apparent motion perception: An EEG study

AQ1

Daria Kleeva*

Saint Petersburg State University, 7/9 Universitetskaya Emb., Saint Petersburg, Russia
**dkleeva@gmail.com*

INTRODUCTION/MOTIVATION

This research was focused on postdictive properties of apparent motion - an illusion of movement as a result of successive presentation of two dots. Obviously, the mechanisms of integration of two dot's representations can take place only after the second dot is presented. There are two alternatives of what exactly happens. Firstly, a person can become aware of the first dot, the second dot and then reconstruct his or her memories of what he or she just saw. Secondly, the person can become aware of the first dot, and before awareness of the second dot unconscious integration can occur, so that the person becomes aware of the sum "sense of motion+second dot" [1, 2]. In order to differentiate between two models presented above several experimental hypotheses were tested. These hypotheses can be summarized as the following: there are significant differences between the primary components of event-related potentials (ERPs) in response to perception of the second dot in conditions of different illusory strength. It should be noted that the predictive properties of visual cortex are not elaborated within this research as far as the previous studies has shown that predictive coding is not crucial for apparent motion perception per se (but for some of its phenomenological characteristics) [3, 4].

METHODS

15 participants took part in experiment. Three types of stimuli were presented: apparent motion (4 levels from weak motion to strong motion), real motion, flicker (no apparent motion). The modulation of stimulus type was reached by the change of the interstimulus interval. The duration of one dot's presentation was constant and was equal to 150 ms. The presentation of stimuli was randomized. EEG was recorded from 14 channels. ERPs were calculated and wavelet analysis performed.

RESULTS AND DISCUSSION

Repeated Measures ANOVA revealed the next significant results. The amplitude of P100 at the site O1 in the condition of the 2nd level illusion (M = 3.82, SD = 2.53) was significantly higher than the amplitude of the same component in the condition of the 3rd level illusion (M = 1.76, SD = 1.82), $p < .01$, 4th level illusion (M = 1.48, SD = 1.5), $p < 0.001$, and flicker (M = 1.55, SD = 2.01), $p < 0.05$. Thus, the amplitude of P100 in response to perception of strong apparent motion was higher than in response to perception of weaker apparent motion and flicker. The power of alpha rhythm until 250 ms after second dot's onset at the site O1 in the condition of flicker (M = .49, SD = .59) was significantly higher than in the conditions of 1st level illusion (M = .043, SD = .36), $p < .05$, 2nd level illusion (M = -. 16, SD = .41), $p < .01$, 3rd level illusion (M = -. 26, SD = .16), $p < .01$, and 4th level illusion (M = -. 027, SD = .24), $p < .05$ [Fig. 1]. Analogous results were presented at right hemisphere (the site O2). EEG-activity

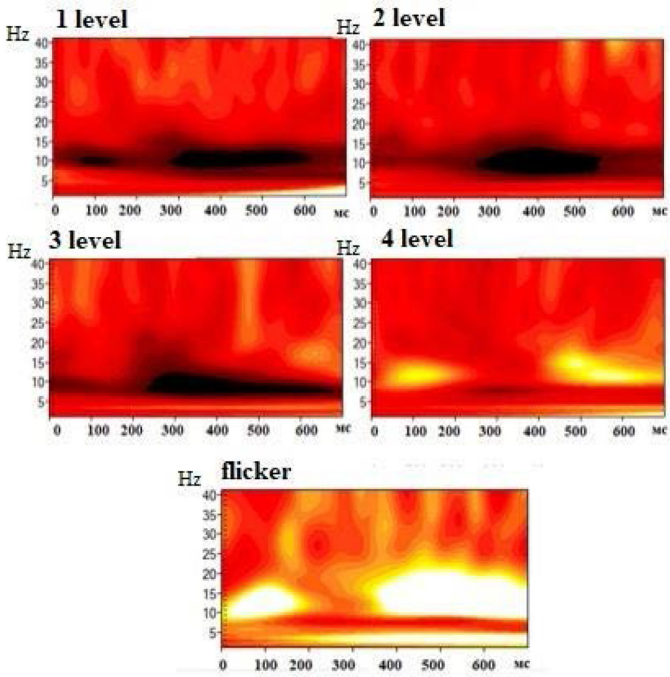

FIGURE 1: Time-frequency dynamics related to different types of stimuli.

occuring in the time window from 0 to 300 ms after the stimulus onset is considered to be related to visual awareness [5]. This means that the differences of activity between different conditions of apparent motion perception can point out that these differences are determined by unconsious integration that happened before awareness. Thus, the results of this research support the second model presented in the introduction. The detected differences in the power of alpha rhythm indicate that the integration of the percept can occur due to rhythm's suppression, given its inhibitory role. To sum up, this research demonstrates that visual perception itself is a recurrent proccess.

AQ2

REFERENCES

[1] D. Dennett. Consciousness explained. Little Brown. 2017.

[2] M. H. Herzog, T. Kammer, F. Scharnowski. Time slices: what is the duration of a percept? PLoS biology, 14(4), 2016.

[3] G. Edwards, P. Vetter, F. McGruer, L. S. Petro, L. Muckli. Predictive feedback to V1 dynamically updates with sensory input. Scientific reports, 7(1), 2017.

[4] R. Sekuler. Motion perception: A modern view of Wertheimer's 1912 monograph. Perception, 10(25), 1996.

[5] M. Koivisto, A. Revonsuo. Event-related brain potential correlates of visual awareness. Neuroscience&Biobehavioral Reviews, 34(6): 922-934, 2010.

Self-organization of event-based visual data for stereoscopy

AQ1

Lea Steffen[1], Jing Peng[1], Stefan Ulbrich[1], Daniel Reichard[1]*, Arne Roennau[1]*, Rüdiger Dillmann[1,2]*

[1]FZI Research Center for Information Technology, Karlsruhe, Germany. steffen, jpeng, sulbrich
[2]Karlsruhe Institute of Technology (KIT), Germany
**daniel.reichard, roennau@fzi.de; *ruediger.dillmann@kit.edu*

MOTIVATION

In order to obtain depth information from 2D-images, multiple views provide a reliable method for stereo reconstruction. In nature, disparity is computed energy efficiently, accurately and robustly. Machine stereo vision, even though it has been an active research topic for decades, is still struggling to compete with biological systems at all three points. Solving the correspondence problem, hence finding matching points of two 2d-images of the same scene from different viewpoints, causes the computing complexity. Silicon retinas, also known as event-based sensors, exploit the potential of human vision. Their high data transfer rate, low latency and low redundancies open up new possibilities for biologically inspired stereoscopy [1], [2]. Event-based sensors are a very biological way to obtain visual information. In that manner, the data processing shall be inspired by nature as well and thus be done by networks of neurons.

METHODS

The data acquisition is realised by two event-based sensors recording the same scene out of slightly shifted perspectives. Many approaches for obtaining depth information from event-based 2D-data, like [3], are based on cooperative algorithms [4]. Here we present a very different alternative. The stereo correspondence problem can be seen as a dimensionality reduction. An efficient way to reduce high dimensional data by use of artificial neural networks (ANN) is given by self-organizing maps (SOM) [5]. The data of two 2D-images, hence 4D-data, is reduced to an underlying latent 3D representation that corresponds with the real-world spatial coordinates. Thus, stereoscopic perception is achieved by a SOM creating a topological representation of event-based 2D-data. In our approach, divergent from the common use, the neural

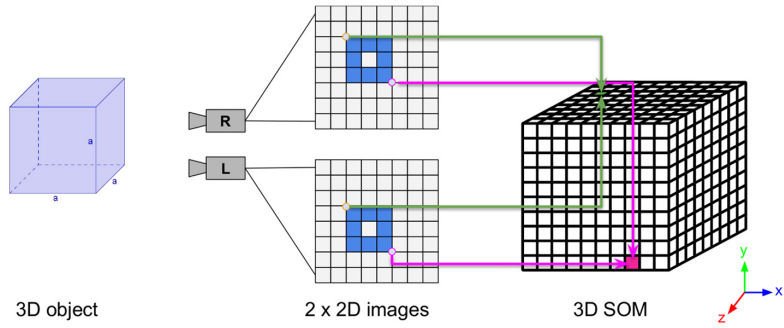

FIGURE 1: Overview of the system architecture. A 3D cube is perceived as slightly shifted 2D squares by two sensors. The 3D SOM maps the resulting 4D data to a 3D representation. In the lower right part it is visualized which axis is represented by which of the RGB-colors.

grid of the SOM is 3D, in order to cover the real-world space. The object's representation in 4D is formalized as the following mapping:

$$f : x \rightarrow [x_L, x_R], \quad x \in R^3 \text{ and } x_L, x_R \in R^2$$

This object represented in 4D is used as the input of the SOM projecting the 3D-object, represented in R^4, into R^3. An overview about the workflow is given in Fig. 1.

RESULTS AND DISCUSSION

At this point, we only tested the implementation with artificial data by picking random samples from a cube. Since the visualization of a SOM with more than two dimensions is not trivial, we applied a method introduced in [6]. First results exposing the progress of the SOM during 1000 iterations are shown in Fig. 2. The authors use a color code to illustrate the neighboring relations. Therefore, each primary color of the RGB color scheme is assigned to one dimension of the 3D-SOM. As shown at the bottom of Fig. 1, the x-axis is blue, the y-axis green and the z-axis red. These colors are then utilized to depict the topology of the SOM. The graphics a, b, c and d all display the output space for both input images. Dots of the left and right part with the same coloration, are corresponding to each other and hence matches. As a next step, we want to use simulated event-based data, provided by the

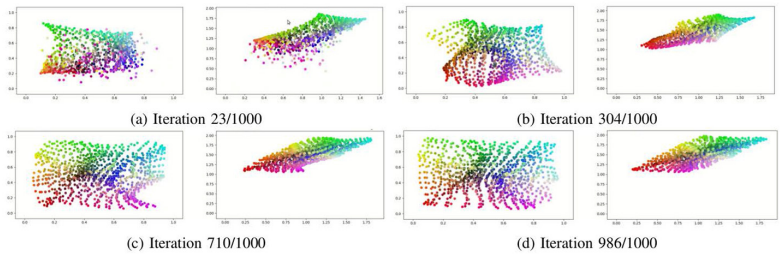

FIGURE 2: For visualization an RGB-cube is used as the 3D-SOM output space. Therefore, every point in the output space is color coded according to its position on the three axis. In a, b, c and d is always the coloration for the left and the right image shown. Identically colored dots from each image are potential matches.

DAVIS simulator [7], as input. Subsequently, we want to test our implementation with the stereo head introduced in [3].

ACKNOWLEDGEMENT

The research leading to these results has received funding from the Baden-Württemberg Stiftung under the research program Neurorobotik as well as the European Union's Horizon 2020 Framework Programme for Research and Innovation under the Specific Grant Agreement No. 785907 (Human Brain Project SGA2).

Keywords: stereoscopy, event-based perception, self-organisation, topological representation

REFERENCES

[1] P. Lichtsteiner, C. Posch, and T. Delbrück, "A 128 x 128 120 db 15 us latency asynchronous temporal contrast vision sensor," IEEE Journal of Solid-State Circuits, vol. 43, no. 2, p. 566576, 2008.

[2] C. Posch, T. Serrano-Gotarredona, B. Linares-Barranco, and T. Delbrück, "Retinomorphic event-based vision sensors: Bioinspired cameras with spiking output," Proceedings of the IEEE, vol. 102, no. 10, pp. 1470–1484, Oct 2014.

[3] J. Kaiser, J. Weinland, P. Keller, L. Steffen, C. Vasquez Tieck, D. Reichard, A. Roennau, J. Conradt, and R. Dillmann, "Microsaccades for neuromorphic stereo vision," 27th International Conference on Artificial Neural Networks, 2018.

[4] D. Marr and T. Poggio, "Cooperative computation of stereo disparity," Science, vol. 194, pp. 283–287, 1976.

[5] T. Kohonen, "Self-organized formation of topologically correct feature maps." Biological Cybernetics, vol. 43, pp. 59–69, 1982.

[6] J. Gorricha and V. Lobo, "On the use of three-dimensional self-organizing maps for visualizing clusters in georeferenced data," Information Fusion and Geographic Information Systems, pp. 61–75, 05 2011.

[7] E. Mueggler, H. Rebecq, G. Gallego, T. Delbruck, and D. Scaramuzza, "The event-camera dataset and simulator: Event-based data for pose estimation, visual odometry, and slam," The International Journal of Robotics Research, vol. 36, no. 2, pp. 142–149, 2017.

Enriching the human connectome: Digitizing the von Economo & Koskinas human cytoarchitectonic atlas

AQ1

Anastasia Brovkin[1]*, René Werner[1], Julia Michel[1], Sarah F. Beul[1], Alexandros Goulas[1]*, Claus C. Hilgetag [1,2]

[1]Department of Computational Neuroscience, University Medical Center Hamburg-Eppendorf, Germany

[2]Department of Health Sciences, Boston University, Commonwealth Avenue, Boston, USA

**a.brovkin@uke.de*

INTRODUCTION

Fundamental relations between architecture, connectivity and function of the cerebral cortex still remain elusive. This is partly due to a lack of detailed, quantitative cytoarchitectonic data for the human brain. Currently, the only comprehensive source of such information is the classic work of von Economo and Koskinas (vEK), which, however, is only available in a paper-based 2D atlas in non-standard space. Our project is aimed at constructing a virtual 3D model of the von Economo and Koskinas atlas in stereotactic space. Recent efforts manually mapped the von Economo and Koskinas parcellation onto the FreeSurfer Desikan-Killiany atlas based on the textual description and 2D drawings.

METHODS

To overcome related problems, we aimed at explicitly defining a virtual 3D von Economo and Koskinas model independent of existing reference geometries – which became possible using 2 different 3D plaster models of the cortical parcellation of manufactured in the era of von Economo. We will present our solution to the 3D reconstruction of the vEK atlas and provide an update of the current efforts in integrating the extracted information into the BigBrain atlas and by extensition, The Virtual Brain neuroinformatics platform – demonstrating the progress in a subtrask of (Co-Design Project) CDP8.

Exploring long range interactions in neural networks

AQ1 **Alejandro Tlaie[1], Inmaculada Leyva[2], Irene Sendiña-Nadal[1]**

AQ6 *[1]Rey Juan Carlos University, Madrid*

[2]Center for Biomedical Technology, Technical University of Madrid, Madrid

INTRODUCTION

Complex networks have attracted more and more interest during recent years. They have been used to describe a wide spectrum of physical processes (from gene manifestation [1] to power grid optimization [2]), human interactions (social networks [3], for example) or to describe the brain [4], among many other applications. Usually, there are two main ingredients when working with complex networks: the structural part -and the graph theory-based tools used to describe them- and the dynamical part -usually studied by means of statistics and non-linear dynamics. When studying the temporal dynamics of a network's nodes, the paradigm is to account for the interactions among closest-neighbours (meaning, only directly structurally connected nodes are able to interact).

A recent novel approach, proposed by Estrada et al [5] was to characterize the dynamics in complex networks taking into account more subtle interactions (they propose the term 'indirect peer pressure' when dealing with social networks, for example). This is not only revolutionary because of the technique they introduced but also due to the paradigm shift it would imply.

MATHEMATICAL MODEL

Following their insights, we have delved into the study of a well known single cell model, the Morris-Lecar neuron [6]:

$$C\dot{V}_i = \sum g_X . f(V_i - E_X) + I_{syn,i} + q\xi_i \quad (1)$$

$$\dot{W}_i = \phi \tau_W(V_i) . \left[W_\infty(V_i) - W_i \right] \quad (2)$$

where V_i is the main variable (it represents the membrane potential of the cell), the X subindex reflects that there are various ionic channels (Na, K) and a leaky term; W_i is the recovery variable and ξ_i is the noisy term (Gaussian white noise) that goes into each neuron's dynamics. The synaptic current is the way of incorporating these novel higher-order interactions:

$$I_{syn,i} = \frac{\sigma}{K}\left[\sum_{D=1}^{2} D^{-\alpha}\left(\sum_{d(i,j)=D} e^{-2(t-t_j)}(V_0 - V_i)\right)\right] \quad (3)$$

given by the superposition of all the post-synaptic potentials emitted by the neighbours of node i in the past, being t_j the time of the last spike of node j. The synaptic conductance σ, normalized by the largest node degree present in the network K, plays the role of coupling intensity. For nodes at topological distance $D > 1$, the coupling is modulated by the suppression constant α (this is the way in which we incorporate the astrocytes in the neuronal network's activity). When the summation is limited to the first order term $D = 1$, only the usual nearest-neighbour coupling is being considered. We already studied this case in Ref. [9], whose results are going to be used for comparison. In that work we careful characterized the conditions for the apparition in the network of synchronization waves, by measuring its global synchronization (S) and comparing it to the local one (S_ρ): the discrepancy between these two gives us an idea of the "waveness" of the network's activity.

RESULTS

The first promising result in this line of research is that we can still preserve the travelling wave phenomenon that Leyva et al. [9] evidenced [fig 1]; this is interesting because it shows that, if anything, we have generalized the results reported in [9]. Furthermore, we see that there appears a new phenomenon that did not manifest for $D = 1$: there is an optimal value of σ for each curve (in a sense, that value of the coupling strength implies that the wave-like behavior is the strongest it can be for a given topology). Moreover, we report [fig 2] another appealing phenomenon: we can produce broader wavefronts of information transmission when allowing higher-order interactions than when we use the classical approach. A potential and suggestive explanation for this is that astrocytes make the neuronal signal more synchronous for lower coupling strength values (i.e., neurons can communicate through different channels than the axonal ones).

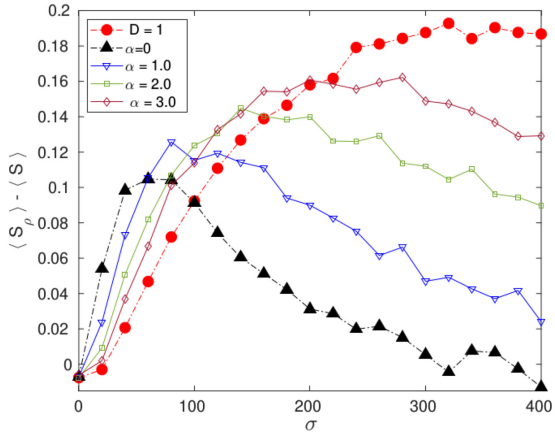

FIGURE 1: Synchronization discrepancy for different coupling strengths. Each curve is the result of averaging ten different realizations of a spatial network of 150 nodes. We see that a greater synchronizations is achieved before in the case that we let higher-order interactions take place.

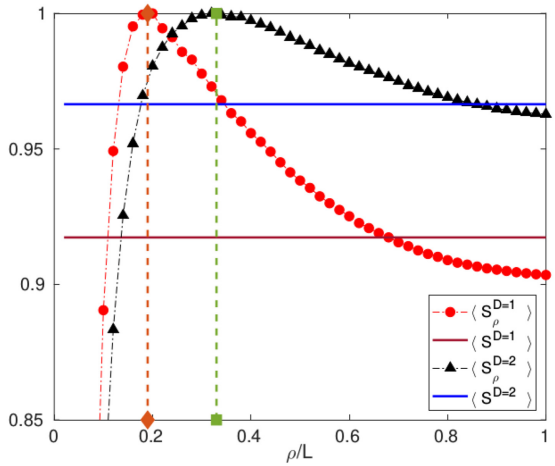

FIGURE 2: Synchronization values for different sizes of the local. This is the result of averaging five different realizations of a Scale-Free network of 150 nodes with < k >= 4. We see that a greater synchronizations is achieved before in the case that we let higher-order interactions take place.

CONCLUSIONS

This work is a pioneering one because it is a potential solution to the irreconcilable problem of not modelling the role of glial cells (in particular, astrocytes) in neuronal activity. As different physiological measures have shown [8], these cells not only serve as glue and maintenance cells for neurons but they also participate in the modulation and release of neurontransmitters. We believe it is of capital importance to start exploring the field of incorporating astrocytes into the theoretical efforts throughout different scales (from synapses to cortical columns). Therefore, we have started this path towards the attainment of a mesoscale model of neuron-astrocyte network interactions.

AQ2

REFERENCES

[1] Lopes FM, Cesar RM and Costa Lda F., Gene expression complex networks: synthesis, identification, and analysis, J. Comp. Biol., Oct 10 10, 1353-67 (2011).

[2] S. Arianos, E. Bompard, A. Carbone and F. Xue, Power grid vulnerability: A complex network approach, Chaos, Feb 19, 013119 (2009).

[3] Grandjean M., A social network analysis of Twitter: Mapping the digital humanities community, Cogent Arts and Humanities 3, (1) (2016).

[4] Sporns, O.: Structure and function of complex brain networks. Dialogues Clin Neurosci.; 15(3): 247262. (2013).

[5] Estrada E. and Silver G., Accounting for the role of long walks on networks via a new matrix function, J. Math. Analysis and App., Volume 449 Issue 2, 1581-1600 (2017).

[6] Morris C. and Lecar H., Voltage Oscillations in the barnacle giant muscle fiber, Biophys. J., 35 (1), 193-213 (1981).

[7] Tlaie A., Leyva I. and Sendiña-Nadal, Dynamical complexity as a proxy for the network degree distribution, To appear in Phys. Rev. E.

AQ3

[8] Perea, G., Navarrete, M., Araque, A., (2009) Tripartite synapses: astrocytes process and control synaptic information. Trends in Neurosciences (32), Issue 2, 421-431.

[9] Leyva, I., Navas, A., Sendia-Nadal, I., Buld, J. M., Almendral, J. A., Boccaletti, S. (2011): Synchronization waves in geometric networks. PRE (84) 065101.

The attention difficulties in adults with history of institutionalization: An ERP study

AQ1 **Iuliia An*, Olga Titova*, Maxim Petrov**

[1]*Saint Petersburg State University, 6 Makarova Emb., Saint Petersburg, Russia*
**iuliia.o.an@gmail.com; *olga.tiitova@gmail.com*

INTRODUCTION

If not properly remediated children brought up in institutional care setting demonstrate atypical brain functioning (Marshall et al., 2008), general cognitive deficits (van Ijzendoorn et al, 2005) and are at risk of attention and behavior regulation difficulties (Loman et al., 2013). However, little is known about the neurophysiological markers of attention difficulties in this subpopulation. Moreover, there is currently a relative lack of research on the long-term effects of institutionalization on cognitive development. The current study is aimed to investigate deferred effects of institutionalization on behavioral performance and modulations of the P1, N1 and P3 event-related potentials (ERPs) associated with attentional networks in adults with a history of institutionalization.

METHODS

The study sample consisted of 30 young adults with at least 6 month experience of institutionalization (Institutional Care Group, 15 males, mean age = 21 yrs, SD = 3.9, min = 17, max = 32) and a group of 30 matched in age and level of education control adults raised by biological parents (Biological Family Group, 14 males, mean age = 21.5 yrs, SD = 4, min = 17, max = 31). All participants had a non-verbal IQ score above 80 and there was no significant difference in IQ between groups.

During EEG recording the participants performed the original Attention Network Test (Fan et al., 2002; fig. 1), developed to evaluate three attentional networks: alerting, orienting and executive control (Posner & Petersen, 1990). Efficiency of alerting and orienting in this paradigm are assessed by measuring how response times (RT) are influenced by alerting cues and spatial cues. The efficiency of the executive network is examined by changes in RT related to

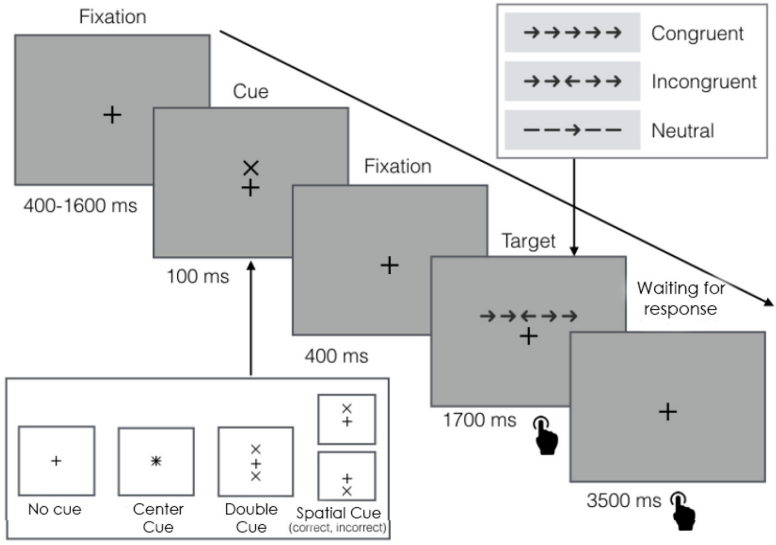

FIGURE 1: Scheme of the experiment.

congruent, incongruent and neutral flankers. The participants were asked to determine whether a central arrow points left or right.

RESULTS AND DISCUSSION

The following four conditions were analyzed: no cue congruent flankers (NC-C), no cue incongruent flankers (NC-I), central cue congruent flankers (CC-C), central cue incongruent flankers (CC-I). Response time analysis revealed significant effects of the Group ($F(1) = 99$, $p < .001$) and Condition ($F(3) = 21.5$, $p < .001$) factors. IC group responded slower (post-hoc Group x Condition test, $p < .005$) in all conditions. In the accuracy analysis significant results were also found for the Group ($F(1) = 14.3$, $p < .001$) and Condition ($F(3) = 33.3$, $p < .001$) factors. IC group was less accurate in the NC-I condition (post-hoc Group x Condition test, $p < .005$). We examined P1, N1 and P3 ERP components amplitude in midline central (M-C), midline parietal (M-P), right parietal (R-P) and left parietal (L-P) electrode clusters using general linear model. No significant differences between IC and BF groups were identified. Although postinstitutionalized adults demonstrate a lack of attentional

resources related to alerting and executive networks on behavioral level, we did not observe any group differences in the amplitudes of the attention-related ERPs so far. Our data collection is still in progress.

ACKNOWLEDGEMENTS

This research was supported by the Government of the Russian Federation (grant No 14.Z50.31.0027; PI: Elena L. Grigorenko).

AQ2

REFERENCES

[1] Fan, J., McCandliss, B. D., Sommer, T., Raz, A., & Posner, M. I. (2002). Testing the efficiency and independence of attentional networks. Journal of Cognitive Neuroscience, 14(3), 340-7.

[2] Loman, M. M., Johnson, A. E., Westerlund, A., Pollak, S. D., Nelson, C. A., & Gunnar, M. R. (2013). The effect of early deprivation on executive attention in middle childhood. Journal of Child Psychology and Psychiatry, 54(1), 37-45.

[3] Marshall, P. J., Reeb, B. C., Fox, N. A., Nelson, C. A., & Zeanah, C. H. (2008). Effects of early intervention on EEG power and coherence in previously institutionalized children in Romania. Development and psychopathology, 20(3), 861-880.

[4] Posner, M. I., & Petersen, S. E. (1990). The attention system of the human brain. Annual review of neuroscience, 13(1), 25-42.

[5] Van Ijzendoorn, M. H., Juffer, F., & Poelhuis, C. W. K. (2005). Adoption and cognitive development: a meta-analytic comparison of adopted and nonadopted children's IQ and school performance. Psychological bulletin, 131(2), 301.

Individual Brain Charting, a high-resolution fMRI dataset for cognitive mapping of the human brain

AQ1

Ana Luísa Pinho[1,2,3]*, Juan Jesus Torre[1,2,3]*, IBC team[2], Bertrand Thirion[1,2,3]*

[1]Parietal team, Inria-Saclay, 1 Rue Honoré d'Estienne d'Orves, Palaiseau, France
[2]NeuroSpin, CEA Saclay, Bâtiment 145, Gif-sur-Yvette, France
[3]ParisSaclay University
**ana.pinho@inria.fr; *juanjesus.torretresols@inria.fr; *bertrand.thirion@inria.fr*

INTRODUCTION/MOTIVATION

Mapping functional neuroanatomy of the human brain has become a central challenge in cognitive neuroscience and it constitutes an essential step toward linking brain systems and behavior. While there is a rich literature on the neural correlates underlying performance of standardized tasks, little is still known about the overall functional organization of the brain and how it can be translated into cognition. Neuroimaging techniques, such as Functional Magnetic Resonance Imaging (fMRI) have contributed to the investigation of brain regions involved in a variety of cognitive processes. However, to date, no data collection has systematically addressed the functional mapping of cognitive mechanisms within a broader scope. The Individual Brain Charting (IBC) project stands for a multi-task fMRI dataset, to be shared with the neuroimaging community, featuring an univocal encoding between task descriptors and brain imaging data. It is intended to support the investigation of the functional principles underlying the cognitive representation of the human brain, allowing for (e.g.) a detailed parcellation of the brain volume into functional-specialized regions. Additionally, the IBC project pertains to the development of a neurocognitive atlas based on the functional signatures of mutual cognitive components between task descriptors.

METHODS

The first release of the IBC dataset accounts for high-resolution (1.5mm) fMRI maps of human brain activations from a permanent cohort of thirteen individuals, during the performance of a dozen of tasks. The dataset is complemented by the task-stimuli protocols and the corresponding behavioral data extracted from each subject. Such tasks were, in their majority, replicated

from previous studies and they comprise a variety of psychological domains, addressing both perceptual and high-level cognitive functions, e.g. retinotopy, tonotopy, somatopy, calculation, language comprehension, social cognition and theory-of-mind [1, 2, 3]. The organization of both neuroimaging and behavioral datasets follows Brain Imaging Data Structure specification [4]. Contrasts from conditions within tasks were computed, in order to capture the effects-of-interest elicited by the responses. Volume-based functional signatures of these effects-of-interest were then obtained from classical inference of the contrasts. Variability of such functional signatures was also investigated across participants.

RESULTS AND DISCUSSION

Pinho et al. (2018) provides a complete description of the first release of the IBC dataset [5]. Raw data from this release is available in the OpenNeuro repository, under the data accession number ds000244, as well as in HBP Knowledge Graph Data Platform. Derived statistical maps can also be found in the NeuroVault public repository, with the id=2138. Figure 1 represents the total area of the brain significantly covered by all tasks featuring the present release. Despite the low statistical power at group level due to the limited sample size, results were overall replicated from the original studies. Figure 2 shows both the individual and group-level functional signatures obtained for a working-memory task [2], upon visualization of four different classes of pictures. It highlights also the variability of such functional signatures across participants. Although there's some consistency of the activation patterns when one considers the whole brain, size and precise location of homologous clusters are quite diverse between participants. These results thus provide clear evidence supporting not

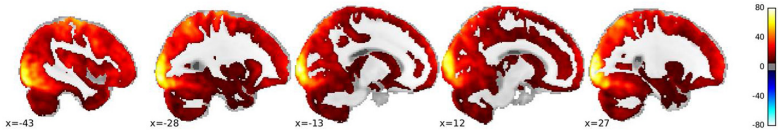

FIGURE 1: Group-level F-map, at a threshold of p<.05, Bonferroni-corrected, representing the total area of the brain significantly covered by all tasks featuring the first release of the IBC dataset (fixed-effects model across tasks and subjects). One can readily see that all the brain is covered, with higher values in sensory cortices and weaker values for the temporal and pre-frontal cortex, as well as subcortical structures.

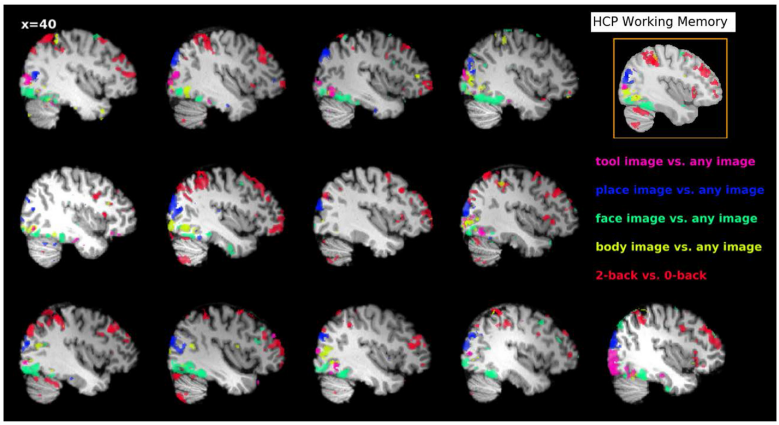

FIGURE 2: Activation maps of the contrasts estimated from the conditions in the HCP Working Memory task. Individual maps for fixed effects are displayed for every participant, using an FDR-corrected threshold q = 0.05. The corresponding group-level conjunction map is shown inside the orange frame. All maps correspond to the slice x=40 in the sagittal view.

only the individual mapping approach but also alternative methods to the classic univariate, task-specific, between-subject level analysis. Future outcomes will rely on mega-analytic encoding models towards the development of a brain-atlasing framework, by systematically mapping the functional networks associated with the cognitive components of the tasks.

AQ2

REFERENCES

[1] Pinel, P. et al. Fast reproducible identification and large-scale databasing of individual functional cognitive networks. BMC Neurosci 8, 91.

[2] Barch, D. M. et al. Function in the human connectome: Task-fMRI and individual differences in behavior. Neuroimage 80, 169-89.

[3] Humphries, C., Binder, J. R., Medler, D. A. & Liebenthal, E. Syntactic and semantic modulation of neural activity during auditory sentence comprehension. J Cogn Neurosci 18, 665-679.

[4] Gorgolewski, K. J. et al. The brain imaging data structure, a format for organizing and describing outputs of neuroimaging experiments. Sci. Data 3, 160044.

[5] Pinho, A. L., Amadon, A., Ruest, T., Fabre, M., Dohmatob, E., Denghien, I., Ginisty, C., Desmidt, S., Becuwe, S., Laurier, L., Doublé, C., Martins, B., Pinel, P., Eger, E., Varoquaux, G., Pallier, C., Dehaene, S., Hertz-Pannier, L., & Thirion, B. (2018). Individual Brain Charting, a high-resolution fMRI dataset for cognitive mapping. Sci. Data 5, 180105.

Using Bayesian Networks for differential analysis of gene regulatory networks

AQ1

Nikolas Bernaola*, Concha Bielza, Pedro Larrañaga

Departamento de Inteligencia Artificial, Computational Intelligence Group, Universidad Politecnica de Madrid, Spain

**n.bernaola@alumnos.upm.es*

INTRODUCTION/MOTIVATION

Differential functional analysis of genetic expression aims to identify which genes are responsible for functional differences when in different conditions. The usual methods to carry out these analysis work by doing uni-variant statistical tests which allow us to identify which genes have different expression levels between the control and experimental conditions [1]. These helps with identifying which genes might be responsible for the functional differences but it gives a very limited picture about the interactions between genes and how they are affected. Gene regulatory networks [1] (from now GRNs) allow us to study the relationships between genes and to identify candidates for transcriptional regulation by using metrics like the correlation or mutual information between the expression levels of different genes. Using Bayesian Networks (BNs) instead of Correlation or Mutual Information Networks allows us to expand on these models by ensuring that statistically independent genes are separated in the network and by being able to use well known methods of probabilistic inference to study the effects of different gene expression levels in the rest of the network[1][2]. In this work we train BN GRNs with microarray data from the Allen Brain Institute's Human Brain Atlas [3] to get GRNs from different areas of the brain. The aim is to improve on current tools like the JuGEx atlas [4] and on previous analysis using Allen Institute data like [5] by giving researchers the ability to do differential functional analysis on groups of genes instead of the usual uni-variant tests.

METHODS

Using the microarray data from the Allen Human Brain Atlas, we have been able to train Gaussian Bayesian Networks of up to a few hundred nodes using the Chow Liu algorithm implemented in the bnlearn package for the

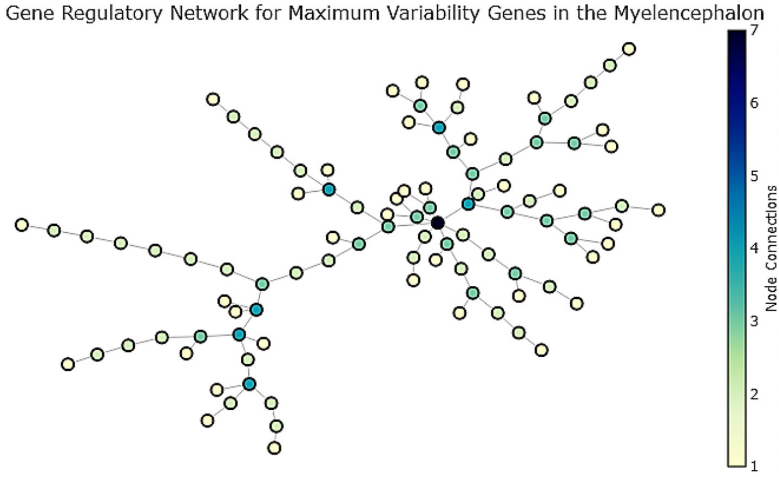

FIGURE 1: Bayesian Network model of a Gene Regulatory Network for the hundred genes in the myelencephalon with the most variable expression level.

R programming language [5], which we then visualize using pygraphviz and plotly [6] in Python (see figure 1). We are currently implementing a better learning algorithm in C++ and Python to improve performance and size of the model based on Edwards' work. [2]

CURRENT RESULTS AND FUTURE WORK

We currently have a working prototype of the tool using a simple structure learning algorithm for the Bayesian Networks. In the following months we expect to create an improved learning algorithm and increased computing time to build a full model incorporating up to the 20000 genes in the Allen Human Brain Atlas dataset. We will also validate the model with known genetic regulation modules introduce a tool to allow users to explore small regions of interest in the model and do inference on them, exploring the effect of the expression of one gene on the rest of the network. We expect to add the tool we develop to the HBP joint platform as part of our work in SP5.

AQ2

REFERENCES

[1] Larrañaga, Pedro, Iñaki Inza, and Jose L. Flores. "A Guide to the Literature on Inferring Genetic Networks by Probabilistic Graphical Models." In Data Analysis and Visualization in Genomics and Proteomics, 215–38. Wiley-Blackwell, 2005. https://doi.org/10.1002/0470094419.ch13.

[2] Edwards, David, Gabriel CG de Abreu, and Rodrigo Labouriau. "Selecting High-Dimensional Mixed Graphical Models Using Minimal AIC or BIC Forests." BMC Bioinformatics 11, no. 1 (2010): 18. https://doi.org/10.1186/1471-2105-11-18.

[3] Sunkin, Susan M et al. "Allen Brain Atlas: an integrated spatio-temporal portal for exploring the central nervous system" Nucleic acids research vol. 41, Database issue (2012): D996-D1008.

[4] Bludau, Sebastian et al. "Integration of transcriptomic and cytoarchitectonic data implicates a role for MAOA and TAC1 in the limbic-cortical network" Brain structure & function vol. 223,5 (2018): 2335-2342.

[5] Chen, Lei, Chen Chu, Yu-Hang Zhang, Changming Zhu, Xiangyin Kong, Tao Huang, and Yu-Dong Cai. "Analysis of Gene Expression Profiles in the Human Brain Stem, Cerebellum and Cerebral Cortex." PLOS ONE 11, no. 7 (July 19, 2016): e0159395. https://doi.org/10.1371/journal.pone.0159395.

[6] Marco Scutari. Learning Bayesian Networks with the bnlearn R Package. Journal of Statistical Software, 35(3), 1-22. (2010) URL http://www.jstatsoft.org/v35/i03/.

AQ3

[7] Plotly Technologies Inc. Collaborative data science. Montréal, QC, 2015. https://plot.ly.

A Brainet of pigeons

Lifang Yang[1,3], Mengmeng Li[1,3]*, Kun Zhao[2]*, Hong Wan[1,2,3]*, Zhigang Shang[1,2,3]*

[1]Industrial Technology Research Institute, Zhengzhou University, Zhengzhou, China
[2]School of Electrical Engineering, Zhengzhou University, Zhengzhou, China
[3]Henan Key Laboratory of Brain Science and Brain-Computer Interface Technology, Zhengzhou, China.
{flyer1014, limengmeng1014}@163.com; zhaokun2046@126.com; {wanhong, zhigang_shang}@zzu.edu.cn

AQ1

INTRODUCTION/MOTIVATION

Ramakrishnan *et al.* proposed a new concept of "Brainet" composed of multiple brains in 2015 [1]. Three monkeys coordinately control a robot arm in their experiment. Paisvieira *et al.* combined the concepts of brain-to-brain interface (BtBI) [2] and "Brainet". A "Brainets" was constructed by interconnecting the brains of four rats to realize real-time information collaboration and interaction [3]. In 2018, Jiang *et al.* successfully established a multi-person BtBI cooperation system. A human "Brainet" was constructed to complete a game collaboratively [4]. These studies show that mammals can synchronize their neural signals and construct a "Brainet". Whether this is universal in nature and whether multiple birds can construct a "Brainet" is unclear. Therefore, we choose pigeon as model animal and design expriment to construct a synchronous "Brainet".

METHODS

Based on the plasticity and neural feedback mechanism [5] of the neural system, reinforcement learning based paradigms are designed to train multiple pigeons synchronize their signals and construct a "Brainet". The paradigms of the two-stage experiment are shown in Figure 1 (a) and (b). In the first stage, three LEDs are illuminated simultaneously. Three pigeons are trained to peck the key during the lighting period and adjust their neural response to be synchronized. In the second stage, the pigeons need not peck the key after visual stimuli. Instead, they get food rewards by synchronizing their neural signals. Behavior synchronization transfer to neural signal synchronization in this two-stage experiment finally. Implantable neural signals in the Nidopallium

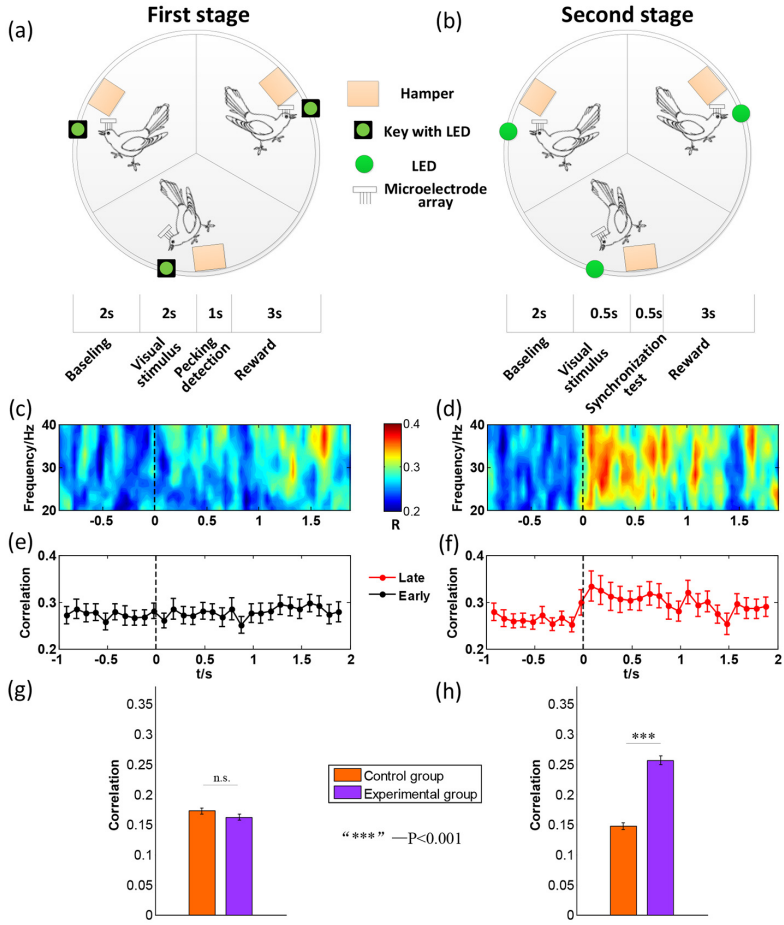

FIGURE 1: Paradigms and dynamic correlation changes of the rwo-stage synchronous learning experiment. (**a**) and (**b**) for paradigms. (**c**), (**d**), (**e**) and (**f**) for dynamic correlation changes. (**g**) and (**h**) for LFPs correlation statistical results.

Caudolaterale (NCL) of three pigeons are acquired and preprocessed. The local filed potential (LFP) signals belonging to specific response time and frequency band related to the synchronization task are obtained. Pearson correlation coefficient between signals is used to measure the synchronization degree of pigeons and the learning process of synchronization is analyzed.

RESULTS AND DISCUSSION

The early period data of the first stage and late period data of the second stage are analyzed, the corresponding dynamic correlation changes are shown in Figure 1 (c), (d), (e) and (f). Results show that the pigeons can synchronize their signals under coordinated task. The LFPs correlation statistical results among three pigeons learnt to synchronize their signals (experimental group) and other untrained ones (control group) during the two stages are shown in Figure 1 (g) and (h). The LFPs correlation among three pigeons of experimental group during early period of the first stage have no significant difference with that of control group, whereas during late period of the second stage, the correlation of experimental group is significantly higher than that of control group. It indicates that the well-trained pigeons can successfully construct a synchronous "Brainets".

Brainet can realize intercommunication among multiple brains, break new ground of communication and cooperation, and help us understand the operation of the brain deeply. This study focuses on NCL of the pigeon, which is a comprehensive brain region integrating perceptual information and decision-making output. Is there a similar phenomenon in other regions, such as the hippocampus, and the neural activity changes of the individual pigeon in Brainet remain to be further analyzed and explored.

AQ2

REFERENCES

[1] Ramakrishnan A, Ifft P J, Paisvieira M, et al. Computing Arm Movements with a Monkey Brainet. *Scientific Reports*, 5: 10767, 2015.

[2] Paisvieira M, Lebedev M, Kunicki C, et al. A Brain-to-Brain Interface for Real-Time Sharing of Sensorimotor Information. *Scientific Reports*, 3:1319, 2013.

[3] Paisvieira M, Chiuffa G, Lebedev M, et al. Corrigendum: Building an organic computing device with multiple interconnected brains. *Scientific Reports*, 5:14937, 2015.

[4] Jiang L, Stocco A, Losey D M, et al. BrainNet: A Multi-Person Brain-to-Brain Interface for Direct Collaboration Between Brains. *arXiv:1809.08632*, 2018.

[5] Mcwhinney S R, Tremblay A, Boe S G, et al. The impact of goal-oriented task design on neurofeedback learning for brain-computer interface control. *Medical & Biological Engineering & Computing*, 56(2):201-210, 2018.

A novel experimental design for investigating dialogue features in the context of cognitive decline

AQ1

Sofia de la Fuente[1]*, Craig Ritchie[2], Saturnino Luz[1]

[1]Edinburgh Medical School: Usher Institute of Population Health Sciences and Informatics. The University of Edinburgh
[2]Centre for Dementia Prevention, The University of Edinburgh
**sofia.delafuente@ed.ac.uk*

INTRODUCTION

Decreasing the incidence of Alzheimer's Disease (AD) is a global public health priority for which the characterisation of early stages of the disease has become paramount, being regarded as a requisite for the implementation of prevention strategies [1]. Accordingly, dementia researchers worldwide are exploring different methods to detect signs of early stages of AD, since it is plausible that preclinical patients may exhibit subtle behavioural neurodegeneration, yet neuropsychological tests do not seem appropriate to detect them. Our research focuses on linguistic and paralinguistic interactions, as recent studies indicate that spontaneous speech data, which can be collected frequently and naturally, provide good predictors for AD detection in cohorts with a clinical diagnosis [2,3]. However, the potential of models based on such data for detecting preclinical AD remains unknown, and there is a growing interest in the analysis of spontaneous dialogues [4], as opposed to narrative speech data. Hence, we have developed an experimental design to collect and process conversational data, and obtain a range of features, yet to be specified, that not only are likely to be relevant for AD modelling, but also do not rely upon the content, or the language, of what is said.

METHODS: TASK PROCEDURE, PARTICIPANTS AND ANALYSIS

The Map-Task we developed consists of two tasks and three different maps. The first is the "Wayfinding task", which requires two maps: one of which has landmarks as well as routes and is given to the participant, the other one has only landmarks and is given to the researcher. They navigate cooperatively through an imaginary land thanks to the directions given by the participant.

About 15 minutes of speech data are recorded through this "give and take", conforming the core data our spoken dialogue study. The third map contains neither landmarks nor routes and is given to the participant afterwards, in order to complete a "landmark allocation" task. This assesses allocentric allocation, which is known to be impaired in AD earlier than other aspects of spatial navigation [5].

Our Map-Task has been carefully designed to meet research and ethic criteria for the PREVENT-ED study (ED: Elicitation of Dialogues), which builds on a larger project (PREVENT [6]) to investigate whether early behavioural signs of AD may be detected in dialogue interaction. Participants aged 40-59 at baseline are currently undertaking this task, generating a corpus of spoken dialogue and data on visuospatial abilities. We use speech processing, natural language processing and machine learning methods to assess how well speech and visuospatial markers agree with neuropsychological, biomarker, clinical, lifestyle and genetic data from the PREVENT cohort.

RESULTS AND CONCLUSIONS

The study is currently in a data collection phase (to be finished in February 2019) with promising feedback and successful interactions. The purpose of this communication is giving dissemination to the map-task, which is a new method for cognitive assessment, originally developed by our research group.

ACKNOWLEDGMENTS

Our research is supported by the UK Medical Research Council.

AQ2

REFERENCES

[1] W. H. Organization et al., "First who ministerial conference on global action against dementia: meeting report, who headquarters, Geneva, Switzerland, 16-17 March 2015," 2015.

[2] C. Thomas, V. Keselj, N. Cercone, K. Rockwood, and E. Asp, "Automatic detection and rating of dementia of Alzheimer type through lexical analysis of spontaneous speech," IEEE International Conference Mechatronics and Automation, 2005, vol. 3, no. February, pp. 1569–1574, 2005.

[3] K. C. Fraser, J. A. Meltzer, and F. Rudzicz, "Linguistic features identify Alzheimer's disease in narrative speech," Journal of Alzheimer's Disease, vol. 49, no. 2, pp. 407–422, 2015.

[4] Mirheidari B, Blackburn D, Reuber M, et al. Diagnosing people with dementia using automatic conversation analysis. In: Proceedings of Interspeech. San Francisco: 2016.1220–4.

[5] Allison SL, Fagan AM, Morris JC, et al. Spatial navigation in preclinical Alzheimer's disease. J Alzheimer's Dis 2016;52:77–90. doi:10.3233/JAD-150855.Spatial.

[6] Ritchie CW, Ritchie K. The PREVENT study: a prospective cohort study to identify mid-life biomarkers of late-onset Alzheimer's disease. BMJ Open 2012;2:1–6. doi:10.1136/bmjopen-2012-001893.

Altered modularity and disproportional integration in functional networks are markers of abnormal brain organization in schizophrenia

AQ1

Cinelli, M.[1]*, Echegoyen, I.[2,3], Oliveira, M.[4], Orellana, S.[5], Gili, T.[6]*

[1]University of Rome "Tor Vergata", Rome, Italy
[2]Centre for Biomedical Technology, Technical University of Madrid, Madrid, Spain
[3]Rey Juan Carlos University, Madrid, Spain
[4]GESIS -- Leibniz Institute for the Social Sciences, Cologne, Germany
[5]Utrecht University, Utrecht, Netherlands
[6]IMT School for Advanced Studies, Lucca, Italy
**nacho.e.blanco@gmail.com*

INTRODUCTION/MOTIVATION

Schizophrenia (SZ) is a severe psychiatric disorder that manifests through positive (hallucinations, disorganized speech and delusions) and negative symptoms (grossly disorganized or catatonic behavior, diminished emotional expression and anhedonia). The disease is commonly accompanied with alterations in sleep, inappropriate affect, depersonalization or derealization [1], and may have an insidious or sudden onset. A myriad of correlates can be found at every level, from genes to whole-brain structural and functional networks. Regarding the last, it has been found that network architecture in SZ patients tend to be more disconnected than in healthy populations [2,3].

Modularity and network partitioning are related to a balance between integration and segregation of information across brain regions [6], and has proven to play an important role in shaping different topologies between subjects suffering from SZ and healthy population [4,5]. SZ of childhood onset has been consistently related to community bounds dissolution [7], while adult onset schizophrenia reports range from altered to intact overall modularity [8,9]. Yet, findings on community structure (i.e., communities in which different nodes participate) are consistent regardless of diagnostic status [8,10,11], indicating regular changes in topology. All in all, it is still unclear how modularity diverges in these clinical populations. The goals of our research are i) to unveil differences concerning ii) overall connectivity, iii) community structure and iv) robustness in terms of connectivity of brain areas associated to healthy subjects and patients of schizophrenia.

METHODS

In the present work, we analyze resting state fMRI functional networks of 65 healthy subjects (HC) and 44 patients of schizophrenia (SZ), 28 of them in a chronic state (CR) of illness, and 16 at early stage (ES). Parcellation follows the template proposed by Shen et al. (2013) [12], weights are calculated with Pearson correlation between all pair of regions' time series and corrected with surrogate permutation testing (i). We then apply the Louvain [13] and Surprise [14] algorithms to detect communities, and compare groups with the Rand index [15] (ii). Finally, we prune the network cutting edges with a weight smaller to a threshold. We explore the value of the threshold and observe how the giant component and the density of the network react to the prune at each group (iii).

RESULTS AND DISCUSSION

In comparison to healthy subjects, we found that networks from SZ patients exhibits wider weight distribution, larger overall connectivity [(i) Fig. 1], and are more consistent in the community structure across subjects [(ii) Fig. 2]. On the other hand, as the pruning threshold increases, density [(iii) Fig. 3] and size of the giant component decreases [(iii) Fig 4]. Given that average synchronization is higher in the SZ group, the giant component is more robust than in the HC group (iii), as it survives better edge removal. Density is notably smaller in the chronic group in comparison to the other two groups (iii), with HC being higher, and early stage in between. That is, even though-functional networks are less dense in SZ patients, they are also more robust to disconnection of the giant component. This tendencies (i and ii) seem to evolve with time, as the early stage group is systematically between the other two groups. This might be due to the chronification of the desease or to the medication. Further research is needed to assess the stability of this evolution.

AQ5

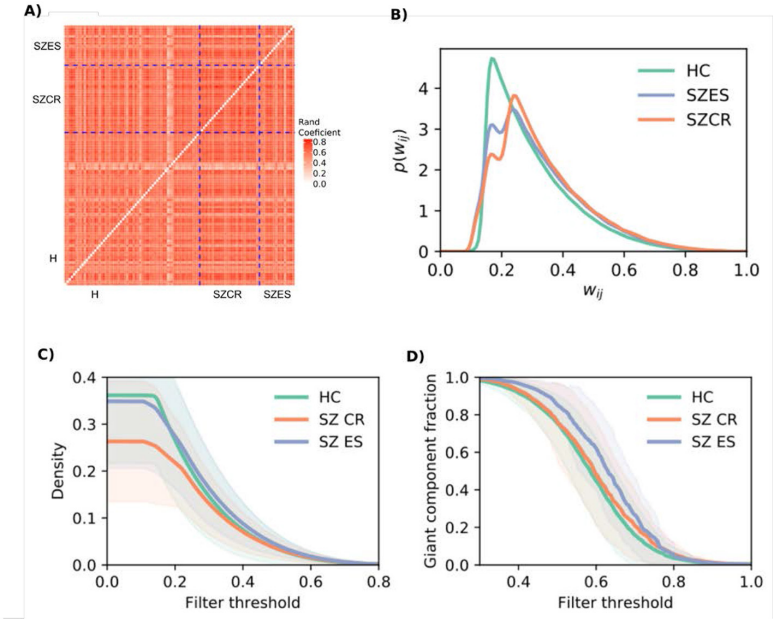

FIGURE 1: (**A**) Community comparison with rand-index. (**B**) Weights distributions. (**C**) Networks density against threshold. (**D**) Robustness of the giant component to threshold.

ACKNOWLEDGEMENTS

This work is the output of the Complexity72h workshop, held at IMT School in Lucca, 7-11 May 2018 (https://complexity72h.weebly.com/) and is already published in arXiv: https://arxiv.org/abs/1805.04329

AQ2

REFERENCES

[1] Association, A. P. Diagnostic and statistical manual of mental disorders (Washington, DC, 2013), 5th ed.

[2] Fornito, A., Zalesky, A., Pantelis, C. & Bullmore, E. T. Schizophrenia, neuroimaging and connectomics. Neuroimage 62, 2296–2314 (2012).

[3] van den Heuvel, M. P. & Fornito, A. Brain networks in schizophrenia. Neuropsychol. review 24, 32–48 (2014).

[4] Sun, Y., Dai, Z., Li, J., Collinson, S. L. & Sim, K. Modular-level alterations of structure–function coupling in schizophrenia connectome. Hum. brain mapping 38, 2008–2025 (2017).

[5] Reinen, J. M. et al. The human cortex possesses a reconfigurable dynamic network architecture that is disrupted in psychosis. Nat. communications 9, 1157 (2018).

[6] Sporns, O. Network attributes for segregation and integration in the human brain. Curr. Opin. Neurobiol. 23, 162–171 (2013).

[7] Alexander-Bloch, A. F. et al. Disrupted modularity and local connectivity of brain functional networks in childhood-onset schizophrenia. Front. systems neuroscience 4, 147 (2010).

[8] Yu, Q. et al. Modular organization of functional network connectivity in healthy controls and patients with schizophrenia during the resting state. Front. systems neuroscience 5, 103 (2012).

[9] Lerman-Sinkoff, D. B. & Barch, D. M. Network community structure alterations in adult schizophrenia: identification and localization of alterations. NeuroImage: Clin. 10, 96–106 (2016).

[10] Alexander-Bloch, A. et al. The discovery of population differences in network community structure: new methods and applications to brain functional networks in schizophrenia. Neuroimage 59, 3889–3900 (2012).

[11] Lerman-Sinkoff, D. B. & Barch, D. M. Network community structure alterations in adult schizophrenia: identification and localization of alterations. NeuroImage: Clin. 10, 96–106 (2016).

[12] Shen, X., Tokoglu, F., Papademetris, X. & Constable, R. T. Groupwise whole-brain parcellation from resting-state fMRI data for network node identification. NeuroImage 82, 403–415 (2013).

[13] Blondel, V. D., Guillaume, J.-L., Lambiotte, R. & Lefebvre, E. Fast unfolding of communities in large networks. J. statistical mechanics: theory experiment 2008, P10008 (2008).

[14] Aldecoa, R. & Martín, I. Surprise maximization reveals the community structure of complex networks. Sci. reports 3, 1060 (2013).

[15] Rand, W. M. Objective criteria for the evaluation of clustering methods. J. Am. Stat. Association 66, 846–850 (1971).

Multivariate comparison of human and mouse pyramidal cell dendritic morphologies

AQ1

Bojan Mihaljević*, Concha Bielza*, Pedro Larrañaga*

Universidad Politécnica de Madrid

**bmihaljevic@fi.upm.es; *mcbielza@fi.upm.es; *pedro.larranaga@fi.upm.es*

INTRODUCTION/MOTIVATION

Better understanding the differences between human and mouse pyramidal cells is important for the modelling efforts of the Human Brain Project. We know, for example, that human pyramidal cells have larger dendritic arbors [1] and more synaptic connections [2] than those of the mouse. Previous comparative studies have largely been univariate, comparing each morphological feature in isolation. Yet, there might be meaningful interactions among the features. Furthermore, these interactions might differ between the species. Such interactions can be captured with probabilistic multi-variate models such as Bayesian networks [3].

METHODS

We will use morphology reconstructions from Neuromorpho.org [4], taking into account the cells' brain area, reconstruction procedure specifics, and cortical layer when comparing cells across species. We will compute a wide array of morphometrics with the NeuroSTR software (https://computational-intelligencegroup.github.io/neurostr/). We will learn one Bayesian network for the human cells and another for mouse cells, with the same morphological features as their variables. These are interpretable models encoding probabilistic independencies among sets of variables. Comparing the two models can reveal differences and similarities between the species. For example, we might find that the distance from the soma is related to branch length differently in mouse than in human cells.

RESULTS AND DISCUSSION

We are performing initial analyses and have no results at this point.

AQ2

REFERENCES

[1] Mohan, Hemanth, Matthijs B. Verhoog, Keerthi K. Doreswamy, Guy Eyal, Romy Aardse, Brendan N. Lodder, Natalia A. Goriounova, et al. 2015. "Dendritic and Axonal Architecture of Individual Pyramidal Neurons Across Layers of Adult Human Neocortex." Cerebral Cortex 25 (12): 4839–53. https://doi.org/10.1093/cercor/bhv188.

[2] DeFelipe, Javier, Lidia Alonso-Nanclares, and Jon I Arellano. 2002. "Microstructure of the Neocortex: Comparative Aspects." Journal of Neurocytology 31 (3-5). Springer: 299–316.

[3] Bielza, Concha, and Pedro Larrañaga. 2014. "Bayesian Networks in Neuroscience: A Survey." Frontiers in Computational Neuroscience 8: 131.

[4] Ascoli, Giorgio A, Duncan E Donohue, and Maryam Halavi. 2007. "NeuroMorpho.Org: A Central Resource for Neuronal Morphologies." The Journal of Neuroscience 27 (35). Soc Neuroscience: 9247–51.

MRI-based stroke outcome prediction and treatment planning

AQ1

A. Kuzina[1,2]*, E. Kondrateva[1]*, V. Alferova[3]*

[1]Skolkovo Institute of Science and Technology, Moscow, Russia
[2]National Research University "Higher School of Economics"
[3]Center of Speech Pathology and Neurorehabilitation, Moscow, Russia
**Anna.Kuzina@skoltech.ru; *E katerina.Kondarteva@skoltech.ru; *v.alferova@mail.ru*

INTRODUCTION/MOTIVATION

The stagnation or complication of post-stroke cognitive dysfunction could be associated with an unfavourable prognosis of the disease [1-4]. Cognitive rehabilitation including intensive speech therapy and physiotherapy is used in order to increase the effectiveness of restorative treatment. However, the question of the therapeutic effectiveness of cognitive rehabilitation courses remains controversial and is being extensively researched [5, 6]. The research became especially crucial as right rehabilitation potential and stroke outcome prognosis became crucial for effective treatment planning [7-9]. The goal of the presented study is the analysis of T1-weighted structural MRI to assess the patient's condition at the time of admission to the rehabilitation center and forecast the dynamics of recovery as a result of restorative therapy.

METHODS

In the current study, we observe the dataset containing 41 patients, mean age 57.31 (11.72) years, with clinical aphasia after the first hemispheric ischemic stroke in the anamnesis 3-12 months onset. Patients were examined before and after the course of rehabilitation treatment (4.7 weeks), which includes intensive speech therapy (15 hours of exercise per week). For each patient in the dataset MRI was performed on the MAGNETOM Avanto MR scanner (Siemens, Germany) with a 1.5 Tesla magnetic field induction right after the admission to the rehabilitation center (3 months after the stroke). All the analysis was done on T1-weighted imagery, which were skull stripped in Brainsuite toolbox, centered and aligned. Effectiveness of the course of treatment was evaluated based on the dynamics of the results of neuropsychological, neurological and neurovisual examination of patients before and after treatment. The estimated parameters included: the dynamics of focal deficiency the

National Institutes of Health Stroke Scale (NIHSS) [10] and functional recovery of the patients (Barthel Index (BI), modified Rankin Scale (mRS)). MRI scans obtained at the time of admission were used to predict NIHSS, Barthel and mRS before and after cognitive rehabilitation courses. Additionally, we fitted models where value of the target parameter at the acute phase (21 days after the stroke) which was concatenated to the feature vector, extracted from the image. The Vox Convolutional and residual neural networks [11] with smooth L1 loss was used to solve all regression tasks. The plain convolutional network exploits 3D convolutional layers, followed by ReLU activations and max pooling layers for gradual dimensionality reduction, while residual network also add skip connections between blocks of layers. The calculations were performed in python with the use of PyTorch framework.

RESULTS AND DISCUSSION

Table 1 depicts mean absolute error for all the regression tasks, estimated on the 5-fold cross validation with two repetitions. We observe rather low errors, which supports the hypothesis that the sMRI-based deep learning models can be considered as relevant predictive tools for the stroke outcome prognosis. Surprisingly, model performs better when predicting the value of interest after the rehabilitation treatment, which is even more important than prediction of the same parameter before treatment. It is also worth mentioning, that addition of the acute phase value increases accuracy of all the models. Presumably, the reason for that is high correlation between initial and future value of the corresponding variable.

Table 1: Regression results: Mean absolute error and its standard deviation on repeated 5-fold cross validation

Target	Possible Values	MAE (SD) before treatment		MAE (SD) after treatment	
		Without acute phase value	Including acute phase value	Without acute phase value	Including acute phase value
Barthel	1 - 100	11.40 (3.346)	7.77 (2.222)	7.65 (2.287)	5.86 (2.124)
mRS	0 - 5	0.66 (0.115)	0.53 (0.251)	0.65 (0.174)	0.45 (0.217)
NIHSS	1 - 31	3.33 (0.907)	3.05 (1.179)	2.54 (0.989)	1.78 (0.895)

AQ2

REFERENCES

[1] Butler, R. A., Ralph, M. A. L., & Woollams, A. M. (2014). Capturing multidimensionality in stroke aphasia: Mapping principal behavioural components to neural structures. Brain, 137 (12).

[2] Grefkes, C., & Fink, G. R. (2014). Connectivity-based approaches in stroke and recovery of function. The Lancet Neurology, 13 (2), 206–216.

[3] Hartwigsen, G., & Saur, D. (2017). Neuroimaging of stroke recovery from aphasia - Insights into plasticity of the human language network. NeuroImage.

[4] Yourganov, G., Fridriksson, J., Rorden, C., Gleichgerrcht, E., & Bonilha, L. (2016). Multivariate Connectome-Based Symptom Mapping in Post-Stroke Patients: Networks Supporting Language and Speech. The Journal of Neuroscience, 36 (25), 6668–6679.

[5] Pustina, D., Coslett, H. B., Ungar, L., Faseyitan, O. K., Medaglia, J. D., Avants, B., & Schwartz, M. F. (2017). Enhanced estimations of post-stroke aphasia severity using stacked multimodal predictions. Human Brain Mapping, 38 (11), 5603–5615.

[6] Itabashi, R., Nishio, Y., Kataoka, Y., Yazawa, Y., Furui, E., Matsuda, M., & Mori, E. (2016). Damage to the left precentral gyrus is associated with apraxia of speech in acute stroke. Stroke, 47 (1), 31–36.

[7] Nenert, R., Allendorfer, J. B., Martin, A. M., Banks, C., Ball, A., Vannest, J., ... Szaflarski, J. P. (2017). Neuroimaging Correlates of Post-Stroke Aphasia Rehabilitation in a Pilot Randomized Trial of Constraint-Induced Aphasia Therapy. Medical Science Monitor, 23, 3489–3507.

[8] Kreisel, S. H., Hennerici, M. G., & Bäzner, H. (2007). Pathophysiology of stroke rehabilitation: The natural course of clinical recovery, use-dependent plasticity and rehabilitative outcome. Cerebrovascular Diseases, 23 (4), 243–255.

[9] Saur, D., & Hartwigsen, G. (2012). Neurobiology of language recovery after stroke: Lessons from neuroimaging studies. Archives of Physical Medicine and Rehabilitation, 93 (1 SUPPL.), S15–S25.

[10] The National Institute of Neurological Disorders and Stroke rt-PA Stroke Study Group. Tissue plasminogen activator for acute ischemic stroke. N Engl J Med. 1995;333:1581–1588. http://doi:10.1056/NEJM199512143332401.

[11] Korolev, S., Safiullin, A., Belyaev, M., & Dodonova, Y. (2017). Residual and plain convolutional neural networks for 3D brain mri classification. Sergey Korolev Amir Safiullin Mikhail Belyaev Skolkovo Institute of Science and Technology Institute for Information Transmission Problems, 835–838.

The mouse brain at different scales

AQ1

Lionel Kusch*, Viktor K. Jirsa*

Institut de Neurosciences des Systèmes, Aix-Marseille Université, Marseille, France

**lionel.kusch@univ-amu.fr; *Viktor.JIRSA@univ-amu.fr*

INTRODUCTION

An important part of simulations of the whole brain is based on the connectome-based modelling of large scale brain networks [1]. This approach is relevant for understanding neuroimaging signals. Nevertheless, these models are great simplification of neural population and the loss of description means that they can capture only some part of brain dynamics. The identification of the missing behaviour of neurons is important to avoid establishing wrong conclusions from the simulation. The comparison between mean field theory and spiking neural network uses a simple topological structure. The network is composed of adaptive exponential integrate and fire neurons placed on a torus and connected with homogeneous connections and with one long heterogeneous connection [2]. The analysis of the simulated dynamic network demonstrates that the synchronization between neurons is different between mean field model and the spiking neural network. These results implicate significant differences in the simulated dynamics of these two levels of description.

METHODS

We utilize the mean field model to simulate mouse brain dynamics and capture resting state dynamics and functional connectivity [3]. However, the investigation of missing dynamics in the simulation of a mouse brain is crucial for validation of interpretations of the mean field model and for helping the future modelling. For this, we propose to use spiking neurons over a connectome. These simulations will be run on supercomputers due to the size of the network. This analysis should bring some important results about the importance of mean field model in the brain simulations. The result will also allow simulations with the coexistence of difference scale. It will be possible to integrate in our research the impact of our results on the dynamics of the brain.

AQ2

REFERENCES

[1] V. K. Jirsa et al., "The Virtual Epileptic Patient: Individualized Whole-Brain Models of Epilepsy Spread," NeuroImage, Individual Subject Prediction, 145 (January 15, 2017): 377–88, 2017.

[2] Viktor K. Jirsa and Roxana A. Stefanescu, "Neural Population Modes Capture Biologically Realistic Large Scale Network Dynamics," Bulletin of Mathematical Biology 73, no. 2 (February 2011): 325–43, 2011.

[3] Francesca Melozzi et al., "The Virtual Mouse Brain: A Computational Neuroinformatics Platform to Study Whole Mouse Brain Dynamics," ENeuro 4, no. 3 (May 1, 2017): ENEURO.0111-17.2017, 2017.

A Comparison of fMRI data analysis methods for depression classification

AQ1 **Marina Pominova*, Ekaterina Kondrateva*, Alexander Rozhnov***

Skolkovo Institute of Science and Technology, Moscow, Russia.
**Marina.Pominova@skoltech.ru; *Ekaterina.Kondrateva@skoltech.ru; *Alexandr.Rozhnov@sklotech.ru*

INTRODUCTION/MOTIVATION

Although depression is one of the most common psychiatric disorders, there is no biological test for the depression diagnosis currently in clinical practice. Nevertheless, depression patterns have been extensively studied by the means of neuroimaging. In the existing studies, it was shown that depression can be recognized by analyzing the data of functional brain activity, such as fMRI.

The fMRI data analysis could be performed of different levels of processing and feature extraction. The convenient approach assumes classification on functional connectivity matrices, acquired as brain regions of interest (ROI) time series correlations [1-4]. Also, obtained ROI time series could be classified directly with 1-D recurrent neural networks. And finally, fMRI data could be classified with minimal preprocessing using 3-D Convolutional Neural Networks with recurrent structure. It should be noted that although deep learning methods are known for requiring more data to achieve high performance, existing works [5], [6] show that neural networks of reduced size with strong regularization can be successfully applied to analyze such data as fMRI and EEG even on a small sample. In this work, we compare three possible approaches: classification with SVM algorithm applied to the precomputed features (connectivity matrices), classification with recurrent neural networks trained on ROI's time series and recurrent-convolutional neural networks, applied directly to the fMRI data without any feature extraction.

METHODS

The observed dataset consisted of 1.5 T T2* EPI sequences of 25 patients with major depressive disorder and 25 healthy volunteers, annotated with demographic characteristics as well as BDI-II scores. fMRI imagery was preprocessed in fmriprep [7] software package. For each patient 133 volumes

were corrected by registering and re-slicing for head motion, field unwarping, normalization, bias field correction, and brain extraction. Next, images were handled via nilearn package to obtain connectivity matrices. Images were spatially smoothed with a Gaussian filter, detrended and standardized. The 116 time series were obtained for each ROI as major SVD component for all region voxel according to AAL atlas. Then we evaluated functional connectivity between each pair of regions using Pearson correlation coefficient. Thus, for each patient, we obtained a 116 × 116 symmetric matrix, pulling 1-dimensional vector we describe every subject with (116 × 115)/2 = 6670 features.

The 1-D Recurrent neural network on ROI time series [8] takes the rsfMRI time series of each patient as input and predicts the class label, taking into account dependence between their sequential changes.

The 3-D Recurrent-Convolutional Neural Network [9] architecture consists of a convolutional part followed by a recurrent part. During the training process, convolutional part takes as input 3D brain images at each time step of fMRI series and transforms them into the feature vectors. Then obtained vectors are transmitted to the recurrent part of the network, which tries to capture temporal information and predict the class label [10].

For both neural networks, we considered configurations with one or two recurrent layers with LSTM memory units. We also experimented with the number of blocks of convolutional layers and the number of filters in R-CNN and the number of LSTM memory units in RNN. The quality of model predictions is estimated by metric ROC AUC on repeated 5-fold cross-validation with 3 petitions.

RESULTS AND DISCUSSION

We compared results obtained with basic fMRI preprocessing and three methods of data analysis, included SVM classification on reduced dimensionality features Recurrent-Convolutional Neural Network modifications for depression recognition problem (Table 1). As can be seen, recurrent CNN's outperform methods requiring feature extraction and pre-processing. Also, we observe statistically significant correlation (p-value 0.02) between probabilistic predictions of the R-CNN's models and BDI-II scores of the patients.

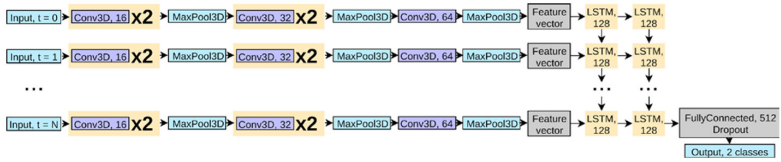

AQ4

FIGURE 1: Recurrent-convolutional neural network applied to 4D fMRI data.

Table 1: Performance obtained on the depression recognition tasks. Reported as ROC-AUC

Data for the analysis	Classifier	AUC	STD
Functional connectivity matrix	SVM (kernel = rbf, C = 1, gamma = 0.01, dim_reduction = PCA)	0.60	0.16
ROI time series	RNN-1	0.54	0.15
ROI time series	RNN-2	0.57	0.18
Full size fMRI data	R-CNN-1	0.75	0.19
Full size fMRI data	R-CNN-2	0.77	0.18

AQ2

REFERENCES

[1] Sheline, Yvette I., et al. "Resting-state functional MRI in depression unmasks increased connectivity between networks via the dorsal nexus." Proceedings of the National Academy of Sciences 107.24 (2010): 11020-11025.

[2] Greicius, Michael D., et al. "Resting-state functional connectivity in major depression: abnormally increased contributions from subgenual cingulate cortex and thalamus." Biological psychiatry 62.5 (2007): 429-437.

[3] Zeng, Ling-Li, et al. "Identifying major depression using whole-brain functional connectivity: a multivariate pattern analysis." Brain 135.5 (2012): 1498-1507.

[4] Veer, Ilya M., et al. "Whole brain resting-state analysis reveals decreased functional connectivity in major depression." Frontiers in systems neuroscience 4 (2010): 41

[5] Plis, Sergey M., Hjelm, Devon R., Salakhutdinov, Ruslan, Allen, Elena a., Bockholt, Henry J., Long, Jeffrey D., Johnson, Hans J., Paulsen, Jane S., Turner, Jessica a., and Calhoun, Vince D. Deep learning for neuroimaging: a validation study. Frontiers in Neuroscience, 8(August):1–11, 2014. ISSN 1662-453X. doi: 10.3389/fnins.2014.00229.

[6] Mirowski, Piotr, Madhavan, Deepak, LeCun, Yann, and Kuzniecky, Ruben. Classification of patterns of EEG synchronization for seizure prediction. Clinical Neurophysiology, 120(11):1927–1940, 2009. ISSN 13882457. doi: 10.1016/j.clinph.2009.09.002.

[7] "Usage — Fmriprep Version Documentation". Fmriprep.Readthedocs.Io, 2018, https://fmriprep.readthedocs.io/en/stable/usage.html. Accessed 10 Dec 2018.

[8] Dvornek, Nicha C., et al. "Identifying autism from resting-state fMRI using long short-term memory networks." International Workshop on Machine Learning in Medical Imaging. Springer, Cham, 2017.

[9] P. Bashivan, I. Rish, M. Yeasin, and N. Codella, "Learning representations from eeg with deep recurrent-convolutional neural networks," arXiv preprint arXiv:1511.06448, 2015.

[10] M. Pominova, A. Artemov, M. Sharaev, E. Kondrateva, A. Bernstein, E. Burnaev et. al., Deep Recurrent 3D Convolutional Neural Networks for Epilepsy and Depression Diagnostic from Structural and Functional MRI Data, Proceedings of the IEEE International Conference on Data Mining 2018, Workshops Proceedings volume, IEEE Computer Society, USA, 8 pp., 2018.

Emotional distraction of working memory: Neural responses disentangled

AQ1 **Jenny Zaehringer[1]*, Myrto Alampanou[3]*, Christian Schmahl[1], Gabriele Ende[2], Anne Krause-Utz[2,3], Christian Paret[1]***

[1]Department of Psychosomatic Medicine and Psychotherapy, Central Institute of Mental Health Mannheim, Medical Faculty Mannheim / Heidelberg University, Germany
[2]Department Neuroimaging, Central Institute of Mental Health Mannheim, Medical Faculty Mannheim / Heidelberg University, Germany
[3]Leiden University, Rapenburg 70, EZ Leiden, Netherlands.
**jenny.zaehringer@zi-mannheim.de; *m.alampanou@umail.leidenuniv.nl; *christian.paret@zi-mannheim.de*

INTRODUCTION

Emotional stimuli are very salient even if they are task-irrelevant, due to their relevance to survival (Drevets and Raichle, 1998). Affective stimuli elicit stronger perceptual representations in the brain's visual and other cortices (Vuilleumier, 2005; Satpute et al., 2015). This increased strength of representation at the expense of executive control resources is termed hard prioritization (Pessoa, 2009) and it is proposed to be a function of amygdalergic projections to cortical sensory areas as well as increased direct processing of affective information in the fronto-parietal control network (Amaral, Behniea, & Kelly, 2003; Okon-Singer, Hendler, Pessoa, & Shackman, 2015; Pessoa, 2009; Sah, Faber, Lopez De Armentia, & Power, 2003). Executive resources are thus occupied by the processing of the affective information and no longer available for executive control-demanding activities such as working memory (Eysenck, Derakshan, Santos, & Calvo, 2007). The frontal-parietal network biases sensory processing of information, facilitating goal selection (Awh, Belopolsky, & Theeuwes, 2012). We aimed to directly test the afforementioned suggested processes by using the established Emotional Working Memory Task (EWMT) in a patient group with Borderline Personality Disorder (BPD). The Emotional Working Memory Task (EWMT) is an adapted Sternberg item recognition task (Sternberg, 1966) modified by Oei and colleagues (Oei et al., 2012; Krause-Utz et al., 2012, 2014). It is one of the most established paradigms that can reflect the effects of emotional distraction on working memory processes (Krause-Utz et al., 2014; Dolcos & McCarthy, 2006). A recent meta-analysis by Scweizer and colleagues (2018) has revealed that distraction by emotionally negative pictures is characteried by altered neural

processes such as increased vlPFC recruitment, amygdala and temporo-occipital cortex. However, we still do not know the exact neural mechanisms through which emotional distraction during cognitive processing takes place. The behavioral impact of the emotional distraction appears to be augmented in individuals for whom emotional stimuli have greater significance (Schweizer et al., 2018). Affective disorders like BPD have been linked to an increased response to affective stimuli (Krause-Utz et al., 2014), so the effects that the emotional distractors of the EWMT will have on working memory processes is considered to be more readily detectable. To the best of our knowledge, no other study has tried to disentangle the different working memory and affective processes during the distinct phases of the EWMT. We hypothesized that activation of the occipital cortex and the amygdala would be increased during the emotional distractor. We further hypothesized that the fronto-parietal network activation would be enhanced during the probe phase following an emotional distractor because frontal resources would need to be more actively recruited to compensate for the distraction during the pending response execution (i.e. probe).

METHODS

A total of $N = 22$ (age : 32.50 ± 10.81; mean$\pm$SD) female patients with at least 5 BPD criteria according to DSM-IV (American Psychiatric Association, 2000) participated in the study. The present EWMT version had a duration of 8 minutes and was comprised of 40 trials, each starting with the presentation of a set of three letters (memoranda, 1000ms). After a 1500 ms delay phase another three-letter set appeared on the screen (probe, 2000ms). Participants had to press the button "yes" or "no" indicating whether one of the letters in the memoranda has reappeared in the probe. In half of the trials, one of the three memoranda was present in the probe. During the delay interval, either no distractor (i.e. a fixation cross; "cross condition") or a distractor (i.e. an aversive picture; "negative condition") was presented. Order of condition and pictures were counterbalanced. A 3 Tesla MRI Scanner was used for the data acquisition and MATLAB (vR2012a) SPM12 package was used for the data analysis. Contrasts between the individual EWMT phases (memoranda, negative picture or cross, probe, response) and baseline activity were modeled per subject. One-sample t-tests were computed to get BOLD-activity patterns on a whole-brain level for each contrast with an intensity threshold of $p < .001$ and an extent threshold of $k > 10$ contiguous voxels.

RESULTS AND DISCUSSION (PRELIMINARY)

Prelimiray results suggest that during the distraction of negative pictures, BPD patients show an increase in the ventrolateral prefrontal cortex (vlPFC), the occipital cortex and the amygdala, which is in line with a recent meta-analysis on emotinal working memory (Schweizer et al., 2018). Moreover, we find a significant increase in BOLD activity in the prefrontal cortex, temporo-occipital cortex and amygdala when comparing the probe following a negative distractor with the probe following no distractor. Prelimiary results are in line with our hypotheses and suggest that participants in the retrieval phase need more resources if they become distracted by a negative picture (see Table 1 and Figure 1).

Table 1: Preliminary summary of brain activations per EWMT phase

Talairach coordinate					
x	*y*	*z*	*Aal*	*TD Labels*	*Brodmann*
Negative pictures					
6	-88	-2	Calcarine_R	Lingual Gyrus	-
-24	8	-18	Olfactory_L	Inferior Frontal Gyrus	-
22	-6	-16	Hippocampus_R	Parahippocampa Gyrus	Amygdala
-20	-30	-4	Hippocampus_L	-	-
-2	50	-16	Rectus_L	Medial Frontal Gyrus	-
-44	4	-36	Temporal_Inf_L	Middle Temporal Gyrus	-
34	-6	-38	Fusiform_R	Uncus	-
Probe					
10	14	-2	Caudate_R	Caudate	Caudate Head
-4	-78	46	Precuneus_L	Precuneus	-
-46	-58	22	Temporal_Mid_L	Superior Temporal Gyrus	39
-38	-90	4	Occipital_Mid_L	Middle Occipital Gyrus	19
-30	-84	-22	Cerebelum_Crus1_L	Fusiform Gyrus	19
50	20	-10	Frontal_Inf_ Orb_R	Inferior Frontal Gyrus	47
22	56	24	Frontal_Sup_R	Middle Frontal Gyrus	10
54	-28	-2	Temporal_Sup_R	Superior Temporal Gyrus	22
6	-40	6	Cingulum_Post_R	Extra-Nuclear	Corpus Callosum
-40	-68	40	Angular_L	Inferior Parietal Lobule	39

Note. Probe following a negative distractor versus probe following cross.

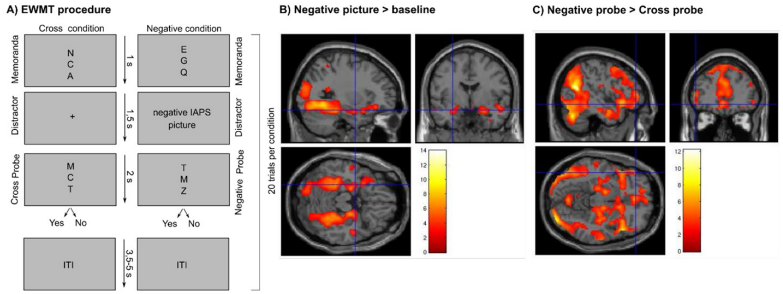

FIGURE 1: Note: This figure is preliminary and subject to change to better depict the EWMT procedure and the main results. (**A**) The present version of the EWMT comprised 40 trials, each starting with the presentation of a set of three letters (memoranda, 1000ms). After a distraction phase of 1500 ms another set of three letters appeared on the screen (probe, 2000ms). Participants had to press the button "yes" or "no" indicating whether one of the letters in the memoranda has reappeared in the probe. In half of the trials, one of the three memoranda was present in the probe. During the distraction interval, either no distractor (i.e. a fixation cross; "cross condition") or a distractor (i.e. an aversive picture; "negative condition") was presented. Target-present and target-absent trials were equal across the negative and the cross condition. The presentation of the two conditions was balanced in a pseudo-random manner with no more than two consecutive conditions. (**B**) Left Amygdala mask (x: -27, y: -3, z: -18) was created with a sphere of 20mm using the MNI coordinates from the negative>neutral contrast reported by Schweizer and colleagues (2018). Small volume correction (SVC) analysis revealed increased activation in the left amygdala in response to the negative picture (negative picture > baseline contrast), $T(21) = 5.70$, $p < .01$, FWE corrected. (**C**) Left vlPFC mask (x: -39, y: 33, z: -6) was created with a sphere of 20mm using the MNI coordinates from the negative>neutral contrast reported by Schweizer and colleagues (2018). Small volume correction (SVC) analysis revealed increased activation in the left vlPFC in response to the probe following a negative distractor (negative probe > cross probe contrast), $T(21) = 6.60$, $p = .00$, FWE corrected.

AQ2

REFERENCES

[1] Amaral, D. G., Behniea, H., & Kelly, J. L. (2003). Topographic organization of projections from the amygdala to the visual cortex in the macaque monkey. *Neuroscience, 118*(4), 1099–1120.

[2] American Psychiatric Association, & American Psychiatric Association. (2000). Diagnostic and statistical manual of mental disorders (revised 4th ed.). *Washington, DC: Author*.

[3] Awh, E., Belopolsky, A. V., & Theeuwes, J. (2012). Top-down versus bottom-up attentional control: A failed theoretical dichotomy. *Trends in Cognitive Sciences, 16*(8), 437-443.

[4] Dolcos, F., & McCarthy, G. (2006). Brain systems mediating cognitive interference by emotional distraction. *Journal of Neuroscience, 26*(7), 2072-2079.

[5] Drevets, W. C., & Raichle, M. E. (1998). Reciprocal suppression of regional cerebral blood flow during emotional versus higher cognitive processes: Implications for interactions between emotion and cognition. *Cognition and Emotion, 12*(3), 353-385.

[6] Eysenck, M. W., Derakshan, N., Santos, R., & Calvo, M. G. (2007). Anxiety and cognitive performance: Attentional control theory. *Emotion, 7*(2), 336–353.

[7] Krause-Utz, A., Elzinga, B. M., Oei, N. Y., Paret, C., Niedtfeld, I., Spinhoven, P., ... & Schmahl, C. (2014a). Amygdala and dorsal anterior cingulate connectivity during an emotional working memory task in borderline personality disorder patients with interpersonal trauma history. *Frontiers in Human Neuroscience, 8*, 848.

[8] Krause-Utz, A., Oei, N. Y., Niedtfeld, I., Bohus, M., Spinhoven, P., Schmahl, C., & Elzinga, B. M. (2012). Influence of emotional distraction on working memory performance in borderline personality disorder. *Psychological Medicine, 42*(10), 2181-2192.

[9] Oei, N. Y., Veer, I. M., Wolf, O. T., Spinhoven, P., Rombouts, S. A., & Elzinga, B. M. (2011). Stress shifts brain activation towards ventral 'affective'areas during emotional distraction. *Social Cognitive and Affective Neuroscience, 7*(4), 403-412.

[10] Okon-Singer, H., Hendler, T., Pessoa, L., & Shackman, A. J. (2015). The neurobiology of emotion–cognition interactions: Fundamental questions and strategies for future research. *Frontiers in Human Neuroscience, 9*.

[11] Pessoa, L. (2009). How do emotion and motivation direct executive control? *Trends in Cognitive Sciences, 13*(4), 160–166.

[12] Sah, P., Faber, E. S. L., Lopez De Armentia, M., & Power, J. (2003). The Amygdaloid Complex: Anatomy and Physiology. *Physiological Reviews, 83*(3), 803–834.

[13] Satpute, A. B., Kang, J., Bickart, K. C., Yardley, J., Wager, T. D., & Barrett, L. F. (2015). Involvement of sensory regions in affective experience: A meta-analysis. *Frontiers in Psychology, 6*.

[14] Sternberg, S. (1966). High-speed scanning in human memory. *Science, 153*(3736), 652-654.

[15] Schweizer, S., Satpute, A. B., Atzil, S., Field, A., Hitchcock, C., Black, M., ... & Dalgleish, T. (2018). The behavioral and neural effects of affective information on working memory performance: A pair of meta-analytic reviews.

[15] Vuilleumier, P. (2005). How brains beware: neural mechanisms of emotional attention. *Trends in Cognitive Sciences, 9*(12), 585-594.

Making good choices: The effects of chronic stress and social isolation on decision-making in mice

Arish Mudra Rakshasa[1,2]*, Michelle T. Tong[1]*

AQ1

[1]Earlham College Neuroscience Program, Richmond, IN
[2]Earlham College Biochemistry Program, Richmond, IN
**araksh15@earlham.edu; *tongmi@earlham.edu*

INTRODUCTION

Chronic stress, which has been correlated with a multitude of physical and mental health issues, can significantly impact cognition and decision-making (Janis and Mann, 1976; Zur and Breznitz, 1981)). Studies using mouse models have demonstrated that chronic stress, induced through repeated immobilisation, can cause mice to evaluate cost-benefit conflicts erratically and engage in riskier behaviour (Friedman et al., 2017). Potential ways of counteracting these stress effects remain largely unexplored. In the current study, we investigate the role of social interaction in attenuating stress-induced aberrant decision-making.

METHODS

This study utilised a pre-post-control mixed-measures design. Mice were housed either in groups or individually throughout the experiment. Both groups of mice underwent a seven-day period of repeated immobilisation to induce chronic stress. Stress levels were determined using behavioural (Open Field Test) and physiological (urine corticosterone ELISA) measures to confirm the efficacy of the chronic stress protocol. Decision-making was assessed through a Cost-Benefit Conflict (CBC) task on a T-maze, in which mice could choose between a high-benefit, high-cost alternative and a low-benefit, lost-cost alternative. All three measures were conducted before and after the chronic stress protocol to compare changes in stress levels and decision-making after chronic stress exposure.

RESULTS AND DISCUSSION

We found that urine corticosterone levels and thigmotaxis in an open field, which are both reliable measures of stress, increased significantly after the chronic stress protocol across housing conditions (Figure 1A, 1B). This suggests that the immobilisation protocol successfully induced chronic stress among the mice. There was no significant interaction of chronic stress and social isolation on decision-making: socially-housed mice did not show a significantly different increase in high-risk decision-making after chronic stress exposure compared to individually-housed mice Crucially, however, significant additive main effects of stress and housing were found. There was a significant increase in high-risk decisions after exposure to chronic stress for both housing conditions, and isolated mice on average made more high-risk decisions than socially-housed mice (Figure 2). These findings suggest that chronic stress and social isolation lead to risky decision-making in mice as individual factors, but the role of social interaction in counteracting this stress effect requires further exploration. This study advances our understanding of stress and cognition in mouse models and lays the groundwork for further research into factors that may attenuate the effects of chronic stress on cognition.

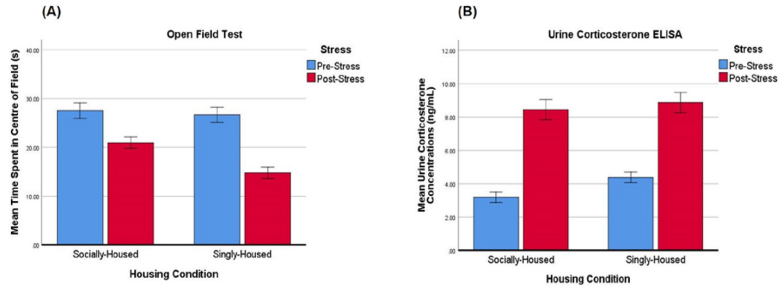

FIGURE 1: (**A**) Performance on an Open Field Test and (**B**) urine corticosterone concentrations (ng/mL) for socially-housed (n = 10) and singly-housed (n = 10) mice. Urine corticosterone concentrations and time spent outside the center of the field (thigmotaxis) increase significantly after repeated immobilisation for both housing conditions, indicating higher stress levels after the chronic stress protocol.

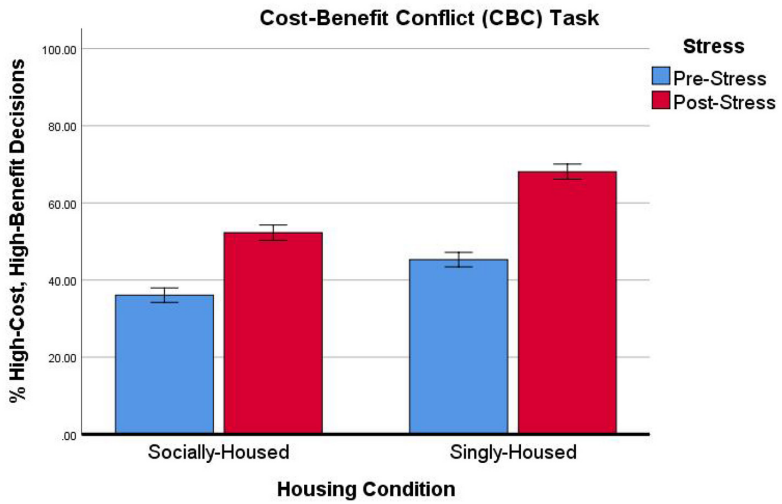

FIGURE 2: Performance of socially-housed (n = 10) and singly-housed (n = 10) mice on a Cost-Benefit Conflict (CBC) task before and after exposure to chronic stress. Proportion of taking high-risk decisions in total decision trials increased significantly ($p < 0.050$) for both conditions after exposure to chronic stress, but this increase was not significantly different ($p > 0.021$) in socially-housed mice than in singly-housed mice.

AQ2

REFERENCES

[1] A. Friedman, D. Homma, B. Bloem, L.G. Gibb, K.I. Amemori, D. Hu ... and K.A. Mikofalyy. Chronic stress alters striosome-circuit dynamics, leading to aberrant decision-making. *Cell*, 171(5):1191-1205, 2017.

[2] I.L. Janis and L. Mann. Coping with decisional conflict: An analysis of how stress affects decision-making suggests interventions to improve the process. *American Scientist*, 64(6):657-667, 1976.

[3] H.B. Zur and S.J. Breznitz. The effect of time pressure on risky choice behavior. *Acta Psychologica*, 47(2):89-104, 1981.

Using KappaNEURON for electrical-biochemical modelling of synaptic plasticity in a hippocampal CA1 pyramidal cell

Domas Linkevičius*, David C. Sterratt

School of Informatics, Institute for Adaptive and Neural Computation, College of Science and Engineering, University of Edinburgh, Edinburgh, United Kingdom
**D.Linkevicius@sms.ed.ac.uk*

INTRODUCTION AND MOTIVATION

Synaptic plasticity, the ability of synapses (connections between nerve cells) to change their strength, is a fundamental property of the brain. Long-term potentiation (LTP), the strengthening of synapses, and long-term depression (LTD), the weakening of the synapses, are among the best researched phenomena in synaptic plasticity [1]. However, understanding of synaptic plasticity is still lacking, due to its very complex expression. One of the main difficulties in understanding synaptic plasticity is the broad range of mechanisms involved, from intracellular biochemical networks, through various neurotransmitters and membrane receptors, to dendritic morphology [2]. Further understanding of synaptic plasticity requires integration of these various levels into coherent and consistent models. In this project, we combine various experimental literature and modelling attempts to assemble a bottom-up model of synaptic plasticity. We employ novel software - KappaNEURON [3] - to merge a detailed model of dendritic spine Ca^{2+} transients and biochemical networks with a model of electrical activity in a neuron. This approach will allow us to show how various experimental synaptic plasticity protocols manifest themselves at the subcellular level and to make novel experimental predictions.

METHODS

KappaNEURON [3] is a hybrid simulator which couples NEURON 7.4 [4] and SpatialKappa 2.1.1 [5] in a consistent and accurate manner. KappaNEURON has the advantage of allowing biochemical interactions to be specified in the rule-based Kappa language, which is particularly suited to describing protein-protein interactions compactly. Relevant biochemical reactions collected

from literature were translated into SpatialKappa's rule-based format, with free or underconstrained reaction rates being tuned to match physiological data. The resulting model includes calcium influx through NMDA receptors and voltage-gated calcium channels, protein interactions dependent on Ca^{2+} levels, such as CaM activation and the resulting phosphorylation or dephosphorylation of proteins pivotal in plasticity, e.g. CaMKII, I1 and AMPA receptors. The biochemical spine model was embedded in a simplified CA1 pyramidal cell model with membrane mechanisms based on [6], with biochemical activity in the spine responding and contributing to electrical activity in the neuron.

DISCUSSION

The simulations incorporating a single biochemically complex spine, in the context of a detailed electrical model of a neuron, allow for deeper understanding of naturally occurring plasticity, as well as pathological plasticity mechanisms, such as in Alzheimer's or Parkinson's [7]. Specifically, studies such as [8], if extended to hippocampus in health and disease, would provide invaluable proteomic and genetic information, which might be translatable to parameter changes or model extensions, representing gene level phenomena. The simulation time due to the biochemical model is much greater than the neural simulation time, and it would therefore be desirable to develop simplified versions of the model that could be incorporated in simulations of networks.

AQ2

REFERENCES

[1] C. R. Raymond. LTP forms 1, 2 and 3: different mechanisms for the 'long' in long-termo potentiation. TRENDS in Neurosciences, 30(4):167-175, 2007.

[2] U. S. Bhalla. Multiscale interactions between chemical and electric signalling in LTP induction, LTP reversal and dendritic excitability. Neural Networks, 24:943-949, 2011.

[3] D. C. Sterratt, O. Sorokina and J. D. Armstrong. Integration of rule-based models and compartmental models of neurons. In *Hybrid Systems Biology: Second International Workshop, HSB 2013, Taormina, Italy, September 2, 2013 and Third International Workshop, HSB 2014, Vienna, Austria, July 23-24, 2014, Revised Selected Papers*, 7699:143–158, 2015.

[4] R. A. McDougal, M. L. Hines and W. W. Lytton. Reaction-diffusion in the NEURON simulator. *Frontiers in Neuroinformatics*, 7(28):1-13, 2013.

[5] O. Sorokina, A. Sorokin, J. D. Armstrong and V. Danos. A simulator for spatially extended kappa models. *Bioinformatics*, 29(23):3105-3106, 2013.

[6] P. Poirazi, T. Brannon and B. W. Mel. Arithmetic of subthreshold synaptic summation in a model CA1 pyramidal cell. *Neuron* 37:977-987, 2003.

[7] D. Y. Kim, L. A. MacKenzie, B. W. Carey, W. H. Pettingell and D. M. Kovacs. Presenilin/y-Secretase-mediated Cleavage of the Voltage-gated Sodium Channel B2-Subunit Regulates Cell Adhesion and Migration. *The Journal of Biological Chemistry*, 280(24):23251-23261, 2005.

[8] M. Roy, O. Sorokina, N. Skene, C. Simonnet, F. Mazzo, R. Zwart, E. Sher, C. Smith, J. D. Armstrong and G. N. Grant. Proteomic analysis of postsynaptic proteins in regions of the human neocortex. *Nature Neuroscience*, 21(1), 130-138, 2018.

Passive forgetting or selective attention? comparing two models of learning in multidimensional environments

AQ1

Guy Davidson[1]*, Angela Radulescu[2,3]*, Yael Niv[2,3]*

[1]Minerva Schools at KGI, San Francisco
[2]Department of Psychology, Princeton University, Princeton
[3]Princeton Neuroscience Institute, Princeton University, Princeton
**guy@minerva.kgi.edu; *angelar,yael@princeton.edu*

INTRODUCTION/MOTIVATION

Using a multidimensional reinforcement learning task in which one of three dimensions determines reward (*Figure 1)*, previous work showed that cognitive models incorporating passive decay of the values of unchosen options explained subject choice data better than competing models (Niv et al., 2015). More recently, models that assume attention-weighted

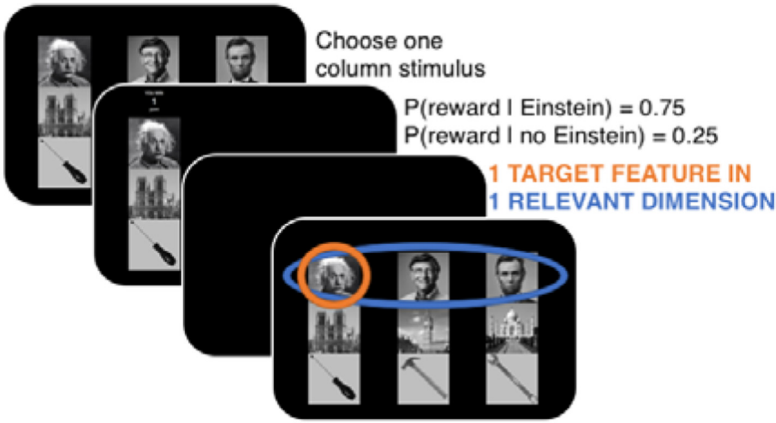

FIGURE 1: The Dimensions task. Subjects are presented with three stimuli, each a column, comprised of three features: a face, a landmark, and a tool. Rewards were contingent only on a single dimension, in which one feature provided a reward with high probability (0.75) and selecting a stimulus with the other two features yielded a reward with low probability (0.25).

reinforcement learning using eyetracking and MVPA (Multivoxel pattern analysis) based measures of attention were shown to predict the data equally well (Leong et al., 2017). We investigate whether the two models, which suggest different cognitive processes, explain the same aspect of the data, or rather different, complementary aspects. We find that the different models capture distinct trial dynamics: models incorporating attention predict subject choice considerably better immediately after they learn the task, while models including decay excel in predicting choices several trials afterward.

METHODS

We fit several different reinforcement learning models to trial-by-trial choice data of N=25 participants from Leong et al. (2017), combining the best-fitting models from the two previous publications. Models were implemented in MATLAB, parameters were fit by maximizing the likelihood of the data using fmincon (Matlab), and models were compared using leave-one-game-out cross-validation. We also designed and implemented additional analyses comparing the cross-validated likelihoods on a trial-by-trial basis, to test for differences between the models at different phases of the task.

RESULTS AND DISCUSSION

We show that combining the two models improves the overall average fit, as measured by cross-validated likelihood on held-out data, suggesting that these two mechanisms explain separate components of the variance (*Figure 2*). Trial-specific prediction accuracies of the models show that each model helps explain different trial dynamics depending on the progress a subject has made in learning the task. In particular, attention-weighted learning predicts choice substantially better in trials immediately following the point at which the subject has successfully learned the task (and made no further mistakes for the remainder of the current game), while passive decay better accounts for choices in trials further into the future relative to the point of

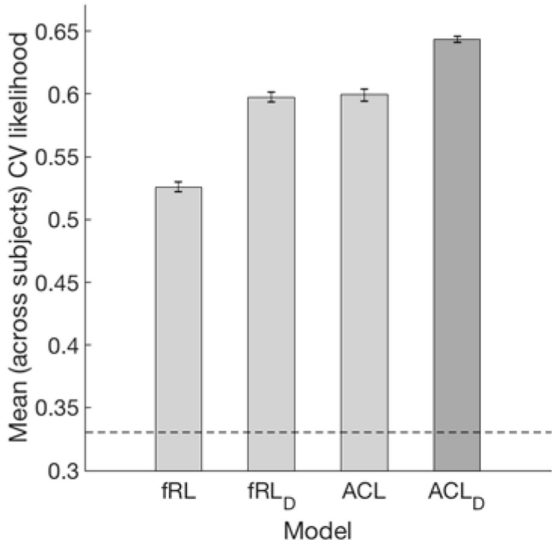

FIGURE 2: Mean cross-validated likelihood for each model (higher is better). fRL: baseline feature-wise reinforcement learning (RL) model. fRLD: feature-based RL model with decay, best-fitting model in Niv et al., (2015). ACL: attention at choice and learning RL model, best-fitting model in Leong et al. (2017). ACLD: attention at choice and learning model with decay, best-fitting model reported.

learning (*Figure 3*). Additional analyses demonstrate that the decay model fails to capture the choice immediately following the last mistake, but recovers quickly afterward, while attention aids in predicting choice both before learning and immediately after it, but not farther into the future. Together, these results suggest a possible role for decay in modeling choices that people make when exploiting learned knowledge of the task, while attention might account for choice behavior as participants actively test hypotheses about task structure early during learning.

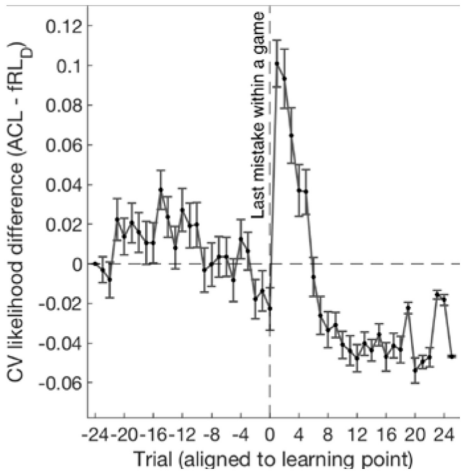

FIGURE 3: Difference between the likelihood of the ACL and fRLD models before, at, and far after the point at which subjects learn the task. The y-axis (x = 0) marks the trial where the subject made the last mistake in a given game, the point at which they learned that game. Before the point of learning (x < 0), both models perform reasonably similarly (i.e., both predict participants' choices with similar accuracy). At and immediately after learning (0 < x < 5), the ACL model performs substantially better, predicting more than 10% of additional variance, as compared to the decay model, while further into the future (x > 5) the decay model predicts choice significantly better.

AQ2

REFERENCES

[1] Niv, Y., Daniel, R., Geana, A., Gershman, S. J., Leong, Y. C., Radulescu, A., & Wilson, R. C. (2015). Reinforcement learning in multidimensional environments relies on attention mechanisms. Journal of Neuroscience, 35(21), 8145–57.

[2] Leong, Y. C., Radulescu, A., Daniel, R., DeWoskin, V., & Niv, Y. (2017). Dynamic Interaction between Reinforcement Learning and Attention in Multidimensional Environments. *Neuron 93*, 451–463.

Childhood trauma and social cognition in schizophrenia

Karolina I. Rokita[1,2], Maria R. Dauvermann[1,2], David Mothersill[1,2], Laurena Holleran[1,2], Jessica Holland[1,2], Laura Costello[2], Catherine O'Donoghue[1], Caroline Cullen[3,4], Niamh Daly Ryan[1,4], Colm McDonald[5], Brian Hallahan[5], Aiden Corvin[4], Michael Gill[4], Gary Donohoe[1,2]

AQ1

AQ6

[1]School of Psychology, National University of Ireland Galway, Ireland
[2]Centre for Neuroimaging and Cognitive Genomics, National University of Ireland Galway, Ireland
[3]Wellcome – HRB Clinical Research Facility, St. James's Hospital, Dublin, Ireland
[4]Department of Psychiatry, Trinity Centre for Health Sciences, St. James's Hospital, Dublin, Ireland
[5]Department of Psychiatry, Clinical Science Institute, National University of Ireland Galway, Ireland

BACKGROUND

In the last two decades, there has been a substantial number of studies indicating a link between schizophrenia (SZ) and early life adversities, such as childhood trauma (CT), which is highly prevalent in psychiatric populations [1]. However, little is known about the association between CT and social cognition, defined as a set of mental operations underlying social interactions and comprising of: Theory of Mind, emotion recognition and regulation, social perception and attributional style. Social cognitive deficits are a hallmark feature of SZ, which may result in impaired social and occupational functioning [2]. In a limited number of studies, childhood trauma has been shown to deleteriously impact on later social cognitive function in individuals with schizophrenia and to a lesser extent, in healthy individuals [3]. The aim of this study is to examine whether childhood adversity is associated with social cognitive abilities in both patients with schizophrenia and healthy controls.

METHODS

Thirty patients with SZ (mean age=43.93; SD=11.80; 18 males, 12 females) and thirty healthy controls (mean age=33.07; SD=9.88; 17 males, 13 females) completed the Childhood Trauma Questionnaire (CTQ), which assesses the frequency and severity of five types of CT: emotional abuse, physical abuse, sexual abuse, emotional neglect and physical neglect. Furthermore, all participants underwent three social cognitive tasks: the Reading the Mind in the

Eyes Task (RME) and the Hinting Task that evaluate the ability to infer emotions and mental states of others, and the Emotion Recognition Task (ERT), which is implemented in the Cambridge Neuropsychological Test Automated Battery and measures the ability to identify six basic emotions in facial expressions (sadness, happiness, fear, anger, disgust or surprise). Pearson's correlation coefficient was carried out to investigate the association between various types of childhood trauma and social cognitive tasks.

RESULTS

We found that a history of CT in patients, specifically physical neglect, was significantly negatively associated with poorer performance on the RME task ($r=-.623$, $p<.001$) and deficits in recognising disgust ($r=.415$, $p<.05$). Physical and sexual abuse were positively correlated with recognition of sad faces ($r=.494$, $p<.01$; $r=.406$, $p<.05$ respectively). In healthy controls, a history of emotional neglect was significantly negatively associated with deficits in recognising disgust ($r=-.434$, $p<.05$) and physical neglect was positively correlated with recognition of fear ($r=.364$, $p<.05$). No significant associations were found between CT and the total score on the Hinting Task in any of the groups.

DISCUSSION

These results suggest that the experience of CT has an impact on emotion recognition and Theory of Mind abilities in patients with SZ. Since deficits in social cognition are suggested to represent a core aspect of disability in schizophrenia and are not generally improved by antipsychotic medication [4,5], a better understanding of the role of early childhood experiences in the development of social cognitive abilities is crucial. Further, the findings highlight the importance of addressing the various types of early childhood social experience and adversity in the assessment and intervention protocols of mental health treatments (e.g.Cognitive Behavioural Therapy), and psychosocial interventions that will specifically target social cognitive deficits. Early interventions (e.g. parenting programs) should also be implemented in an effort to minimise the occurrence of childhood adversities or reduce their impact.

ACKNOWLEDGMENTS

This work was supported by grants from the European Research Council (ERC-2015-STG-677467) and Science Foundation Ireland (SFI-16/ERCS/3787). The PhD is funded by the Hardiman Research Scholarship from NUI Galway.

AQ2

REFERENCES

[1] Read, J., Perry, B.D., Moskowitz, A., Connolly, J. (2001). The contribution of early traumatic events to schizophrenia in some patients: a traumagenic neurodevelopmental model. Psychiatry, 64, 319–345.

[2] Green, M.F. (2016). Impact of cognitive and social cognitive impairment on functional outcomes in patients with schizophrenia. JClinPsychiatry, 77, 8–11.

[3] Rokita, K.I., Dauvermann, M.R., Donohoe, G. (2018). Early life experiences and social cognition in major psychiatric disorders: a systematic review. European Psychiatry, 53, 123-133.

[4] Daros, A.R., Ruocco, A.C., Reilly, J.L., Harris, M.S., Sweeney, J.A. (2014). Facial emotion recognition in first-episode schizophrenia and bipolar disorder with psychosis. Schizophr Res, 153, 32–37.

[5] Kucharska-Pietura, K., Mortimer, A. (2013). Can antipsychotics improve social cognition in patients with schizophrenia? CNS Drugs, 27, 335–343.

Sound, motion, and the brain: Exploring how sounds affect the creation of movements within an improvised performance

AQ1 **Ioannis Sidiropoulos[1]*, Roger Alsop[2]***

[1]University of Melbourne, Building 864, 234 St Kilda Road, Southbank, Victoria, Australia
[2]University of Melbourne, Building 864, 234 St Kilda Road, Southbank, Victoria, Australia
**i.sidiropoulos@student.unimelb.edu.au; *ralsop@unimelb.edu.au*

INTRODUCTION

This paper discusses the specultaive experimental design/methodology intended to be used to explore the coupling of perception-action in the context of understanding creativity influenced by sounds in improvised dance and physical theatre. It intends to examine the effects of auditory perception on movement improvisation and how this informs the creative process of a performance. It questions how sounds affect the brain during the creation of improvised bodily movements while listening to sounds, and how sounds influence the movement choices of the performers. This research combines contemporary dance and physical theatre practices along with cognitive neuroscience. It will explore the response to sound as expressed through movement and how this may be used in analysing movements and developing choreographic processes in dance and physical theatre. The sounds for this experimental process are recorded sounds (blended music and environmental sounds).

METHODOLOGY

The methodology will incorporate movement analysis, brain signal analysis and discussion with participants. The experimental processes has two phases. In phase one (behavioural data), a group of performers (group 1) will improvise while paying specific and primary attention to the sounds (contemporary music blended with man-made environmental sounds) they are hearing – not their movements. These movements will be video captured via digital (DSLR) cameras and three-dimensional recording via Microsoft Kinect System. The captured data will then be parsed for similarities between participants movements which will be distilled to form similar taxonomies.

This will focus on upper, middle and lower body movements, analysing them with the Laban Movement Analysis (LMA), not considering the potential meaning or interpretation of the movement. In phase two (neural activity data), group 1 and a new group of performers (group 2) will be asked to imagine improvising to the same sounds while their brain activity is being recorded via an fMRI (functional Magnetic Resonance Imaging) scanner. They will watch the video recordings made in phase 1 while listening to the same sounds and their brain activity also recorded via an fMRI scanner. All data will be compared and correlated for similarities.

RESULTS AND DISCUSSION

These behavioural and neural activity data will be compared and correlated, informing the creative process of a new experimental choreographic work, based on the combination of the gathered data. This is an ongoing exploration and early stage results will be presented.

AQ2

REFERENCES

AQ3 Anderson, John R., Raluca Budiu, and Lynne M. Reder. 2001. "A theory of sentence memory as part of a general theory of memory." *Journal of Memory and Language* 45 (3):337-367. doi: 10.1006/jmla.2000.2770.

Batson, Glenna, and Margaret Wilson. *Body and mind in motion: dance and neuroscience in conversation*.

Bergland, Christopher. 2018. *Psychology Today*. May 8. Accessed August 25, 2018. https://www.psychologytoday.com/au/blog/the-athletes-way/201805/the-powerful-psychological-benefits-dance.

Bläsing, Bettina, Martin Puttke-Voss, and Thomas Schack. 2010. *The neurocognition of dance: mind, movement and motor skills*. Hove, East Sussex England; New York: Psychology Press.

Finke, R. A. 1996. "Imagery, creativity, and emergent structure." *Conscious Cogn* 5 (3):381-93. doi: 10.1006/ccog.1996.0024.

Foster, Ruth. 1976. *Knowing in my bones*. London: A. and C. Black.

Gazzaniga, Michael S. 1984. *Handbook of cognitive neuroscience*. 1st ed. New York: Plenum Press.

Gazzaniga, Michael S., Richard B. Ivry, and G. R. Mangun. 2009. *Cognitive neuroscience: the biology of the mind*. 3rd ed. New York: W.W. Norton.

Grove, Robin, Catherine J. Stevens, and Shirley McKechnie. 2005. "Thinking in four dimensions creativity and cognition in contemporary dance."In. Carlton, Vic.: Melbourne University Press,. http://search.informit.com.au.ezp.lib.unimelb.edu.au/browsePublication;res=IELHSS;isbn=0522851452 Connect to ebook (University of Melbourne only).

Hanna, Judith Lynne. 1979. *To dance is human: a theory of nonverbal communication*. Austin: University of Texas Press.

Humphrey, Doris. 1959. *The art of making dances*. New York: Rinehart.

Kandel, Eric R., James H. Schwartz, Thomas M. Jessell, Steven A. Siegelbaum, A. J. Hudspeth, and Sarah Mack. 2013. "Principles of neural science."In *Neurology Collection*. New York, N.Y.: McGraw-Hill Education LLC.

Limón, J. 1955. *Composing a Dance*: Juilliard School of Music.

Piccinini, G., and S. Bahar. 2013. "Neural computation and the computational theory of cognition."*Cogn Sci* 37 (3):453-88. doi: 10.1111/cogs.12012.

Rizzolatti, G., L. Fadiga, V. Gallese, and L. Fogassi. 1996. "Premotor cortex and the recognition of motor actions."*Brain Res Cogn Brain Res* 3 (2):131-41.

Stevens, Catherine, Stephen Malloch, Shirley McKechnie, and Nicole Steven. 2003. "Choreographic cognition: The time-course and phenomenology of creating a dance." *Pragmatics & Cognition* 11 (2):297-326. doi: 10.1075/pc.11.2.06ste.

Ward, Jamie. 2010. *The student's guide to cognitive neuroscience*. Second edition. Hove; New York: Psychology Press.

Three dimensional analyses of synapses in the human temporal neocortex

AQ1 **Nicolás Cano-Astorga[1], Javier DeFelipe[1,2,3], Lidia Alonso-Nanclares [1,2,3]**

[1]*Laboratorio Cajal de Circuitos Corticales (CTB), Universidad Politécnica de Madrid, Campus de Montegancedo s/n, Pozuelo de Alarcón Madrid, Spain* AQ6

[2]*Centro de Investigación Biomédica en Red sobre Enfermedades Neurodegenerativas (CIBERNED), C/Valderrebollo, Madrid, Spain*

[3]*Instituto Cajal (CSIC), Avda. Doctor Arce, Madrid, Spain*

INTRODUCTION

Brain organization is extremely complex and our current knowledge about it is far from being completed. The cerebral cortex attracts the researcher's attention because it is the region where cognitive process takes place. Concretely, Brodmann's area 21 or Temporal 2 (T2) is an associative six-layered cortex located in middle temporal gyrus [1]. It is strongly connected to others associative cortices trough cortico-cortical layer III projecting neurons [2, 3]. At a functional level, it is a critical node for language-based semantic processing, acting as interface between sensorimotor language and internal mental world [4] as well as leading social animations identification [5]. To understand how neuronal circuits contribute to the functional organization of the cerebral cortex requires a detailed ultrastructural analysis of neuronal connectivity. We have selected layer III from T2 to perform a detailed three dimensional ultrastructural analyses of the neuropil, the region where most of the synaptic contacts are located.

METHODS

T2 samples were obtained from non-pathological tissue of biopsies from epilepsy patients (3 males and 2 females), who reported normal T2 electrophysiological activity during surgery. We have used a focused ion beam/scanning electron microscopy (FIB/SEM) which allows imaging serial sections by removal of 20 nm-thick layers of material, leading to fully reconstruct of a given volume [6]. Stacks of images obtained by the FIB/SEM were analyzed using EspINA software which allows the 3D reconstruction of synapses. Once the synaptic junctions were fully reconstructed, each synapse could be classified as asymmetric (AS) or symmetric (SS) based on its prominent

or thin post-synaptic density, respectively. EspINA also provides the number of synapses in a given volume, which allows the estimation of the number of synapses per volume.

RESULTS

The main goal of this study is to provide T2 layer III neuropil synaptic data, in particular, its synaptic density per unit volume, and the excitatory/inhibitory synaptic balance. Preliminary results (Figures 1, 2) based on 5111 identified synapses, which 3590 were finally analyzed, shows synaptic density ranges 0.52-0.92 synapse/ μm^3 and mean balance were 93.97% for AS and

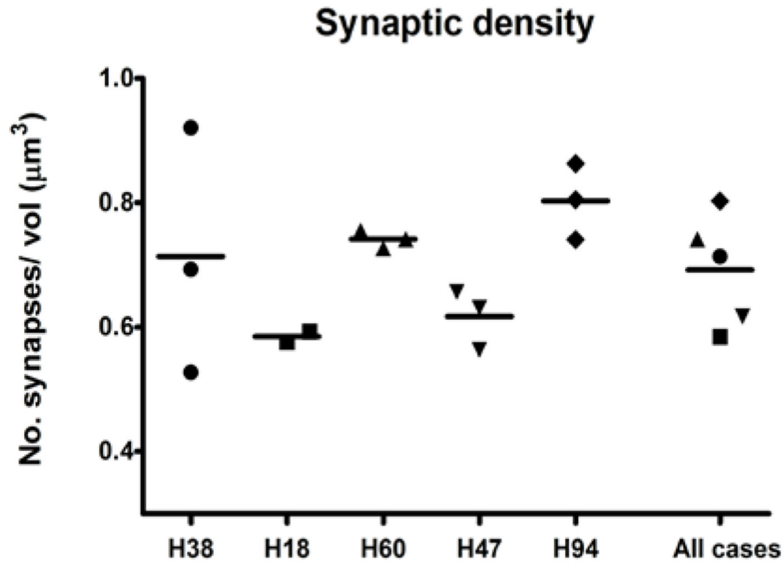

FIGURE 1: Synaptic density.

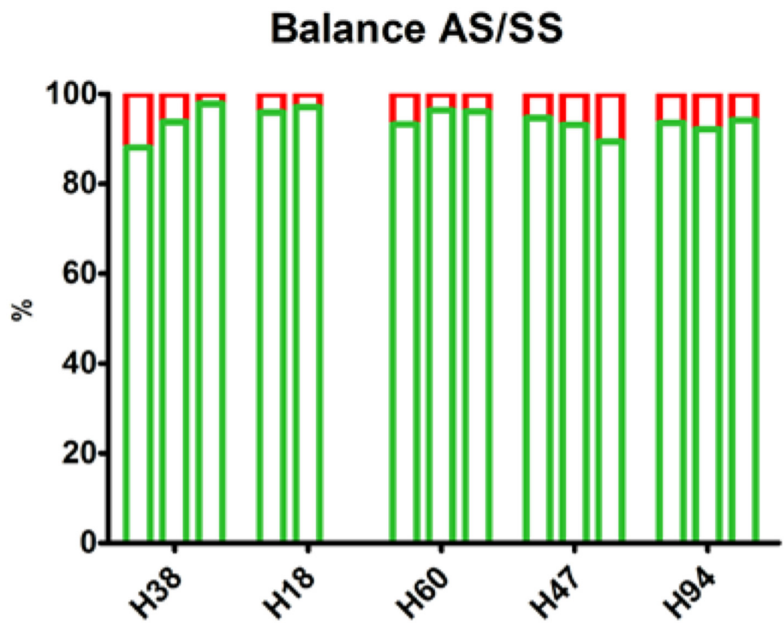

FIGURE 2: Balance AS/SS.

6.03% for SS, which concur with human related literature [7]. Investigating the synaptic properties of cerebral cortex is essential to better understand the human synaptome.

AQ2

REFERENCES

[1] HM Duvernoy. The Human Brain Surface, Three-Dimensional Sectional Anatomy with MRI, and Blood Supply. *SpringerWienNewYork*. 1991.

[2] LC Triarhou. Cellular structure of the human cerebral cortex; translated and edited version of "Zellaufbau der grosshirnrinde des menschen" (von Economo, 1927). *Karger*. 2009.

[3] J. Xu, J.Wang, L.Fan, H.Li, W.Zhang, Q.Hu, et al. Tractography-based parcellation of the human middle temporal gyrus. *Sci Rep*, 5:18883, 2015.

[4] Y. Xu, Q.Lin, Z.Han, Y.He and Y.Bi. Intrinsic functional network architecture of human semantic processing: Modules and hubs. *Neuroimage*, 132:542-55, 2016.

[5] M. Schurz, MG.Tholen, J.Perner, RB.Mars and J.Sallet. Specifying the brain anatomy underlying temporo-parietal junction activations for Theory of Mind: A review using probabilistic atlases from different imaging modalities. *Hum Brain Mapp*, 38:4788-805, 2017.

[6] A. Merchán-Pérez, JR.Rodriguez, L.Alonso-Nanclares, A.Schertel and J.DeFelipe. Counting synapses using FIB/SEM microscopy: a true revolution for ultraestructural volumen reconstruction. *Front Neuroanat*, 3:18, 2009.

[7] M. Domínguez-Álvaro, M.Montero-Crespo, L.Blazquez-Llorca, R.Insausti, J.DeFelipe and L.Alonso-Nanclares. Three-dimensional analysis of synapses in the transentorhinal cortex of Alzheimer´s disease patients. *Acta Neuropathol Commun*, 6:20, 2018.

Multiple alignment of packet sequences for efficient communication in a many-core neuromorphic system

Luca Peres[1,2]*, Gianvito Urgese[2]*, Francesco Barchi[2], Andrea Acquaviva[2], Enrico Macii[2]

AQ1

[1]Department of Control and Computer Engineering, School of Computer Science, University of Manchester
[2]Politecnico di Torino
**luca.peres-2@manchester.ac.uk; *gianvito.urgese@polito.it*

INTRODUCTION

Emerging many-core architectures provide dense interconnection fabrics leading to new communication requirements. In particular, the effective exploitation of synchronous and asynchronous channels for fast communication from/to internal cores and external devices is a crucial issue for these architectures. SpiNNaker and Intel Loihi are two of the promising architectures described in the literature [1]. The direction taken by hardware designers is to integrate many processing elements (PEs) cores and several layers of memory on each chip with custom communication infrastructures. These cores are distributed in computing clusters across the architecture, each with locally shared memory. The SpiNNaker system [2] requires two preliminary phases for setting-up the applications: the task-graph placement [3], where the application is partitioned and placed on the cores and the configuration of the cores with application-specific data structures [4]. This last phase requires to send a list of op-codes (commands to be executed) generated on a host machine to a configurator application (pre-loaded on each core) capable of interpreting these codes and creating the data structures necessary for the final applications. Currently, the host transmits these lists of op-codes to the SpiNNaker cores by instantiating many unicast transmissions (one for each core involved in the application) even though many of the transmitted packets contain the same information and could be potentially clustered in a more efficient stream.

METHOD

We designed a clustering methodology that uses the Multiple Sequence Alignment (MSA) algorithm [5] for transforming the many unicast streams, needed for configuring the system, in a consistent multicast/broadcast stream that fully exploits the features offered by the custom communication infrastructure. Our pre-processing step, implemented in C++ using the SeqAn bioinformatics library [6], is capable of clustering the recurrent pieces into a single stream that can be transmitted using a multicast transmission. Now packets are labeled as Multicast (for multiple destinations), Broadcast (to communicate with all the cores) or Unicast (for a single destination) and sent to the target group of cores depending on the label.

RESULTS AND COMMENTS

Figure 1 shows the number of packets generated for four versions of the Thalamo-Cortical Microcircuit (TCM) [8]. Blue bars represent the number of packets sent using unicast streams, without op-codes alignment, in which data are transmitted as they are. Green/red/yellow stacked bars indicate the number of packets sent using a multicast stream generated with the MSA

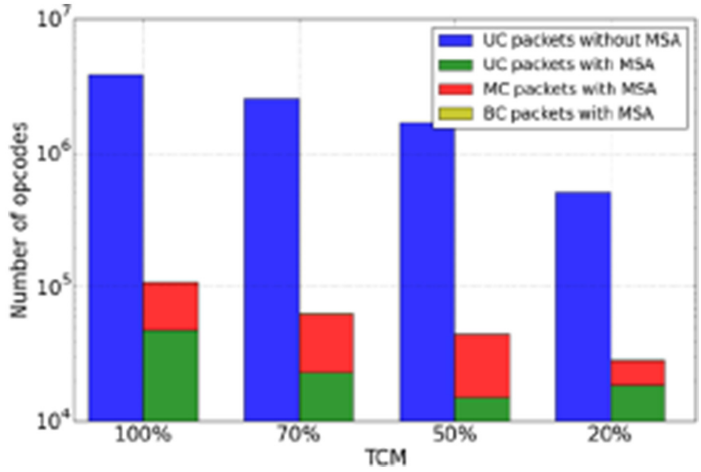

FIGURE 1: Packets comparison.

Table 1: Execution stats

TCM	Number of chips	Number of cores	Saved
100%	157	390	97.1%
70%	70	274	97.5%
50%	40	196	97.3%
20%	17	80	94.3%

procedure designed for clustering recurrent packets. In Table 1 we present the number of saved packets for the four scaled versions of the TCM application alongside with the number of chips and cores allocated for each version.

In conclusion, we developed a system able to cluster the information in order to exploit the multicast network, reducing the number of packets generated of a quantity up to the 97% and improving the host-board communication phase. The described procedure, in principle, can be applied to all type of packet transmissions towards the communication mesh for reducing the bottleneck given by the data transmission phase.

AQ2

REFERENCES

AQ3

[1] Wikipedia. 2018. AI accelerator. (2018). https://en.wikipedia.org/wiki/AI_ accelerator

[2] Steve B Furber et al. 2013. Overview of the spinnaker system architecture. IEEE Transactions on Computers 62, 12 (2013), 2454–2467.

[3] Gianvito Urgese et al. 2016. Optimizing network traffic for spiking neural network simulations on densely interconnected many-core neuromorphic platforms. IEEE Transactions on Emerging Topics in Computing (2016).

[4] Alessandro Siino et al. 2016. Data and commands communication protocol for neuromorphic platform configuration. In MCSoC, 2016 IEEE 10th International Symposium on. IEEE, 23–30.

[5] Cédric Notredame et al. 2000. T-coffee: a novel method for fast and accurate multiple sequencealignment1. Journal of molecular biology 302, 1 (2000), 205–217.

[6] Knut Reinert et al. 2017. The SeqAn C++ template library for efficient sequence analysis: a resource for programmers. Journal of biotechnology 261 (2017), 157–168.

[7] Gianvito Urgese et al. 2018. Multiple Alignment of Packet Sequences for Efficient Communication in a Many-core Neuromorphic System: Work-in-progress. Proceedings of the International Conference on Compilers, Architecture and Synthesis for Embedded Systems, Article No.3.

[8] Potjans, T. C., and Diesmann, M. (2014). The cell-type specific cortical microcircuit: relating structure and activity in a full-scale spiking network model. Cereb. Cortex 24, 785–806. doi: 10.1093/cercor/bhs358.

Mathematical model order reduction in computational neuroscience

AQ1 **Mikko Lehtimäki*, Lassi Paunonen, Marja-Leena Linne**

Tampere University
mikko.lehtimaki@tut.fi

INTRODUCTION

Multi-scale models in neuroscience typically integrate detailed biophysical neurobiological phenomena from molecular level up to network and system levels. Such models are challenging to simulate despite the availability of massively parallel computing systems. Model Order Reduction (MOR) is an established method in engineering sciences, such as control theory. MOR is used in improving computational efficiency of simulations of large-scale and complex nonlinear mathematical models. In this study the dimension of a nonlinear mathematical model of plasticity in the brain is reduced using mathematical MOR methods.

Traditionally, models are simplified by eliminating variables, such as molecular entities and ionic currents. Additionally, assumptions of the system behavior can be made, for example regarding the steady state of the chemical reactions. However, comprehensive models with full system dynamics are needed in order to increase understanding of different mechanisms in the brain. Thus the elimination approach is not suitable for the consequent analysis of neural phenomena. The loss of information typically induced by eliminating variables of the system can be avoided by mathematical MOR methods that approximate the entire system with a smaller number of dimensions compared to the original system. Here, we demonstrate the effectiveness of MOR in approximating the behavior of all the variables in the original system by simulating a model with a radically reduced dimension.

In the present work, mathematical MOR is applied in the context of an experimentally verified signaling pathway model of plasticity [1]. This nonlinear chemical equation based model describes biochemical calcium signaling in plasticity and learning in the subcortical area of the brain. The model consists of 44 variables and is time-dependent, which poses an additional challenge both computational efficiency and reduction wise.

METHODS

The MOR method we employed is Proper Orthogonal Decomposition with Discrete Empirical Interpolation Method (POD+DEIM), a subspace projection method for reducing the dimensionality of nonlinear systems [2]. By applying these methods, the simulation time of the model is radically shortened. However, in very long simulations, steady state of the reduced model might diverge from the original. The tolerated amount of approximation error depends on the final application of the model. Based on these promising results, POD+DEIM is recommended for dimensionality reduction in computational neuroscience.

RESULTS AND DISCUSSION

In summary, the reduced order model consumes a considerably smaller amount of computational resources than the original model, as seen in Figure 1. A low root mean square error between the variables in the original and reduced model is achieved without losing any variables from the model.

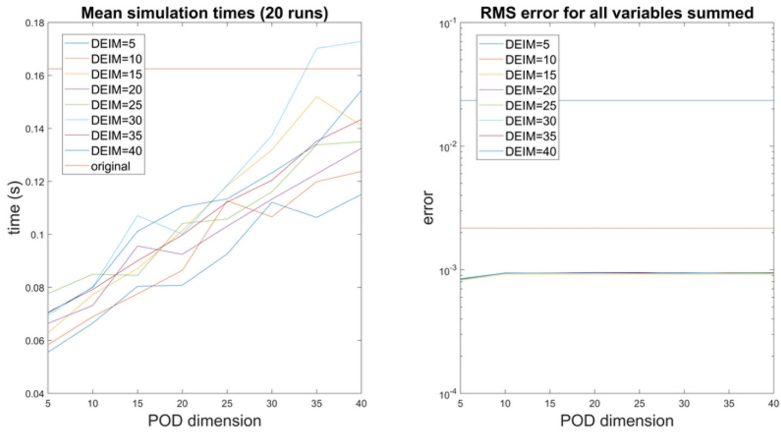

FIGURE 1: Simulation time (left) and Root Mean Square error (right) of the reduced model compared to the full dimensional model, for DEIM dimensions as function of POD dimension.

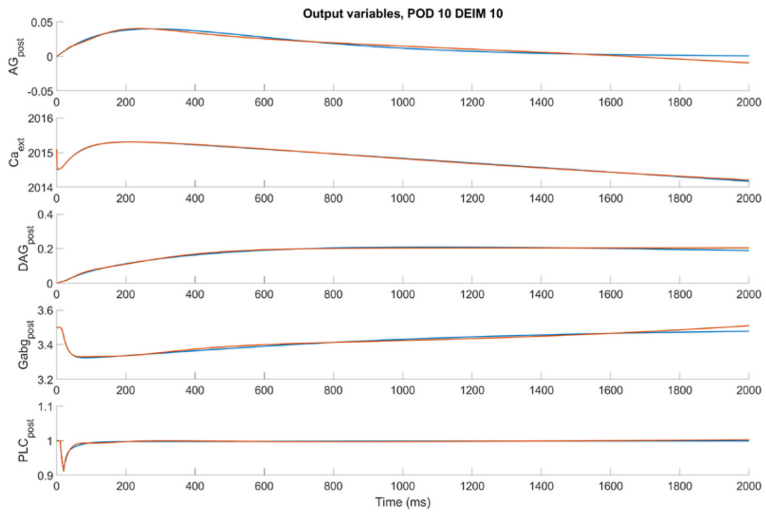

AQ4

FIGURE 2: Trajectories of selected variables from the original model (blue) and the reduced model (red) with POD and DEIM dimension set to 10. Glutamate and Calcium stimulus is indected at t=10 *ms*.

The results presented here are novel as mathematical MOR has not been studied in neuroscience without linearisation of the mathematical model and never in the context of the model presented here.

AQ2

REFERENCES

[1] B. Kim, S. Hawes, F. Gillani, L. Wallace, and K. Blackwell, "Signaling pathways involved in striatal synaptic plasticity are sensitive to temporal pattern and exhibit spatial specificity." PLoS Comput Biol, vol. 9, no. 3, Mar. 2013.

[2] S. Chaturantabut and D. Sorensen, "Nonlinear model reduction via discrete empirical interpolation," SIAM Journal of Scientific Computing, vol. 32, no. 5, pp. 2737–2764, Sep. 2010.

From transcription to projection: Integrative multiscale frameworks for a cell-type specific mouse mesoconnectome

AQ1

Nestor Timonidis[1]*, Rembrandt Bakker[1,2]*, Paul Tiesinga[1]*

[1]Neuroinformatics department, Donders Institute for Brain, Cognition and Behaviour, Radboud University Nijmegen, The Netherlands
[2]Inst. of Neuroscience and Medicine (INM-6) and Inst. for Advanced Simulation (IAS-6) and JARA BRAIN Inst. I, Jülich Research Centre, Germany.
**n.timonidis@donders.ru.nl; *r.bakker@donders.ru.nl; *p.tiesinga@science.ru.nl*

INTRODUCTION

One of the original ambitions of the Human Brain Project was the development of a large-scale cellular level model of the human brain that could be used for comprehending fundamental mechanisms of cognition and brain diseases [1]. For such an achievement to be accomplished, adequate information about the cellularly-resolved structural connectome of the brain must be present. Given the breakthrough in [2] of a fully described mouse mesoconnectome, this study aims to proceed in a cell-type specific description by applying a set of machine-learning based computational approaches on high-throughput molecular and cellular mouse brain related data sources for connectivity inference.

METHODS

High dimensional imaging data from the Allen Brain Institute [3] are being processed by an informatics pipeline[4], resulting in 2-dimensional matrices used for connectivity inference. The two data sources are ISH (in situ hybridization) spatial gene expression patterns and tract-tracing connectivity patterns spanning the whole brain. According to our methodology, supervised machine learning algorithms (Random Forest, Logistic Regression) are being applied to the gene expression dataset, training it to learn the connectivity patterns. The connectivity patterns constitute two categories, namely cell-class speciifc and cell-class inspecific projections [5]. The predictive accuracy for all projection patterns is being evaluated through the use of the cross-validation technique with measurements such as area under the roc curve (AUC) and f-score.

Moreover, the most important genes for each connectivity pattern are being selected and applied to a gene-ontology enrichment analysis, and the molecular function and biological process of those sets are being examined.

RESULTS

There is no significant difference between the cell class specific and inspecific prediction patterns, which suggest that projection patterns are similar in both cases. Results are more significant than random for both classifiers, since in every case they exceed a baseline classification with random assignments.

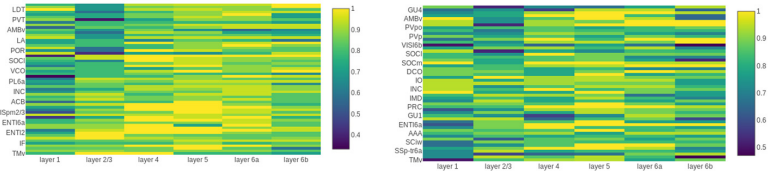

AQ4

FIGURE 1: Prediction accuracy of connectivity patterns from cortical areas to specific laminar-profiles. Left panel: intratelencephalic cell class projections. Right panel: corticothalamic cell class projections. X-axis: cortical areas. Y-axis: laminar profiles (layers 1 – 6b). The legend to the right maps colors to predictive accuracies.

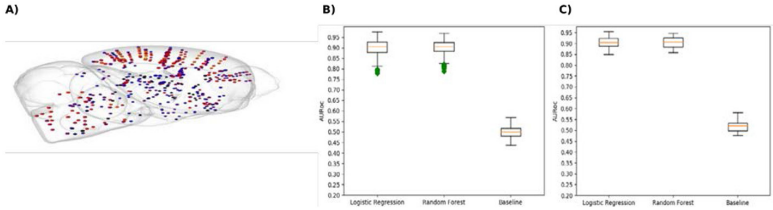

AQ4

FIGURE 2: (**A**) Spatial plot of prediction accuracy for projections in wild-type mouse. (black: 0.7, blue: 0.8; red: 0.9, yellow: 1.0), produced with Scalable Brain Composer (scalablebrainatlas.incf.org/composer). The result suggests that predicting projections to subcortical regions is harder than to cortical regions. (**B**) Box plots corresponding to area under the curve (AUC) values for prediction accuracy of a set of connectivity patterns in cell-class specific patterns. (**C**) Same as B for cell-class inspecific (wild-type mice). X-axis: classification approach. Y-axis: AUC values.

Finally, an average AUC value higher than 80% for each pattern suggests the presence of connectivity signal in the ISH gene expression data which might be explained by the encoding of synapse formation by transcriptional factors.

AQ2

REFERENCES

[1] H Markram. The Human Brain Project. Scientific American 306, 50-55. 2012.

[2] SW Oh, JA Harris, L Ng, et al. A mesoscale connectome of the mouse brain. Nature, 508(7495), 207-214. 2014.

[3] ES Lein, MJ Hawrylycz, N Ao, M Ayres, A Bensinger et al. Genome-wide atlas of gene expression in the adult mouse brain. Nature, 445, 68–176. 2007.

[4] S Ji, A Fakhry, H Deng. Integrative analysis of the connectivity and gene expression atlases in the mouse brain. Neuroimage 84:245–253. 2014.

[5] JA Harris. et al. The organization of intracortical connections by layer and cell class in the mouse brain. bioRxiv. 2018.

Graph signal processing of high density EEG signals in disorders of consciousness

AQ1 **Sepehr Mortaheb[1]*, Jitka Annen[1], Camille Chatelle[1,2], Olivia Gosseries[1], Steven Laureys[1]**

[1]Coma Science Group, GIGA Consciousness - GIGA Research, University of Liège, Liège, Belgium
[2]Laboratory for NeuroImaging of Coma and Consciousness, Massachusetts General Hospital, Boston, MA, USA
**s.mortaheb@uliege.be*

INTRODUCTION

Graph signal processing (GSP) is a novel approach to analyse multi-dimensional neuroimaging data, constraining functional measures by structural characteristics in a single framework (i.e. graph signals) [1-4]. In this approach, functional time series are assigned to the vertices of the underlying structural graph. GSP analysis is performed in each time point of the signal. We used GSP to analyse high density electroencephalography (hd-EEG) in patients with disorders of consciousness (DOC) and healthy subjects. DOC patients suffer from reduced levels of consciousness after a sever brain injury and include unresponsive wakefulness syndrome (UWS), minimally conscious state (MCS, also sub-categorised into MCS- and MCS+ the latter showing signs of language preservation), and emergence from minimally conscious state (EMCS) [5]. In this study, we investigated the use of GSP framework to study functional-structural connectivity relationship of these patients especially in alpha band (8-12 Hz) which has been shown as an important frequency band in these disorders [6].

METHODS

Resting state EEG signals were recorded using a 256 electrode EGI system with a sampling rate of 250 Hz for 30 minutes. A convenient sample of 40 patients (10 UWS, 10 MCS-, 10 MCS+, 10 EMCS, 22 male, age: 40 $\pm$ 15.63 (Median $\pm$ SD)) and 10 age-matched healthy subjects (6 male, age: 44.5 $\pm$ 11.45 (Median $\pm$ SD)) were included. EEG data were preprocessed and segmented into 2 seconds epochs. For each subject, the first 150 clean epochs (i.e. 5 mins) were used for analysis. In order to perform GSP analysis, underlying weighted graphs were constructed based on the Euclidean distances between each

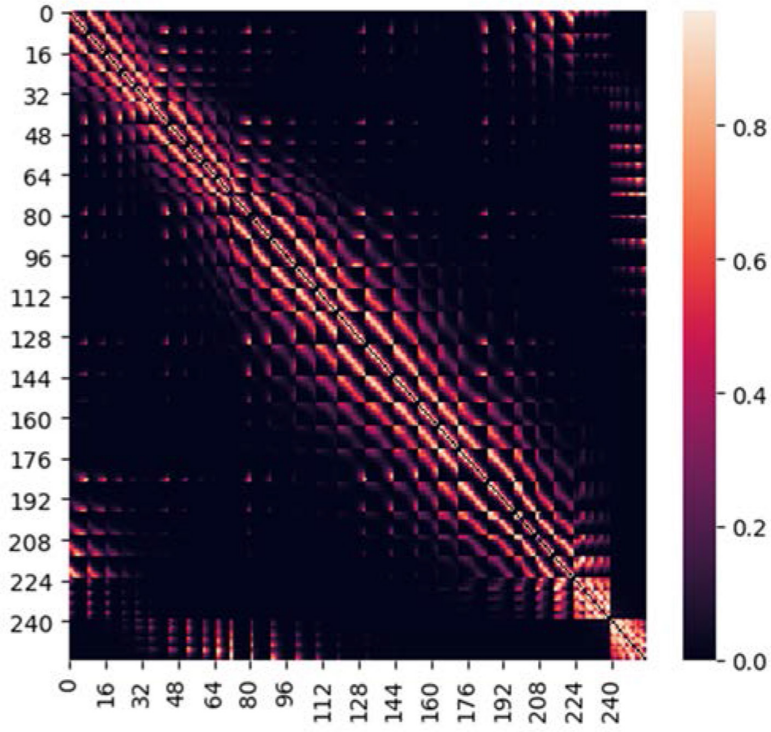

FIGURE 1: Structural connectivity matrix made based on the EGI cap electrode distances.

pair of electrodes (Fig.1). Then, total variation (TV) [2] of EEG in the alpha band (8-12 Hz) at each time point was calculated, supported by the underlying weighted graph. For every subject, the mean TV value was calculated for each epoch and the median TV over epochs was reported. Clinical diagnosis was defined as the best diagnosis based on repeated Coma Recovery Scale-Revised (CRS-R) assessment. To see whether there is a trend in the median TV of subjects in different levels of consciousness a Jonckheere Terpstra (JT) trend test was performed. In addition, a Spearman correlation test was done to investigate any relationship between median TV and CRS-R score.

RESULTS AND DISCUSSION

Increased TV in the alpha band was observed with increasing level of consciousness (JT=4.6195, $p<0.001$, Fig.2). In addition, a positive correlation ($R^2=0.873$, $p<0.001$, Fig.3) between TV in the alpha band and CRS-R score of the patients was observed. TV is theoretically the sum of local variations in each electrode, supported by the weighted structural graph. Our results suggest that as the level of consciousness decreases, the TV in the alpha band decreases. This is possibly related to increased local segregation of information in pathological states of consciousness. In the future, GSP analysis could consider connectivity in the temporal and spatial domain for the supporting graph, to provide a truly multi-modal analysis in DOC patients.

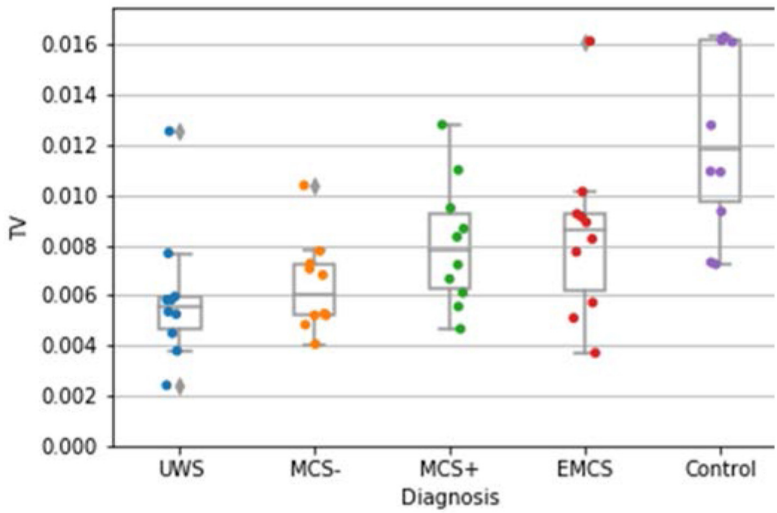

FIGURE 2: Median total variation of graph signals of different DOC patients and healthy controls.

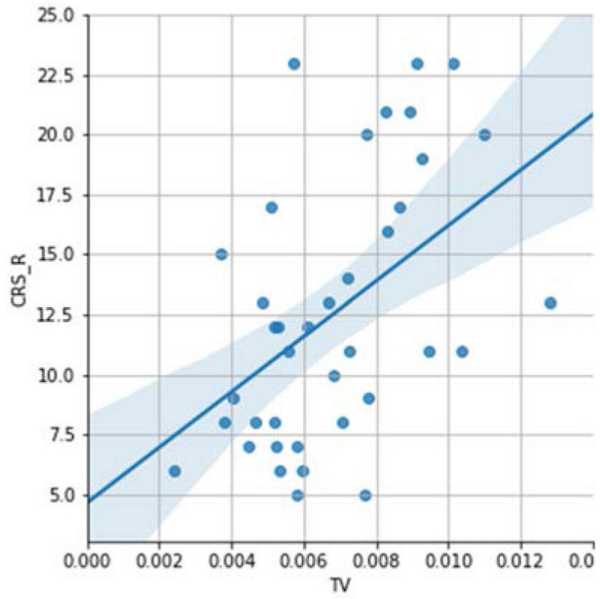

FIGURE 3: Correlation analysis between total variation of graph signals and CRSR score

AQ2

REFERENCES

[1] J. D. Medaglia, W. Huang, E.A. Karuza, et. al., Functional alignment with anatomical networks is associated with cognitive flexibility, *Nature Human Behaviour*, 2(2):156, 2018.

[2] D. I. Shuman, S. K. Narang, P. Frossard, et. al., The emerging field of signal processing on graphs: extending high-dimensional data analysis to networks and other irregular domains, *IEEE Signal Processing Magazine*, 30(3): 83-98, 2013.

[3] M. Menoret, N. Farrugia, B. Pasdeloup, and V. Gripon, Evaluating graph signal processing for neuroimaging through classification and dimensionality reduction, In proceedings of *Signal and Information Processing (GlobalSIP), 2017 IEEE Global Conference on*, 618-622, 2017.

[4] W. Huang, T. A. W. Bolton, J. D. Medaglia, et. al., Agraph signal processing perspective on functional brain imaging, In *Proceedings of the IEEE*, 2018.

[5] C. Schnakers, S. Laureys. Coma and disorders of consciousness. *Springer*. 2017.

[6] S. Chennu, P. Finoia, E. Kamau, et. al., Spectral signatures of reorganised brain networks in disorders of consciousness, *PLoS computational biology*, 10(10):e1003887, 2014.

An evolutionary optimisation framework for SpiNNaker

Edward Jones*, Steve Furber*

School of Computer Science, University of Manchester, Oxford Road, Manchester M13 9PL, UK
**edward.jones-3@manchester.ac.uk; *steve.furber@manchester.ac.uk*

INTRODUCTION/MOTIVATION

Parameter tuning and optimisation of SNN models have applications in both biological models and in the conversion of artificial neural networks (ANNs) models to SNN models 1 . Experimental limits to the data that can be collected in vivo mean that SNN models of biological neural networks often require several parameters to be estimated or tuned. The SNN models that result from the conversion of ANNs 2 could be optimised and so help to develop better conversion methods. An evolutionary algorithm (EA) optimisation framework for SNN models on SpiNNaker 3 was developed with a view to understanding how the weight parameters of a small test network could be optimised for the MNIST digit recognition task 4 . A genetic algorithm (GA) was used in the experiments for its biological relevance and the potential for model evaluation to be parallelised by running multiple models simultaneously on SpiNNaker. Tools such as those developed in this research could help bridge between the fields of machine learning and computational neuroscience and allow for a better understanding of the mechanisms of information processing in neural networks more generally.

METHODS

The test model for the optimisation framework was a simple convolutional SNN model (see Figure 1), the weights of which were optimised for the MNIST digit recognition task using a GA (see Table 1). The input was rate-coded representations generated from the MNIST images. Weights were encoded in a gene representation of 5,785 bases, with the bases taking integer values in the range -1 to +1. Two populations, seeded and unseeded, were evolved over 304 generations to understand the effect of initialisation on the evolved networks. The unseeded population was made up of 24,000 randomly initialised individuals and the seeded population was seeded with 12,000

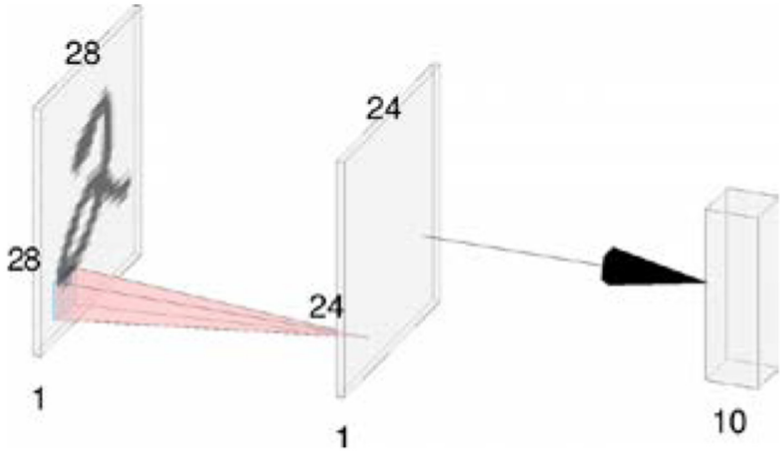

FIGURE 1: The structure of the simple SNN model optimised using a GA.

Table 1: A summary of the GA parameters

Variable	Value
Population Size (individuals)	24000
Mutation Rate	0.10%
Mutation Type	Base substitution
Crossover Rate	50.00%

individuals with a centre-surround filter (6,000 positive, 6,000 negative). In this experiment 1.46×10^7 networks were evaluated on SpiNNaker.

RESULTS AND DISCUSSION

Figure 2 shows the evolution of the training accuracy of the two populations over 304 generations. The five top performing individuals from the final populations were evaluated against the MNIST testing set and the best individuals gave 66.7% and 63.9% testing accuracy, unseeded and seeded respectively. It was observed that the populations do not converge to one filter, possibly due to the high mutation rate or the number of generations the GA was run for.

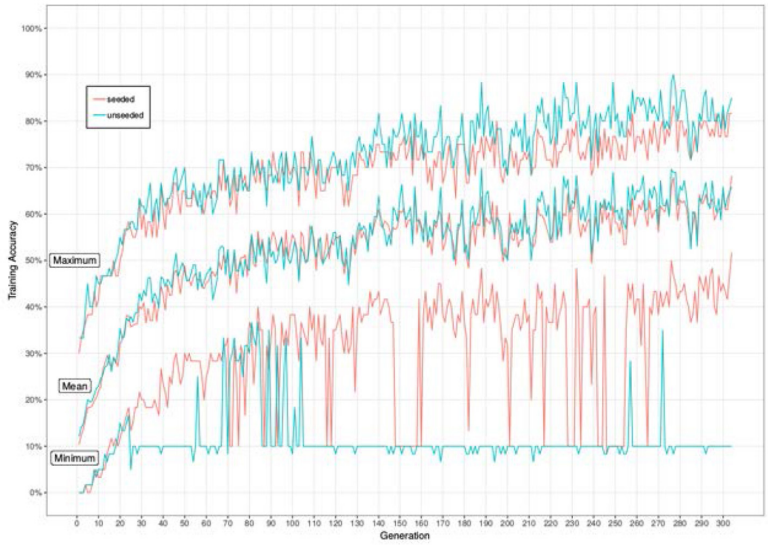

FIGURE 2: A graph comparing the training accuracy of the seeded and unseeded populations over 304 generations.

During the course of these experiments it was found that the overhead of submitting a jobs to SpiNNaker redesigning the framework to allow multiple models to be evaluated in one job. This work demonstrates that it is possible and feasible to use a GA to tune the parameters of a simple SNN model on SpiNNaker. Automated optimisation methods such as GAs and the parallelism afforded by SpiNNaker have the potential to change how research is done, with researchers being able to concentrate on higher levels of abstraction and larger scales in models.

AQ2

REFERENCES

[1] W. Van Geit, E. De Schutter and P. Achard. Automated neuron model optimization techniques: a review. Biological Cybernetics, 99(4):241–251, 2008.

[2] Bodo Rueckauer, Iulia-Alexandra Lungu, Yuhuang Hu, Michael Pfeiffer and Shih-Chii Liu. Conversion of continuous-valued deep networks to efficient event-driven networks for image classification. Frontiers in Neuroscience, 11(1):682, 2017.

[3] S. B. Furber, F. Galluppi, S. Temple and L. A. Plana. The SpiNNaker project. Proceedings of the IEEE, 102(5):652–665, 2014.

[4] LeCun Yann, Cortes Corinna, and Burges Chris. MNIST handwritten digit database, http://yann.lecun.com/exdb/mnist/, 1998.

Spatio-temporal pattern detection in macaque motor cortex during an instructed-delay reach-to-grasp task using SPADE

AQ1 **Alessandra Stella[1], Pietro Quaglio[1], Alexa Riehle[2], Thomas Brochier[2], Sonja Grün[1,3]**

AQ6

[1]Institute of Neuroscience and Medicine (INM-6, INM-10), Institute for Advanced Simulation (IAS-6), and JARA Brain Institute I (INM-10), Jülich Research Centre, Jülich, Germany

[2]Institut de Neurosciences de la Timone, CNRS-AMU, Marseille, France

[3]Theoretical Systems Neurobiology, RWTH Aachen University, Aachen, Germany

INTRODUCTION

Correlation in neuronal spiking activity is considered as an expression of an active cell assembly. The concept was suggested by Donald Hebb in 1949 [1], stating that neurons organize in assemblies of co-activated cells that act as information processing units. We hypothesize that assembly activity is expressed through repeated and precise activations of sequences - spatio temporal patterns (STPs) - of action potentials emitted by the neuron members of the cell assembly. We previously developed a method, called SPADE [2,3], that combines mining and statistical testing techniques in order to detect significant STPs in parallel electrophysiological recordings. The method is designed as following: it first finds repeating STPs using frequent itemset mining [2], and then evaluates them for significance.

In order to test for significance, it pools together patterns of the same signature, i.e. the number of spikes involved, its number of occurrences, and the duration of the pattern (time between first and last spike). The significance of each signature is evaluated by comparing its occurrence count to the number expected in independent processes generated by dithering the original data [4]. The statistics is performed by bootstrapping. The SPADE method is available in the Python library Elephant [5].

METHODS

Our goal is to investigate cell assembly activation in parallel spike train data recorded from pre-/motor cortex of macaque monkeys performing a

reach-to-grasp task [6,7]. More specifically, we aim to test the hypothesis that different cell assemblies are activated at different points in time in relation to the behavior. Therefore we employ the SPADE method in order to detect repeated spike patterns, to the data from different epochs during the trial. We extend a previous analysis that focused on synchronous patterns on the same data [8] to precise patterns with temporal lags, i.e. STPs. Here we first focused on two sessions (each of 15min) that are publicly available [6]. The experimental procedure was structured as such: after a preparatory period, the monkeys had to pull and hold an object by using either a side or a precision grip, and using either high or low force (four total behavioral conditions). The single trial data is segmented into six behavioral epochs (of 500ms) and data from corresponding epochs across the trials are concatenated and analyzed as one data piece. Spike trains are discretized with 3 ms precision.

RESULTS

Preliminary results show firstly that patterns occur mostly during the movement period. The patterns are formed by the same neurons however with many different lag configurations. Secondly, pattern configurations are specific to the different trial types (grip/force combinations). Thirdly, we find that several neurons participate in all patterns within one behavioral condition, and their individual spikes are involved in multiple patterns. Thus, we suggest to consider the latter neurons as hub neurons [9], and plan to investigate further their characteristics. Further we plan to analyze many more recording sessions for the occurrence of significant STPs, their relation to behavior and their specificities.

AQ2

REFERENCES

[1] Hebb, D. O. (1949) The organization of behavior: A neuropsychological approach. John Wiley & Sons.

[2] Torre E, Picado-Muiño D, Denker M, Borgelt C, Grün S (2013) Statistical evaluation of synchronous spike patterns extracted by frequent item set mining. Frontiers in Computational Neuroscience, 7:132.

[3] Quaglio, P., Yegenoglu, A., Torre, E., Endres, D., Grün, S. (2017). Detection and Evaluation of Spatio-Temporal Spike Patterns in Massively Parallel Spike Train Data with SPADE. Frontiers in Computational Neuroscience, 11:41.

[4] Louis, S. G., & Diesmann, M. (2010). Surrogate spike train generation through dithering in operational time. Frontiers in computational neuroscience, 4, 127.

[5] Elephant - Electrophysiology Analysis Toolkit, http://www.python-elephant.org/, RRID:SCR_003833.

[6] Brochier, T., Zehl, L., Hao, Y., Duret, M., Sprenger, J., Denker, M., ... & Riehle, A. (2018). Massively parallel recordings in macaque motor cortex during an instructed delayed reach-to-grasp task. Scientific data, 5, 180055.

[7] Riehle A, Wirtssohn S, Grün S, Brochier T (2013) Mapping the spatio-temporal structure of motor cortical lfp and spiking activities during reach-to-grasp movements. Frontiers in Neural Circuits, 7:48.

[8] Torre, E., Quaglio, P., Denker, M., Brochier, T., Riehle, A., & Grün, S. (2016). Synchronous spike patterns in macaque motor cortex during an instructed-delay reach-to-grasp task. Journal of Neuroscience, 36(32), 8329-8340.

[9] Dann, B., Michaels, J. A., Schaffelhofer, S., & Scherberger, H. (2016). Uniting functional network topology and oscillations in the fronto-parietal single unit network of behaving primates. Elife, 5, e15719.

Feature extraction and dimensionality reduction using ultralow power 2-dimentional MoS 2 based memristor networks

AQ1

Amanov Dovran*

Hong Kong University of Science and Technology, Clear Water Bay, Kowloon, Hong Kong
**damanov@connect.ust.hk*

INTRODUCTION

There have been several experimental demonstrations of machine learning algorithm using memristor, simple two terminal metal/insulator/metal structured device, networks which paved a way to hardware-based machine learning devices 1,2 . However, recently, there have been a lot attention on 2-dimentional materials based memristors as they have higher power efficiency, lower programming voltage, higher integrability, and higher flexibility comparing to traditional metal-oxide based memristor 3,4. This abstract is inspired by our research at School of Engineering and Applied Science, Harvard University laboratory (will be submitted to the journal soon).

METHODS

We have found out that bilayer 2-dimentional MoS2 based memristor have low programming voltage of ~0.2V (see figure 1). Moreover, we were able to demonstrate spike-timing dependent plasticity which is very crucial in learning algorithms (see figure 2). Standby operation power is about micron-Joule order while single weight updating operation consumed around nano-joule order. Therefore, memristor networks built from these kind of energy efficient memristor have crucial potential applications in various technologies which has bottleneck of energy efficiency (e.g. Drones, IoT devices). Fabrication of bilayer 2-dimentional (2 layers of 2D MoS2) MoS 2 based memristor network of size 16 by 2 is anticipated to perform feature extraction and dimensionality reduction. Principal components will be obtained on the memristor conductances using Sanger's rule (generalized Hebbian learning). Henceforth, memristor network will be tested for accuracy using industry-wide data like breast-cancer cell data to evaluate the classification performance. Moreover, energy consumed for training and testing will be measured as main theme of

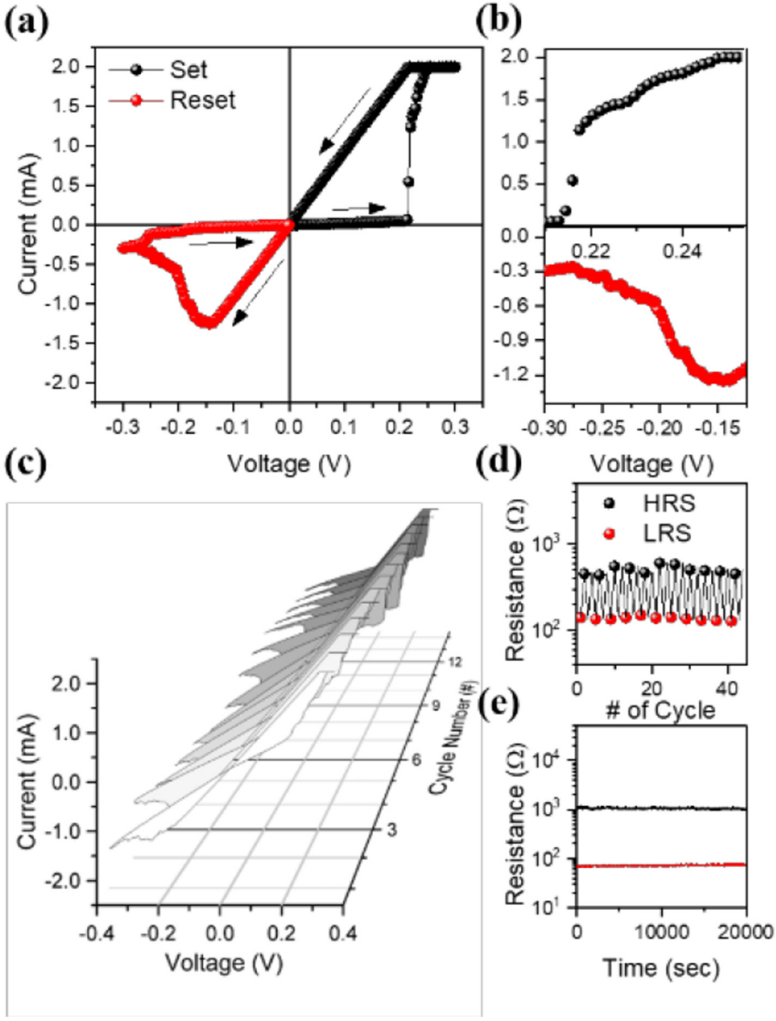

FIGURE 1: Schematic, device, and four-point probe method. (**a**) Optical image of Cu/two-layer MoS2/Au MIM device. Inset: zoom-in optical image. Scale bar: 100 mm (**b**) Schematic plot of devices and four-point probe method (**c**) Representative I-V curve of Cu/two-layer MoS2/Au MIM device with four-point probe method. Inset: the corresponding curve of resistance versus voltage (**d**) The total resistance and resistance across MoS 2 versus voltage with four-point probe measurements.

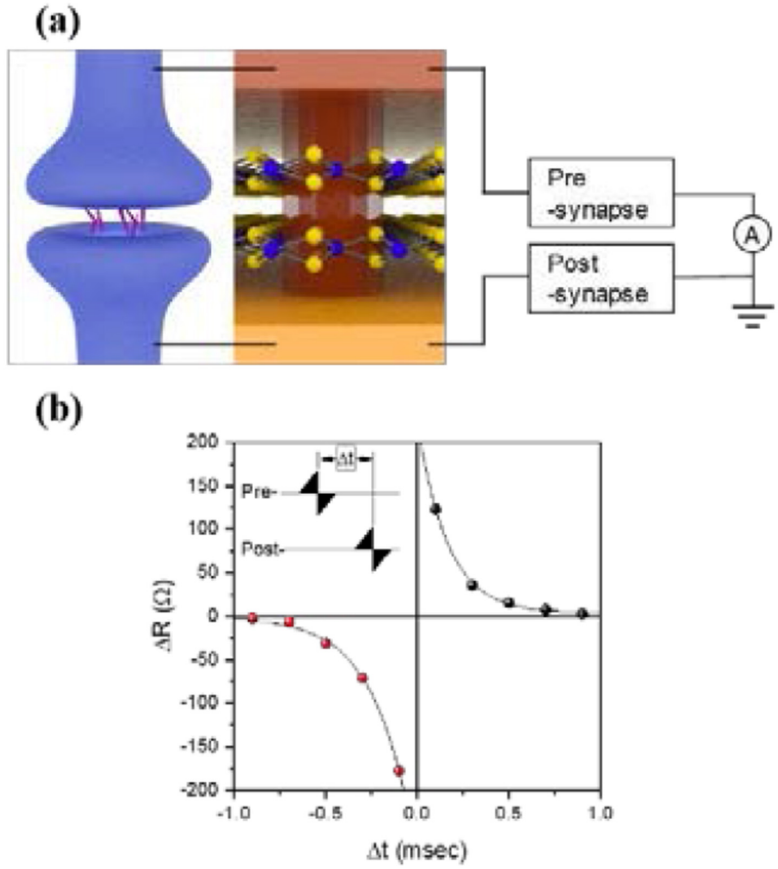

FIGURE 2: Demonstration of STDP in the memristor synapse (a) Schematic plot of the STDP setup (b) The measured change of the memristor resistance (synaptic weight) vs the relative timing Δt of the neuron spikes.

the work is quantifying energy efficiency of the network. The work will take about 1-2 month and therefore results will be demonstrated in conference Feature extraction and dimensionality reduction is crucial component of unsupervised learning which has wide range of application including very impactful ones like pattern recognition and anomaly detection. Therefore, power efficient 2-dimentional material based memristor network integrated

devices/systems will pave a way more to the point applications of various technologies as they will be to analyze the data on board with very low power consumption rather than sending it back to server or trying to do analysis consuming a lot energy. Hence, timely action can be carried out depending on the environment of the application. For instance, integrating proposed memristor networks to drones and using in emergency situations will greatly reduce the effectiveness of the action taken by personnel.

AQ2

REFERENCES

[1] Choi, S., Shin, J. H., Lee, J., Sheridan, P., & Lu, W. D. (2017). Experimental Demonstration of Feature Extraction and Dimensionality Reduction Using Memristor Networks. Nano Letters, 17(5), 3113-3118. doi:10.1021/acs.nanolett.7b00552.

[2] Sheridan, P. M., Cai, F., Du, C., Ma, W., Zhang, Z., & Lu, W. D. (2017). Sparse coding with memristor networks. Nature Nanotechnology, 12(8), 784-789. doi:10.1038/nnano.2017.83.

[3] Ge, R., Wu, X., Kim, M., Shi, J., Sonde, S., Tao, L., . . . Akinwande, D. (2017). Atomristor: Nonvolatile Resistance Switching in Atomic Sheets of Transition Metal Dichalcogenides. Nano Letters, 18(1), 434-441. doi:10.1021/acs.nanolett.7b04342.

[4] Kim, M., Ge, R., Wu, X., Lan, X., Tice, J., Lee, J. C., & Akinwande, D. (2018). Zero-static power radio-frequency switches based on MoS2 atomristors. Nature Communications, 9(1). doi:10.1038/s41467-018-04934.

Communication middleware for spreading data into SpiNNaker

Francesco Barchi*, Luca Peres, Gianvito Urgese, Andrea Acquaviva

Politecnico di Torino, Torino, IT, The University of Manchester, Manchester, UK
**francesco.barchi@polito.it*

MOTIVATION

The main feature of neuromorphic multicore systems is the capability of processing information asynchronously in an event-driven style. The processing units (processors) remain in an idle state until an event arrives, then a reaction is triggered and, after that the processors return to the idle state. Another peculiarity of the Neuromorphic systems is the high number of interconnections between the processing units which speeds-up and simplifies the communications between the cores.

In this domain, SpiNNaker has been the first working example of such architectural structure [1]. Currently, one of the issue for this platform is the time necessary to transfer data from the host server to the SpiNNaker board through *point to point* packets flowing one-by-one to each target core through a single Ethernet enabled chip. In this work we describe a new communication middleware designed for enhancing the *Host to Core* and *Core to Core* data transmission exploiting the Multicast network, thus giving a real speed-up in the overall communication procedure.

METHOD

Data is currently transmitted using the Spinnaker Data Protocol (SDP) in *Host to Core* and *Core to Core* communications using the *point to point* (P2P) network capabilities (one source – single destination) of SpiNNaker chips [2]. The use of the P2P limits the system as it needs the intermediation of the Monitor Processors of the two chips involved in the communication. Furthermore, this type of communication is sequential and does not exploit the full capabilities of the SpiNNaker network and the concurrency of the system.

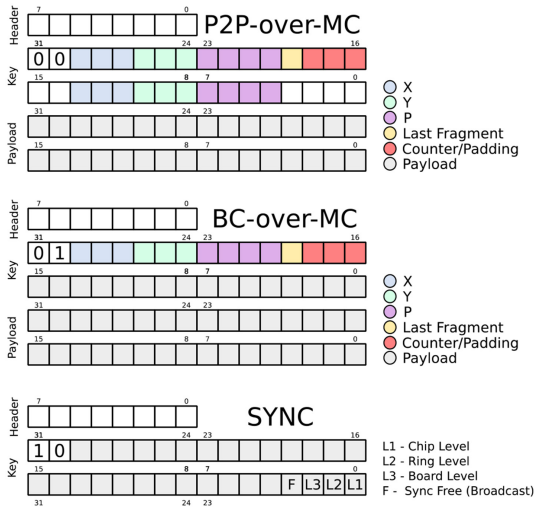

FIGURE 1: Communication Middleware – The Spinnaker Multicast Headers used for implementing the Communication Middleware. The two most significant bits (MSbs) define the communication type. Implementing the point to point connectivity (MSbs 0b00) over the MC network require to use 4 Byte in order to specify the packet source and the packet destination. Implementing the broadcast connectivity (MSbs 0b01) over the MC network require only 2 Byte in order to specify the packet source only. The BC over MC communication can use fragments of 48 bit instead 32 bits with an efficiency of 66% (44% of efficiency using fragments of 32 bits). The SYNC packet provides the capability to synchronise the whole SpiNNaker board using only four packets using a multilevel approach.

Our idea has been to develop a *Communication Middleware* able to exploit the *multicast* (MC) network capabilities (one source - multiple destinations) of SpiNNaker chips to speed-up the *Host to Core* and the *Core to Core* communications. The MC protocol being directly used by Application Processors without the Monitor Processor intermediation. The *Communication Middleware* uses a custom multicast packet header (Figure 1) for providing *unicast*, *broadcast*, and *multicast* communication on the SpiNNaker. We developed a set of APIs, both on host and board sides, capable of managing the routers configuration, the fragmentation and recomposition of data block, and the creation of MC packets. Each processor is capable of fragmenting and assembling a whole SDP packet.

We have developed a routing rule compression system capable of detecting binary overlaps in routing rules and exploiting router capabilities that include

the use of binary masks during routing. In this way, we were able to implement *unicast* and *broadcast* connectivity using only 50 routing rules instead of 1600 making the implementation of the *Communication Middleware* feasible.

RESULTS

We tested the implementation of the communication middleware by sending to the architecture the data necessary to configure a simulation of spiking neural networks (SNN) [3]. By exploiting the concurrency of the system and

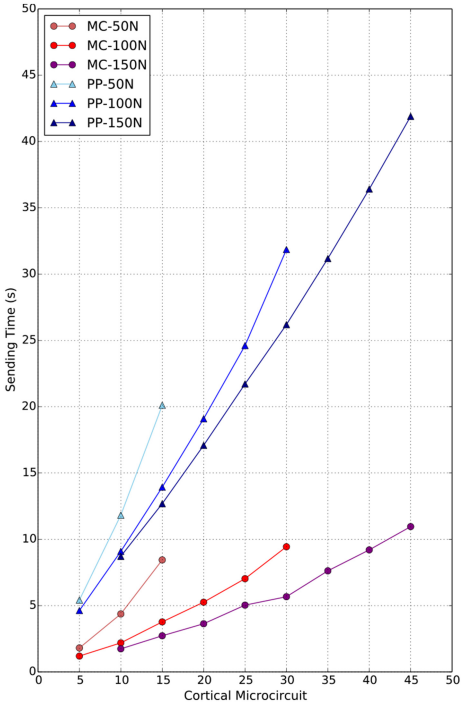

FIGURE 1: Benchmark Results – The Communication Middleware performances measured sending configuration packets for a benchmark simulation of a Cortical Microcircuit using different network dimensions and a different number of neurons per processor. We use the native point-to-point communication middleware (blue lines) and our multicast-based middleware (red lines). The improvement is a speedup of about three times.

the multicast connectivity, we have been able to get an improvement of 3x on the data forwarding inside the board (Figure 2), providing the chance of building more efficient applications through the new middleware.

AQ2

REFERENCES

[1] S.B.Furber, F.Galluppi, S.Temple, and L.A.Plana.2014.TheSpiNNakerProject. Proc. IEEE 102, 5 (May 2014), 652–665.

[2] S.B.Furber, D.R.Lester, L.A.Plana, J.D.Garside, E.Painkras, S.Temple, and A.D.Brown. 2013. Overview of the SpiNNaker System Architecture. IEEE Trans.Comput. 62, 12 (Dec 2013), 2454–2467.

[3] G.Urgese, L.Peres, F. Barchi, E.Macii, and A.Acquaviva. 2018. Work-in-Progress: Multiple Alignment of Packet Sequences for Efficient Communication in a Many-Core Neuromorphic System. In Compilers, Architectures and Synthesis For Embedded Systems (CASES), 2017 International Conference on. IEEE.

Machine learning for cognitive competence assessment

Nikolay Skuratov[1,3], Svetlana Sushchinskaya[1], Evgeny Khalezov[2], Anastasiia Liashenko[2], Maxim Sharaev[1], Ekaterina Kondrateva[1], Marie Arsalidou[2,4]*

AQ1

[1]Skolkovo Institute of Science and Technology, Moscow, Russia
[2]Department of Psychology, National Research University Higher School of Economics, Moscow, Russia
[3]Moscow Institute of Physics and Technology, Moscow, Russia
[4]Department of Psychology, York University, Toronto, Canada
**nikolay.skuratov@skoltech.ru; *svetlana.sushchinskaya@skoltech.ru; *khalezov@gmail.com; *akliashenko@gmail.com; *m.sharaev@skoltech.ru; *ekaterina.kondrateva@skolkovotech.ru; *marie.arsalidou@gmail.com*

Cognitive competence is highly related to academic and professional success. Parametric measures of mental-attentional capacity evaluate cognitive competence across multiple levels of difficulty [1, 2], which allow for assessment of performance of individuals with variable cognitive abilities. Research shows that mental attentional capacity improves gradually over childhood and adolescence [2]. Concurrently, brain related indices significantly change as a function of age. One less used method to evaluate hemodynamic responses in the typically developing brain is ultrasonography. The purpose of this study is to find predictive relations among scores obtained using parametric measures of mental attentional capacity and hemodynamic responses obtained using Doppler ultrasonography in school age children. Specifically, we test Machine Learning predictive models on parametric measures of mental attentional capacity and Doppler ultrasonographic indices recorded from the carotid and vertebral arteries.

MATERIAL AND METHODS

625 children from Moscow schools attending grades 1-4 ages 7-11 years were tested. For them were obtained ultrasonographic data: characteristics of carotid, vertebral, cerebral arteries. Also, children completed a paper-and-pen Figural Intersection Task (FIT) [1-3] and computerized tasks – Colour Matching Task (CMT) [2,3] and Number Matching Task (NMT). Based on behavioral scores (accuracy and reaction time) and ultrasound indices (i.e., vessel diameter

and blood velocity) we built prediction models to estimate a child's age. We selected a final model from a list of regressors (Lasso, Ridge, KNeighbors, XGBoostRegressor and Linear Regression) combined with dimensionality reduction (Principal Component Analysis, Locally Linear Embedding) and feature selection techniques (SelectFromModel, SelectKBest).

RESULTS

Show that the age of children was determined with mean absolute error of 0.85 with Lasso Regression and SelectKBest feature selection for both ultrasound and behavioral scores. In other words, the model can predict the age of the child within 10 months. This result remained unchanged when we examined boys and girls separately. Concluding, it is encouraging to observe agreement in predictive scores for ultrasound and behavioural results. This suggests that both methods can be used in predicting developmental age in school and clinical setting. Findings will be discussed in the context of machine learning approaches, theories of cognitive development as well as practical applications in educational settings that encourage neurocognitive methods for assessing developmental readiness.

This abstract was prepared with the support of the Russian Science Foundation (project No. 17-18-01047).

AQ2

REFERENCES

[1] Pascual-Leone, J. (1970). A mathematical model for the transition rule in Piaget's developmental stages. Acta Psychologica, 32, 301–345

[2] Arsalidou, M., & Im-Bolter, N. (2017). Why parametric measures are critical for understanding typical and atypical cognitive development. Brain Imaging and Behavior, 11, 1214–1224. doi: 10.1007/s11682-016-9592-8

[3] Arsalidou, M., Pascual-Leone, J., & Johnson, J. (2010). Misleading cues improve developmental assessment of working memory capacity: the color matching tasks. Cognitive Development, 25(3), 262-277.

Volr - A declarative approach to learning in spiking neural networks

AQ1

Jens Egholm Pedersen[1]*, Christian Pehle[2]*

[1]Unversity of Copenhagen, Unit for Cognitive Neuroscience, Oester Farimagsgade 2A, 1353 Copenhagen, Denmark

[2]Heidelberg University, Kirchhoff-Institute of Physics, Im Neuenheimer Feld 227, 69120 Heidelberg, Germany

**xtp778@alumni.ku.dk; *c.pehle@kip.uni-heidelberg.de*

INTRODUCTION

For inexperienced users, there are still significant barriers to entry to computational platforms and tools developed by the Human Brain Project (HBP). Experiments involving learning are particularly challenging to program, even for advanced users. Interface libraries such as PyNN translate and replicate experiments across platforms such as SpiNNaker and BrainScales, except when plasticity or learning are involved. Both across backends and over time, where APIs naturally mutate. Experiments with structural plasticity on SpiNNaker [1] or in the loop training on BrainScaleS [2] use platform-specific features to achieve their goals, which are difficult to migrate. As a consequence research within learning-to-learn and in-the-loop paradigm training require extensive customization of current frameworks. Consistent models of simulated and accelerated neural experiments across backends and time will significantly reduce the iteration time and drastically cut experimental costs, to the benefit of the research community as a whole. Further gains in the integration of existing and well-known tools like Python and Jupyter notebooks will likely increase adoption. This work presents a method to avoid the above-mentioned challenges and to improve exposure to HBP technologies. Using the novel modeling language Volr [3], we construct a network and train it to solve a small maze task on BrainScaleS, NEST, and Tensorflow. Volr permits cross-platform training and ensures the reproducibility of the experiment. We believe the use case illustrates the suitability of Volr as a tool for future neurocognitive research.

METHODS

The Volr architecture as shown in the figure to the right illustrates how the neural network model (top) is translated from the Volr language description into various backends. The backend models are trained with backpropagation in Tensorflow and in NEST through a Tensorflow-like [4]. Training on the BrainScaleS system is not yet supported, but because of the universal model description, the NEST weights can be translated into BrainScaleS weights [2].

RESULTS AND OUTLOOK

The domain-specific language, Volr, has been developed to describe reproducible and consistent neural network experiments for artificial (ANN) and spiking (SNN) substrates. Prototypical integration with Jupyter Notebooks has been shown to allow fast iterations of experiments, with immediate access to already familiar Python tools for large-scale data analysis. Three targets are currently supported, but further work is needed to include platforms such as SpiNNaker, Intel's Loihi and the new BrainScaleS 2 system developed in the HBP. Ongoing work is exploring the domain of more complex cognitive experiments with cognitive tasks modeling, reverse differentiation for ANN and the inclusion of high-level abstractions for learning through learning-to-learn integration between ANN and SNN. In this context it would be interesting to incorporate the methods of [2][5] into a generalizable non-experiment specific framework.

Keywords: learning, neuromorphic computing, computational neuroscience, domain-specific language

REFERENCES

[1] Petruț A. Bogdan, Andrew G. D. Rowley, Oliver Rhodes and Steve B. Furber, Structural Plasticity on the SpiNNaker Many-Core Neuromorphic System, Frontiers in Neuroscience | Neuromorphic engineering.

[2] Sebastian Schmitt, Johann Klaehn et al., Neuromorphic Hardware In The Loop: Training a Deep Spiking Network on the BrainScaleS Wafer-Scale System, arXiv/1703.01909.

[3] Jens Egholm Pedersen, Christian Pehle, Volr (2018), Github organization, github.com/volr/.

[4] Jens Egholm Pedersen, Christian Pehle, Volr (2018), Github organization, github.com/volr/volrpynn.

[5] Guillaume Bellec, Darjan Salaj, Anand Subramoney, Robert Legenstein, Wolfgang Maass, Long short-term memory and learning-to-learn in networks of spiking neurons, arXiv/1803.09574 (to appear in NIPS 2018).

A robot arm performs target reaching without planning using spiking neurons

J. Camilo Vasquez Tieck[1*], Lea Steffen[1], Jacques Kaiser[1], Arne Roennau[1], Rüdiger Dillmann[1]

AQ1

FZI Research Center for Information Technology, Germany - SP10 Neurorobotics
**tieck@fzi.de*

MOTIVATION

Target reaching is one of the most important problems in robotics — object interaction, manipulation and grasping tasks require reaching an specific target [2]. A broad accepted concept in neuroscience is that the CNS (Central Nervous System) uses sensory-motor primitives as building blocks for the execution and planning of motions [3], [4]. The combination of simple primitives representing muscle synergies creates more complex and advanced motions [4], [5], [6]. There have been developments in robotics using this principles for dynamic motion primitives [7], [8], for a reactive framework of reflexes [9]. Nevertheless, robotics still relays on the classical methods. In classical robotics the problem of reaching a target is solved by calculating the inverse kinematics (IK) for the target point, then validating the configuration, and finally planning the trajectory. These steps are computational expensive. A complete overview on planing methods is presented in [2], and a detailed analysis on different methods for solving the IK is presented in [10]. Our approach is motivated by the consideration on how human beings estimate positions and distances. Humans can easily determine which object is in front/back or on the left/right of another one, which of two angles is a wider [11]. Studies have shown that the human brain uses the feedback information from vision and from proprioception to execute reaching movements [12], [13]. A coupling between between this two systems suggest that there are other important components involved in the generation of motion. We avoid the complexity of calculating the IK and motion planning, and instead we use a combination of motor primitives to control the robot.

METHODS

The problem definition is that given an initial state of the robot arm, move the tool center point (TCP) to a specific target point in space (see Fig. 1a). Building on previous work with SNN using motor primitives for grasping [14], [15] and manipulation [16], we propose a bio-inspired architecture to perform target reaching with a robot arm without planning. A SNN represents motions in a hierarchy of motor primitives. Different correction primitives are combined using an error signal to control a robot arm in a closed-loop scenario. Three motor primitives — le f t – right, up – down and f ar – near — are defined to move the robot TCP in different directions. An example on how the primitives are modeled for the arm motion is presented in Fig. 1b. To illustrate how the system works, we present a sample run of the whole system in 1c. The first three rows show the current TCP position x, y and z in blue vs. the target's location in orange. The next thee rows show the spike activation of the error signals $\varepsilon\ \varphi$, $\varepsilon\ \theta$ and ε r. In row seven raw ε shows the spike pattern of the error-related population. The spike patterns of the neuron populations, representing the motor primitives, are respectively plotted by raw LR, raw UD and raw NF.

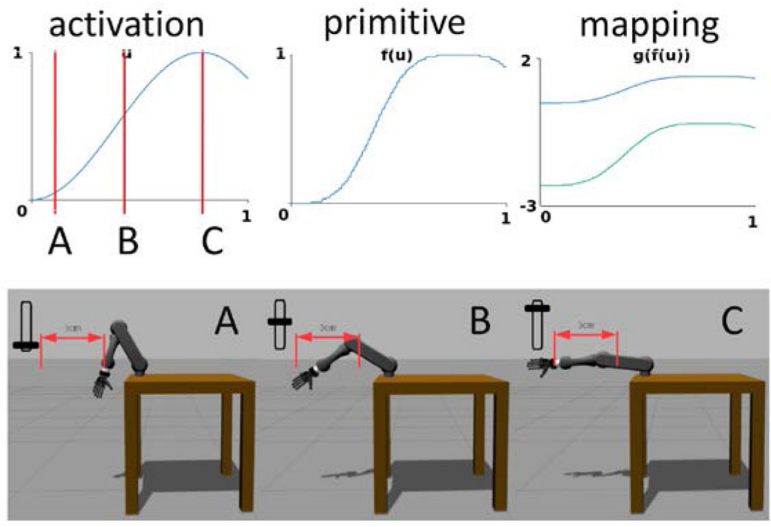

FIGURE 1: (**a**) Arm with target and motor primitives. (**b**) Modeling with motor primitives. (**c**) Spike activation, error signals and TCP position. (Figures adapted from [1]).

RESULTS AND DISCUSSION

We present a holistic system using one SNN. Motor primitives can simplify motor control, reduce amount of parameters, lower amount of necessary information processing, allow motion modelling in a parametric way. Our approach can also be used with different robot arms, by redefining the mapping of the primitives to the robot kinematic. In our method, the TCP position comes from simulation as well as the position of the target. But reaching involves the visual feedback for online motion [13], [12]. In order to test in a real robot, we need to integrate perception with the camera to get tcp and ball "relative positions". The vision system used in [17] could be integrated to perform motion prediction and use that to determine the error signal [18]. Current work also focuses on integrating this experiment and the motion framework in the Neurorobotics Platform [19] from the Human Brain Project.

ACKNOWLEDGMENTS

This research has received funding from the European Union's Horizon 2020 Framework Programme for Research and Innovation under the Specific Grant Agreement No. 720270 (Human Brain Project SGA1) and No. 785907 (Human Brain Project SGA2).

Keywords: target reaching, motor primitives, motion representation, closed-loop, spiking networks

REFERENCES

[1] J. C. V. Tieck, L. Steffen, J. Kaiser, A. Roennau, and R. Dillmann, "Controlling a robot arm for target reaching without planning using spiking neurons," in 2018 IEEE 17th International Conference on Cognitive Informatics & Cognitive Computing (ICCI* CC), 2018.

[2] J.-C. Latombe, Robot motion planning. Springer Science & Business Media, 2012.

[3] R. S. Johansson and K. J. Cole, "Sensory-motor coordination during grasping and manipulative actions," Current opinion in neurobiology, 1992.

[4] A. d'Avella and F. Lacquaniti, "Control of reaching movements by muscle synergy combinations," Frontiers in computational neuroscience, 2013.

[5] K. A. Thoroughman and R. Shadmehr, "Learning of action through adaptive combination of motor primitives," Nature, 2000.

[6] E. Bizzi, V. Cheung, A. d'Avella, P. Saltiel, and M. Tresch, "Combining modules for movement," Brain Research Reviews, 2008.

[7] A. J. Ijspeert, J. Nakanishi, H. Hoffmann, P. Pastor, and S. Schaal, "Dynamical movement primitives: learning attractor models for motor behaviors," Neural computation, 2013.

[8] S. Schaal, "Dynamic movement primitives-a framework for motor control in humans and humanoid robotics," in Adaptive motion of animals and machines, 2006.

[9] T. Kröger, "Opening the door to new sensor-based robot applications the reflexxes motion libraries," in Int. Conf. Robotics and Automation (ICRA), 2011.

[10] S. R. Buss, "Introduction to inverse kinematics with jacobian transpose, pseudoinverse and damped least squares methods," IEEE Journal of Robotics and Automation, 2004.

[11] R. Pfeifer and J. Bongard, How the body shapes the way we think: a new view of intelligence. MIT press, 2006.

[12] J. A. Saunders and D. C. Knill, "Humans use continuous visual feedback from the hand to control fast reaching movements," Experimental brain research, 2003.

[13] F. Filimon, J. D. Nelson, R.-S. Huang, and M. I. Sereno, "Multiple parietal reach regions in humans: cortical representations for visual and proprioceptive feedback during on-line reaching," Journal of Neuroscience, 2009.

[14] J. C. V. Tieck, H. Donat, J. Kaiser, A. Roennau, and R. Dillmann, "Towards grasping with spiking neural networks for anthropomorphic robot hands," ICANN, 2017.

[15] J. C. V. Tieck, S. Weber, T. C. Stewart, A. Roennau, and R. Dillmann, "Triggering robot hand reflexes with human emg data using spiking neurons," IAS-15, 2018.

[16] J. C. V. Tieck, L. Steffen, J. Kaiser, A. Roennau, and R. Dillmann, "Multi-modal motion activation for robot control using spiking neurons," BioRob, 2018.

[17] J. Kaiser et al., "Towards a framework for end-to-end control of a simulated vehicle with spiking neural networks," in Simulation, Modeling, and Programming for Autonomous Robots (SIMPAR), IEEE International Conference on, 2016.

[18] J. Kaiser, R. Stal, A. Subramoney, A. Roennau, and R. Dillmann, "Scaling up liquid state machines to predict over address events from dynamic vision sensors," Bioinspiration & biomimetics, 2017.

[19] E. Falotico et al., "Connecting artificial brains to robots in a comprehensive simulation framework: The neurorobotics platform," Frontiers in neurorobotics, 2017.

Brain signals classification technique for EEG data

Illia Skarha-Bandurov[1]*, Tetiana Boloborodova[2]*, Vitalii Honcharov[1], Inna Skarga-Bandurova[2]*

AQ1

[1]Luhansk State Medical University, 32 Budivelnikiv Street, Rubizhne, Lugansk region, Ukraine
[2]Volodymyr Dahl East Ukrainian National University, 59-a Tsentralny Prospekt, Severodonetsk, Ukraine
**ioskarga@gmail.com; *biloborodova@snu.edu.ua; *milostiprosim@i.ua; *skarga-bandurova@snu.edu.ua*

INTRODUCTION/MOTIVATION

The data extracted from the electroencephalogram (EEG) measures can be a rich source of information. They can be used not only in clinical research to understand the patient status and their diagnosis, but they are also heavily used in the gaming industry, IoT devices as well as for emotion recognition, military scenarios, etc. Hence, many approaches to machine classification have been proposed in this area. At the same time, when using these methods, a number of issues associated with the implementation of a multi-criteria parameter estimation in real time remain are unsolved. One of these issues is to classify the human biophysical state by EEG indicators. It is still unclear which machine classifier can be sufficient for clinical application when we have several monitoring data. To analyze signal structures of very different sizes, we need to perform a multi-sensor analysis on the recorded EEG signal. As a first stage to solve this problem, we propose a classification technique based on the combined multi-criteria probability estimates.

METHODS

The experiment was carried out using the dataset available in the open access UCI Machine Learning Repository [1]. Multichannel EEG dataset consists of 14977 instances obtained from 14 scalp electrodes in two eye states, open eyes and closed eyes. Detailed description EEG eye state data is given in [2].

Our EEG data processing methodology consists of six stages. At the first stage, we perform the data normalization by applying the Euclidean distance. Then, we analyze data using the ARIMA model; it allows us to run exponential smoothing, a one-dimensional autoregressive integrated moving average for the time series and to obtain a forecast of the data. To assess the quality of

the ARIMA model we use the Bayesian information criterion (BIC). To perform prediction the human biophysical state we chose the model with the minimum BIC value as the optimal. The obtained forecast values are used to calculate the residuals, which are the basis for further data fusion. The calculation of the base probability distribution is carried out using residues of variables of the human biophysical state. Next, we check the conflicts of probabilities of variables and select the method of data fusion. In this work, we use the Dempster-Shafer theory as a base approach for data fusion. After that, data classification is performed. For learning the model, we use the Random Forest algorithm and fivefold cross-validation. And at the last stage, we assess the classification accuracy.

RESULTS AND DISCUSSION

The probability of the human eyes states is calculated by the combined probabilities of the data obtained from the 14 EEG electrodes. For test dataset, the accuracy of EEG data classification is 0.93. There is a reason to believe that the proposed method provides accuracy comparable to other more popular algorithms and is a promising further basis for real-time data classification due to its low computational power and the possibility of using incomplete information.

AQ2

REFERENCES

[1] UCI Machine Learning Repository. Available at: https://archive.ics.uci.edu/ml/datasets/EEG+Eye+State (accessed 23 September 2018).

[2] O. Rösler, and D. Suendermann. A first step towards eye state prediction using EEG. In proceedings of the AIHLS, 2013.

Mind, brain, education: Pitfalls and potential connecting cognitive science and neuroscience with education

AQ1 **Jie GAO[1,2]***

[1]*Sorbonne University*
[2]*Institut Jean Nicod*
**jie.gao@paris-sorbonne.fr*

MOTIVATION

In philosophy, from Socrates onwards, one could count as many significant intellectual and social trends as favoured methods of argument and schools of thought, and almost all significant trends (Plato's idealism, Aristotle's realism, Dewey's pragmatism, Vygotski's social constructivism) have contemplated on learning/teaching and sought for strategies to develop autonomous learners and critical thinkers. They may be right about the general aim of education, but none of them provides concrete knowledge about the means to achieve the goal, not to mention that more complexities have been introduced by information overload, globalisation, digital revolution, etc. On the other hand, tremendous efforts have been made to achieve a scientific understanding of the brain as "an integrated system supporting the entire array of the mental functions" [1]. Mind, brain, education science (MBE) is a pioneering educational initiative where cognitive science and education science join force to inform us about how we learn best, how to most effectively advance the 21st century skills, such as elaboration, communication and rational autonomy, both for the immediate gain and the long run. This encounter raises several epistemological and ethical issues; some objections mirror those against evidence-based education.

METHODS

Using methods of philosophy and history of science, the present work inform the debate with a systematic descripiton of how MBE works in theory and in practice. First, we examine the coherence of the arguments leveled against and in favor of evidence-based education. Then we propose an analytical framework ideal for conceptualising such projects involving multiple actors

and scales of operation. Finally, we use the case of numerical cognition and numeracy education to see how it has (not) worked and how it may work in the future.

CONCLUSION

Education practices are best served by incorporating research findings. However, sustained impact of neuromyths calls for caution with (solely) bain-based agenda. The analysis suggests that to be a worthy field of educational research, MBE has to improve research design and integrate methods of social interventions and cognitive sciences. Specifically, there are much potential for MBE if it can (1). improve causal validity by balancing internall & external validity (2). increase explanatory power with mixted methods and cross-cultural examinations (3). balance level of involvement and build intermediacy between different actors with shared values, fundings, journals and criteria of instituiional evaluation (4). motivate educational thinking and practice through models arising from neural and behavioural evidence that inform us about the "what", the "why" and the "how" it works in the cognitive-cultural ecosystem of education.

Keywords: neuroscience and education, transdisciplinary, translational, philosophy of cognitive science

REFERENCES

[1] Andler, Daniel. "Philosophy of cognitive science." *French Studies In The Philosophy Of Science*. Springer, Dordrecht, 2009. 255-300.

[2] Baberousse, A., Bonnay, D., & Cozic, M. (2018). The Philosophy of Science: A Companion. Oxford University Press.

[3] Biesta, G. J. (2010). Why 'what works' still won't work: From evidence-based education to value-based education. Studies in philosophy and education, 29 (5), 491–503.

[4] Chang, H. (2009). Ontological principles and the intelligibility of epistemic activities. Scientific understanding: Philosophical perspectives, (pp. 64–82).

[5] Chang, H. (2011). The philosophical grammar of scientific practice. International Studies in the Philosophy of Science, 25 (3), 205–221.

[6] Davies, P. (1999). What is evidence-based education? British journal of educational studies, 47 (2), 108–121.

[7] Dillon, M. R., Kannan, H., Dean, J. T., Spelke, E. S., & Duflo, E. (2017). Cognitive science in the field: A preschool intervention durably enhances intuitive but not formal mathematics. Science, 357 (6346), 47–55.

[8] Fischer, K. W. (2008). Dynamic cycles of cognitive and brain development: Measuring growth in mind, brain, and education. The educated brain: Essays in neuroeducation, (pp. 127–150).

[9] Izard, V., Sann, C., Spelke, E. S., & Streri, A. (2009). Newborn infants perceive abstract numbers. Proceedings of the National Academy of Sciences, 106 (25), 10382–10385.

[10] McMillan, J. H., & Schumacher, S. (2010). Research in education: Evidence-based inquiry, myeducationlab series. Pearson.

[11] Pica, P., Lemer, C., Izard, V., & Dehaene, S. (2004). Exact and approximate arithmetic in an amazonian indigene group. Science, 306 (5695), 499–503.

AQ3

[12] Tokuhama-Espinosa, T. (2010). Mind, brain, and education science: A comprehensive guide to the new brain-based teaching. WW Norton & Company.

[13] Weisberg, D. S., Keil, F. C., Goodstein, J., Rawson, E., & Graye, J. R. (2008). The seductive allure of neuroscience explanations. Journal of cognitive neuroscience, 20 (3), 470–477.

[14] Willingham, D. T. (2009). Three problems in the marriage of neuroscience and education. cortex, 45 (4), 544–545.

Advantages of publishing in Frontiers

OPEN ACCESS
Articles are free to read for greatest visibility and readership

FAST PUBLICATION
Around 90 days from submission to decision

HIGH QUALITY PEER-REVIEW
Rigorous, collaborative, and constructive peer-review

TRANSPARENT PEER-REVIEW
Editors and reviewers acknowledged by name on published articles

Frontiers
Avenue du Tribunal-Fédéral 34
1005 Lausanne | Switzerland

Visit us: www.frontiersin.org
Contact us: info@frontiersin.org | +41 21 510 17 00

REPRODUCIBILITY OF RESEARCH
Support open data and methods to enhance research reproducibility

DIGITAL PUBLISHING
Articles designed for optimal readership across devices

FOLLOW US
@frontiersin

IMPACT METRICS
Advanced article metrics track visibility across digital media

EXTENSIVE PROMOTION
Marketing and promotion of impactful research

LOOP RESEARCH NETWORK
Our network increases your article's readership